

THE UNIVERSITY OF CHICAGO

ENGINEERING APPROACHES FOR THE TREATMENT OF NON-HEALING  
DIABETIC WOUNDS

A DISSERTATION SUBMITTED TO  
THE FACULTY OF THE PRITZKER SCHOOL OF MOLECULAR ENGINEERING  
IN CANDIDACY FOR THE DEGREE OF  
DOCTOR OF PHILOSOPHY

BY  
ABIGAIL LEIGH LAUTERBACH

CHICAGO, ILLINOIS

JUNE 2023

To my parents, Shane and Karen Lauterbach, who taught me the value of hard work and fostered my curiosity and love of learning. To my siblings, Lauren, Will, and Jack, for their love, encouragement, and support. And to Avery, my incredible husband who held my hand and built me up every step of the way.

"The most beautiful thing we can experience is the mysterious. It is the source of all true art and science." - Albert Einstein

# TABLE OF CONTENTS

|  |      |
|--|------|
| LIST OF FIGURES . . . . .  | vii  |
| LIST OF TABLES . . . . .   | viii |
| ACKNOWLEDGMENTS . . . . .  | ix   |
| ABSTRACT . . . . .   | xiii |
| 1 INTRODUCTION . . . . .   | 1    |
| 1.1 Phases of Wound Healing . . . . .  | 1    |
| 1.1.1 Phase I: Hemostasis . . . . .  | 2    |
| 1.1.2 Phase II: Inflammation . . . . .   | 3    |
| 1.1.3 Phase III: Proliferation . . . . .   | 5    |
| 1.1.4 Phase IV: Remodeling . . . . .   | 5    |
| 1.1.5 How the Diabetic Disease State Impacts Wound Healing . . . . .   | 6    |
| 1.2 Current Standards of Care in Diabetic Wound Healing . . . . .  | 9    |
| 1.2.1 Physical Measures . . . . .  | 10   |
| 1.2.2 Dressings . . . . .  | 11   |
| 1.2.3 Growth Factors . . . . .   | 12   |
| 1.2.4 Emerging Technologies for the Treatment of Non-Healing Diabetic Wounds . . . . .   | 13   |
| 2 TOPICALLY APPLIED COLLAGEN-BINDING SERUM ALBUMIN FUSED IL-4 FOR THE TREATMENT OF DIABETIC WOUNDS . . . . .                         | 15   |
| 2.1 Abstract . . . . .   | 15   |
| 2.2 Introduction . . . . .   | 16   |
| 2.3 Results . . . . .  | 19   |
| 2.3.1 CBD-SA-IL-4 Binds to Collagen, Induces M2 Macrophages <i>in vitro</i> , and is Retained Within Wounds <i>in vivo</i> . . . . . | 19   |
| 2.3.2 CBD-SA-IL-4 Therapy Promotes Diabetic Wound Healing . . . . .  | 23   |
| 2.3.3 CBD-SA-IL-4 Induces Macrophage Recruitment to the Wound Microenvironment Through Soluble Signals . . . . .                     | 28   |
| 2.3.4 CBD-SA-IL-4 Treatment Increases M2 Macrophages and Pro-angiogenic Cell Populations in the Wound . . . . .                      | 30   |
| 2.3.5 Single Systemic Administration of CBD-SA-IL-4 did not Upregulate Toxicity Markers . . . . .                                    | 32   |
| 2.4 Discussion . . . . .   | 34   |
| 2.5 Materials and Methods . . . . .  | 37   |
| 2.6 Author Contributions . . . . .   | 42   |
| 2.7 Funding . . . . .  | 42   |
| 2.8 Acknowledgements . . . . .   | 42   |
| 2.9 Conflicts of Interest . . . . .  | 42   |

|       |   |    |
|-------|---|----|
| 3     | SYSTEMICALLY ADMINISTERED FLT3L FOR THE TREATMENT OF DIABETIC WOUNDS . . . . .  | 43 |
| 3.1   | Abstract . . . . .  | 43 |
| 3.2   | Introduction . . . . .  | 43 |
| 3.3   | Results . . . . .   | 44 |
| 3.3.1 | Systemically Administered Flt3L Enhances Wound Healing in Type 2 Diabetic Mouse Model . . . . .                       | 44 |
| 3.3.2 | Flow Cytometric Analysis of Wound Tissue Following Flt3L treatment . . . . .  | 46 |
| 3.4   | Discussion . . . . .  | 48 |
| 3.5   | Materials and Methods . . . . .   | 48 |
| 3.6   | Author Contributions . . . . .  | 49 |
| 3.7   | Funding . . . . .   | 50 |
| 3.8   | Acknowledgements . . . . .  | 50 |
| 3.9   | Conflicts of Interest . . . . .   | 50 |
| 4     | MANNOSE-DECORATED CO-POLYMER FACILITATES CONTROLLED RELEASE OF BUTYRATE TO ACCELERATE CHRONIC WOUND HEALING . . . . . | 51 |
| 4.1   | Abstract . . . . .  | 51 |
| 4.2   | Introduction . . . . .  | 51 |
| 4.3   | Results . . . . .   | 53 |
| 4.3.1 | Tunable, Sustained Release of Butyrate from Mannose Co-Polymer . . . . .  | 53 |
| 4.3.2 | pMan-But and pMan-PhBut Modulate Inflammation <i>In Vitro</i> . . . . .   | 56 |
| 4.3.3 | pMan-But but not pMan-PhBut Modulate Soluble Signals <i>In Vivo</i> . . . . .   | 61 |
| 4.3.4 | pMan-But Treatment Accelerates Wound Healing in Type 2 Diabetic Murine Model . . . . .                                | 64 |
| 4.4   | Discussion . . . . .  | 68 |
| 4.5   | Materials and Methods . . . . .   | 71 |
| 4.5.1 | Small Molecule Synthesis . . . . .  | 71 |
| 4.5.2 | Polymer Synthesis and Characterization . . . . .  | 73 |
| 4.5.3 | Butyrate Release Kinetic Characterization . . . . .   | 74 |
| 4.5.4 | In Vitro Bioactivity Characterization . . . . .   | 75 |
| 4.5.5 | Mouse skin chronic wound healing model . . . . .  | 76 |
| 4.5.6 | Cytokine profile in wound tissue . . . . .  | 76 |
| 4.5.7 | Histomorphometric analysis of wound sections . . . . .  | 77 |
| 4.6   | Author Contributions . . . . .  | 77 |
| 4.7   | Funding . . . . .   | 77 |
| 4.8   | Acknowledgements . . . . .  | 77 |
| 4.9   | Conflicts of Interest . . . . .   | 78 |
| 5     | DISCUSSION, LIMITATIONS, FUTURE DIRECTIONS, AND CONCLUSIONS . . . . .   | 79 |
| 5.1   | Discussion, Limitations, and Future Directions in Cytokine Engineering . . . . .                                      | 79 |
| 5.2   | Discussion, Limitations, and Future Directions in Polymer Based Therapeutics . . . . .                                | 83 |
| 5.3   | Conclusions . . . . .   | 83 |

REFERENCES . . . . . 84

## LIST OF FIGURES

|      |  |    |
|------|--|----|
| 1.1  | Schematic of Cellular Infiltrates During Wound Healing . . . . .   | 2  |
| 2.1  | CBD-SA-IL-4 schematic and production . . . . .   | 19 |
| 2.2  | CBD-SA-IL-4 binds its receptor and signals through pSTAT6 . . . . .  | 20 |
| 2.3  | CBD-SA-IL-4 induces M2-like macrophage phenotype . . . . .   | 21 |
| 2.4  | CBD-SA-IL-4 binds collagen I and collagen III . . . . .  | 22 |
| 2.5  | <i>In vivo</i> Pharmacokinetic of CBD-SA-IL-4 . . . . .  | 23 |
| 2.6  | Topically applied 1% HA + CBD-SA-IL-4 enhances skin wound healing . . . . .  | 25 |
| 2.7  | Topically applied 1% HA + CBD-SA-IL-4 enhances granulation tissue formation . . . . .                                | 27 |
| 2.8  | CBD-SA-IL-4 reduced inflammatory cytokines and induced regenerative cytokines and chemokines in the wounds . . . . . | 29 |
| 2.9  | CBD-SA-IL-4 induces M2 macrophage proliferation and angiogenesis in the wounds . . . . .                             | 31 |
| 2.10 | CBD-SA-IL-4 does not show toxicity after a single subcutaneous administration . . . . .                              | 33 |
| 3.1  | Flt3L treatment promotes reepithelialization . . . . .   | 45 |
| 3.2  | Flt3L treatment representative histology images . . . . .  | 46 |
| 3.3  | Flt3L treatment modulates immune cell compartments in the wound bed . . . . .  | 47 |
| 4.1  | Structure and characterization of pMan-But and pMan-PhBut . . . . .  | 54 |
| 4.2  | Proton NMR characterization of butyrate-containing copolymers . . . . .  | 55 |
| 4.3  | Butyrate release from pMan-But and pMan-PhBut . . . . .  | 56 |
| 4.4  | pMan-But and pMan-PhBut are non-toxic to mBMDCs . . . . .  | 57 |
| 4.5  | <i>In vitro</i> characterization of butyrate polymer bioactivity . . . . .   | 58 |
| 4.6  | pMan-But suppresses pro-inflammatory cytokine and chemokine signaling from mBMDCs . . . . .                          | 60 |
| 4.7  | pMan-But alters cytokine signals from RAW 246.7 cells. . . . .   | 61 |
| 4.8  | <i>In vivo</i> characterization of butyrate polymer immune milieu modulation . . . . .                               | 63 |
| 4.9  | Polymer addition increases the viscosity of HA gel. . . . .  | 65 |
| 4.10 | <i>In vivo</i> wound closure efficacy of butyrate polymer . . . . .  | 66 |
| 4.11 | <i>In vivo</i> wound closure with butyrate polymer representative images . . . . .                                   | 67 |
| 4.12 | PBS vs. pHEMA healing efficacy . . . . .   | 68 |
| 5.1  | <i>In vivo</i> RIOM ulceration area . . . . .  | 82 |

## LIST OF TABLES

|     |  |    |
|-----|--|----|
| 2.1 | CBD-SA-IL-4 Treated Wound Characterization Panel Details . . . . . | 41 |
| 3.1 | Flt3L Treated Wound Characterization Panel Details . . . . .       | 50 |

## ACKNOWLEDGMENTS

I am incredibly thankful to all the people - friends, family, colleagues - for their endless support, encouragement, and help throughout my graduate studies. It takes a village, and I am fortunate to have an incredibly strong one.

To Jeffrey Hubbell, my graduate advisor, thank you for the opportunity to work in such a special place. The independence I have learned as a scientist and professional will be invaluable to me as I move into my next position. I came into graduate unsure of what I wanted to study, but after our conversations I was so excited to be in the environment you fostered that the nature of the work became less important than the breadth of incredible science happening in the lab. Your willingness and support for my pushing into new models, molecules and techniques was crucial to my development as a scientist and creative thinker. Your passion for new and meaningful science is motivating. Furthermore, your desire to pursue clinically impactful science truly resonated with me, and in watching your entrepreneurial endeavors, I learned about a whole field of work that prior I had no knowledge of but have found an excitement for. Thank you for your consistent support in pursuing opportunities outside of my doctoral studies, especially within professional development.

I would like to thank my many mentors that have guided me throughout the years. I would like to thank Yuping Bao, my first research advisor at The University of Alabama, who encouraged me to apply to graduate programs and continued to support me beyond my time with her lab. She also showed me the power of being a female researcher, something that has stuck with me and will continue to stick with me. Aslan Mansurov, who taught me many of the fundamental lab skills I needed to complete my work (protein production, ELISAs, and much more). I would also, especially, like to thank Jun Ishihara who brought me into the field of wound healing. His kindness and patience enabled me to make huge strides as a scientist. I will never forget my first time working with mice and being visibly so nervous and Jun just told me to take a deep breath and put on some relaxing music, a truly

formative experience. Even from London, Jun has provided me with support and guidance in navigating my graduate studies and subsequent professional steps.

The Hubbell lab is a truly special place and there are many people to whom I owe my development as a researcher, scientist, and individual. Aaron Alpar and Rachel Wallace who have had crucial leadership roles in the lab, building up everyone around them and making the science that happens here better. Aaron has saved me from many near-crisis research situations and Rachel was formative in learning how to conduct spectral flow cytometry (almost missing my engagement in the process). Rachel also pushed me to explore countless opportunities outside of research, she was always willing to extend her knowledge, network, and experiences to me, thank you for being a fantastic role model and supporter (and bocce partner)! Lisa Volpatti, while we never worked on the same project, I feel fortunate to have had such a strong woman to look up throughout my graduate studies. Watching you consistently aim higher has been endlessly motivating to me. Thank you for always taking the time to troubleshoot and discuss science as well as personal life. I look forward to continuing to learn from you. Thank you to Kirsten Refvik, who's endless knowledge was so exciting to learn from and work with, if you had a problem Kirsten could come up with some sort of solution. Thank you for also never letting me take anything too seriously and always being available to walk to Starbucks for a break (needed or not). Thank you Suzana Gomes, for your endless support, you always have taken such great care of everyone in the lab and I am blessed to have gotten to know you. Thank you, Taryn Beckman, for being my first true mentee, your drive and creativity are inspiring, and you are such a gifted scientist. Thank you for your patience in watching me learn to teach. More importantly thank you for your unwavering friendship, you made the last year of my graduate work immeasurably better, and I am thrilled to continue to learn from you. Thank you to Anna Slezak, who I became such fast friends with. I am truly grateful for your support as a colleague but more so as a friend. Your abilities as a scientist are bar none and it has been an absolute joy

and privilege to work alongside you. You pushed me to be a better scientist and motivated me to push my own boundaries inside and outside of my work. Thank you to the rest of the Hubbell lab: Jenni Antane, Priscilla Briquez, Erica Budina, Shijie Cao, Kevin Chang, Angie Chun, Camryn Garza, L. Taylor Gray, Isabella Hansen, Ande Hesser, Seonghun Kang, Marcin Kwissa, Ryne Montoya, Michal Raczy, Joe Reda, Lucas Shores, Ivan Vuong, Ruyi Wang, Thomas Wang, and Elyse Watkins

Thank you to the core facilities at The University of Chicago, in particular the Flow core, David Leclerc and Laura Johnston whose expertise has been invaluable to me. Thank you to the Histology core, these projects simply would have not been possible without your incredible work. Finally the light core, Shirley Bond and Christine Labno who facilitated data collection and answered many imaging analysis questions of mine.

I would like to thank my cohort, in particular Madison Plaster, Calixto Mattos Salles, Susan Okrah, Killian Tracey, and Paul Joekin. You all made graduate school much more fun that I think I could have ever imagined. Thank you for all the game nights, practice talks, pep talks, and consistent support.

Most importantly I would like to thank my family. My parents Shane and Karen Lauterbach, who have always put me first, provided endless support, many tearful calls and visits after failed experiments and the encompassing trudge that is graduate school. It is through both of your example that I learned how to work hard and be self-sufficient through tough times (which don't last, but tough people do). Thank you for allowing me to pursue anything I could dream of and providing endless support along the way. Thank you to my amazing siblings, Lauren, Will and Jack. Lauren, to have such a strong and determined sister is a gift. Watching your relentlessly pursue what you want is an inspiration. While I have had countless mentors, you are first among them and what a role model for me to have. Thank you. Will and Jack, thank you for all the visits and making sure I could see into the long-term, always answering my distraught phone calls when something didn't go

as planned and helping me move past it. You both have been my loudest supporters from the beginning. Thank you to my grandparents (Grandma Lauterbach and Nana) who were always so excited to hear about my work and quick to share my progress with those around them, I love you both! Thank you to my soon-to-be, but also has been for some time now, family — Al, Michelle, Keaton and Kierra Schmitz thank you for always taking the time to listen to all my graduate study experiences, the good and the bad. Reading drafts of proposals, sitting through practice talks, you all have been amazing supporters throughout this time and I am so thankful to be apart of your family, thank you for making me feel like I am.

Above all, I would like to thank my almost husband Avery. Words cannot describe how thankful I am for you. You have always supported me, in every single endeavor. You are my strongest believer and fiercest advocate. Through many instances of self-doubt your faith in me remained. Through all the weekends of work, bizarre hours, and failed experiments you always met me where I was at and provided nothing but love and support. Thank you for seeing in me what sometimes I could lose sight of, and bringing out the very best in me. This would not have been possible without you (or Bear). I know I have the most amazing partner in you and look forward to our next great adventure, whatever it may be.

## ABSTRACT

The overall goal of my thesis is to develop molecules to induce wound healing in an otherwise non-healing, diabetic wound by adjusting the microenvironment within the wound. To do this we utilized protein engineering strategies to target the exposed collagen in a cutaneous wound to ensure localization of protein constructs, we also took advantage of cellular deficits within the wound and systemically delivered appropriate soluble signals to the wound, and finally we as utilized a polymerized form of butyrate to disrupt the nonfunctional microenvironment by means of other dysfunctional pathways.

In Chapter 1, I introduce the groundwork for why a diabetic wound becomes chronic and non-healing. I discuss the key differences between healthy, healing wounds and diabetic, non-healing wounds, these differences span soluble signals, cellular populations and gene expression levels. I discuss the current standard of care used to treat diabetic wounds and the clinical shortcomings of these standards of care. Finally, I introduce new and emerging strategies being used to heal diabetic wounds.

Non-healing diabetic wounds are complex and multifaceted, many immune cells play a specific and crucial role in moving the wound towards healing. This allows us the opportunity to view the wound through many different lenses, represented by key cellular players of the wound healing process. In Chapter 2, I look at the wound through a macrophage focused lens and expand upon previously developed cytokine engineering techniques utilized in the laboratory to target exposed collagen with a cytokine payload, interleukin-4 (IL-4). We characterize the protein through bioactivity and macrophage polarization assays and determine our construct is biologically active and capable of pushing macrophages towards a pro-regenerative phenotype *in vitro*. I then move into efficacy studies using the well-established Type 2 diabetic murine model for non-healing diabetic wounds where CBD-SA-IL-4 shows to promote wound closure. Finally, I describe the mechanism through which CBD-SA-IL-4 promotes wound closure by characterizing the soluble signal changes in the wound

microenvironment and subsequent cellular changes that occur after topical administration of our construct.

In Chapter 3, I expand the approach to treat non-healing, diabetic wound through a different cellular lens focusing instead on dendritic cells and the role they carry in wound healing. We again use the Type 2 diabetic, db/db, mouse model to assess the efficacy of systemically administered Flt3L therapy in wound healing. Finally, we quantify the cellular changes within the wound to understand how Flt3L improves wound closure of chronic cutaneous wounds.

In Chapter 4, we utilize a polymer, instead of a protein, to again manipulate the microenvironment of a non-healing diabetic wound and induce changes toward pro-regenerative signals. We characterize the changes in soluble signals in the wound after topical administration of pManButyrate. We test the efficacy of pManButyrate as a therapeutic for wound healing in the Type 2 diabetic, db/db, mouse model and show improved closure after topical administration.

In Chapter 5, I discuss limitations, conclusions and future directions of this work within the context of both diabetic wound healing and other forms of non-healing wounds.

# CHAPTER 1

## INTRODUCTION

### 1.1 Phases of Wound Healing

The skin serves as a semi-permeable barrier to protect from the damage caused through the outside environment, such as physical trauma, dehydration, temperature, ultra-violet light, toxins and micro-organisms. When damage to the skin occurs, it leaves the rest of body susceptible to perturbations to these factors (e.g. infection by micro-organism infiltration) [1, 2]. To minimize the body's exposure to such environmental factors the skin has a highly complex mechanism for repairing itself. This wound healing process is tightly controlled and relies on the interactions between many different classes of cells; epithelial, endothelial, stem, stromal, and immune cells [3, 4, 5]. These cells produce different soluble signals and mediators that direct the re-epithelization of the skin in tight temporal fashion. In this chapter I will delineate the four phases of wound healing, as well as how the diabetic disease state impacts the cellular players in these phases. Additionally, I will discuss the current standards of care used to treat chronic wounds. Finally, I will discuss the emerging technologies that are being explored to improve clinical outcomes of patients with non-healing wounds.

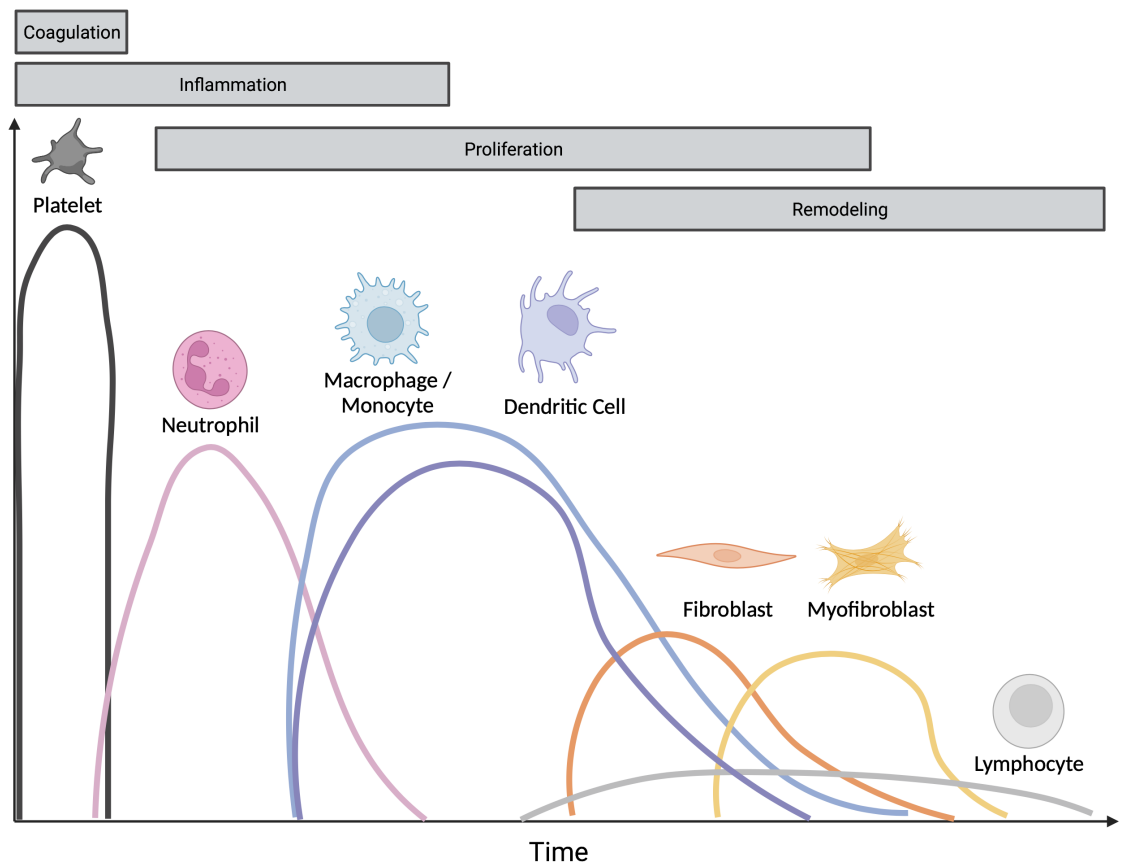


Figure 1.1: Schematic of Cellular Infiltrates During Wound Healing. Adapted from Guillamat-Prats, 2021

### 1.1.1 Phase I: Hemostasis

When damage is incurred to the skin, hemostasis is the first step in the multi-step process of restoring skin integrity. This first phase wound healing is highly conserved in many species through a range of organism complexity, indicating its importance to survival [6]. Hemostasis enables damage-management through the closure off damaged blood vessels, preventing exceptional blood loss. These processes are initiated upon vessel damage, when platelets will adhere to the damaged site through a variety of interactions [7]. These interactions stem from two major pathways of initiation to clot formation - the extrinsic system that

stems from the injured skin tissue itself and the intrinsic system through the activation and aggregation of thrombocytes by exposed collagen. These two pathways converge to form the common pathway at the point of factor X. Factor X is activated to factor Xa - which goes on to activate factor II (prothrombin) and on to factor IIa (thrombin). Thrombin is then generated and converts fibrinogen into fibrin. Thrombin also activates other factors in the intrinsic pathway - creating a positive feedback loop creating more fibrin [8]. This creation of fibrin ultimately resulting in a polymerized fibrin clot [7, 9]. This clot, stops bleeding, releases growth factors such as transforming growth factor- $\beta$  (TGF- $\beta$ ) and epidermal growth factor (EGF), as well as provides a preliminary scaffold for infiltrating cells to repair damage as the wound moves into the next phase of healing [10, 11].

### *1.1.2 Phase II: Inflammation*

Inflammation, often villainized, serves a crucial role in the wound healing process. Inflammation provides a means to alert cells to the damage incurred and recruit the necessary players to restore the barrier integrity of the skin. Inflammation of a wound is incurred through many different mechanisms. Increases of intracellular  $\text{Ca}^{2+}$  occur at the edges of the wound and propagate inward, production of reactive oxygen species (ROS) such as hydrogen peroxide, release of damage-associated molecular patterns (DAMPs) such as DNA, ECM components, and ATP, as well as the release of chemokines can serve as recruitment signals of inflammatory cells to the wound environment [11]. Neutrophils are often regarded as the 'first responders' cell type to the site of injury, and are not observed in healthy skin at homeostasis [12]. They are responsible for controlling infection and are capable of doing so through the release of toxic granules which produce an oxidative burst, initiating phagocytosis, and generate neutrophil extracellular traps (NETs) [13].

Monocytes are the next cellular recruit to the wound environment, they are recruited from the bone marrow, blood, and spleen upon tissue injury or infection as both effectors and

progenitors of macrophages and dendritic cells [14, 15, 16]. Both dendritic cells (DCs) and macrophages act as 'professional phagocytes' as they engulf apoptotic or necrotic neutrophils [17]. While macrophages are certainly better understood in the context of cutaneous skin repair it has recently been seen that enhancing efferocytosis in dendritic cells had a positive effect on wound healing capabilities in both healthy and diabetic wounds [18]. These findings point to a clear participation of DCs in clearing apoptotic debris following cutaneous skin injury, adding both a new lens to how the wound healing process works as well as a new potential point of intervention for treatment of non-healing wounds.

The cellular recruitment dynamics within a wound are complex and many unknowns persist, but in healthy wounds it is known that macrophages peak at around day three post injury after being recruited through soluble factors as monocytes [19]. These macrophages then in turn recruit more monocytes through secretion of chemokines such as CCL2 [20, 21, 22]. Based on the milieu present in the wound microenvironment macrophages can be polarized on a spectrum of phenotypes, ranging from inflammatory (coined M1 or M1-like macrophages) to anti-inflammatory/pro-regenerative (coined M2 or M2-like macrophages) [19, 23, 24]. These different macrophage phenotypes serve different functions and produce different soluble factors, further influencing the milieu present in the wound microenvironment. It is thought that in the transition from the inflammatory phase of wound healing into the proliferative phase, macrophages in the wound microenvironment transition from the M1 phenotype to the M2 phenotype [25, 26]. The macrophage population in the wound begins to decrease around day five post injury, reaching near-baseline levels ten days post injury [27]. Other immune cells such as T cells and mast cells also play a role in wound healing, though their role is not as well characterized when compared to neutrophils and macrophages, as well as dendritic cells which are becoming more well understood. [28, 29].

### *1.1.3 Phase III: Proliferation*

As the inflammation in the wound resolves, the proliferation phase begins. This phase of healing consists of three main components: re-establishing vascular channels (angiogenesis), generating granulation tissue, and re-epithelializing the wound surface [30]. Formation of blood vasculature is crucial to the repair of tissue, as without vasculature the wound bed cannot receive proper oxygenation and nutrition [31]. Angiogenesis is primarily facilitated through the M2 macrophage cell subset and the secretion of angiogenic factors such as VEGF-A [32, 33, 34]. The newly formed vasculature runs through temporary stromal framework, the granulation tissue. Mainly formed by activated infiltrating immune cells such as macrophages as well as fibroblasts, the granulation tissue also serves as a scaffold for other cells and newly synthesized ECM components [35]. Finally, re-epithelialization constitutes the last component of the proliferation phase of wound healing. The primary cell populations responsible for re-epithelialization are keratinocytes and fibroblasts, both of which are influenced by soluble factors [36, 37, 38]. Keratinocytes communicate with fibroblasts to secrete many signals that potentiate tissue repair, for example IL-6 produced by fibroblasts and acts on keratinocytes when sequestered has been shown to decrease angiogenesis and collagen deposition [39, 40]. These signals in turn induce collagen production by the fibroblasts, rebuilding the damaged ECM of the wound with temporary Type III collagen that is replaced with Type I collagen in the final phase of healing [41].

### *1.1.4 Phase IV: Remodeling*

Though the wound is closed in terms of barrier function after the proliferative stage, there is more to be done to restore the maturity of the repaired tissue. The collagen III produced in the proliferative phase of healing is replaced with collagen I, which is much stronger due to its more organized alignment [42, 35]. The remodeling phase of wound healing is also where scar formation occurs. This phase of wound healing is where fibrosis can occur, if fibroblasts

do not display the proper "eat me" signals to macrophages they are capable of depositing excessive matrix components and cause scarring [11]. Additionally, during the remodelling phase of healing leaky blood vessels that were formed during angiogenesis are pruned - in order to form stable and well-perfused blood vessels that can maintain homeostasis [43]. This is done through the release of 'anti-angiogenic factors' that can modulate the responsiveness to VEGFs [44, 45, 11]. One example is CXCL10, which when bound to its receptor CXCR3 (found on endothelial cells) inhibits endothelial tube formation. This process is important as it has been found without this negative regulation of angiogenesis hypertrophic scarring occurs [46]. Healed skin tissue does not return to its pre-damaged strength though, and even after remodelling is complete the skin is only 80% as strong when compared to its pre-injury tensile strength [47].

### *1.1.5 How the Diabetic Disease State Impacts Wound Healing*

Many aspects of the tightly controlled wound healing process are perturbed within the diabetic disease state. These perturbations are multifaceted and intertwined; high blood sugar can cause immune dysfunction impacting the soluble signals present that direct wound closure [48]. When these signals are not regulated, cellular infiltrates become disorganized and the progression between phases of wound healing is hampered, ultimately leading to a non-healing wound [19, 28, 49, 50]. In particular, the transition between the inflammatory phase into the proliferative phase is cited as the primary point of dysfunction within a chronic, diabetic wound [26]. Elevated levels of proinflammatory cytokines even in unwounded diabetic skin, blunts the functionality of the acute inflammatory response that signals for the recruitment of immune cell infiltrates such as neutrophils and macrophages upon tissue injury [51, 52]. The chronic low-grade inflammation associated with diabetes instead numbs the immune system to these inflammatory signals and thus there is a baseline inflammatory signature associated with the diabetic wound, that ultimately proves to be nonproductive

inflammation [51]. The dysfunction created by the hampered recruitment of cells, and the chronically inflamed milieu in turn prevent the proliferation of keratinocytes, fibroblasts, and endothelial cells which prevent re-epithelialization and angiogenesis [53].

An example of a perturbation in soluble signal that impacts cellular recruitment and phenotype is the 'pro-inflammatory' chemokine CCL2 (MCP-1). CCL2 is a well known macrophage recruitment signal and it has been successfully used in mouse models of diabetic wounds to restore this blunted macrophage response [54]. The findings of this study demonstrate that the diabetic wound exhibits a significant delay in macrophage infiltration that was the result of reduced CCL2 expression and when CCL2 was applied to the wound the macrophage response could be restored. This study very clearly supports the growing paradigm shift that the diabetic might not be 'hyper-inflamed' but rather the chronic inflammation experienced by the diabetic wound desensitizes the environment - preventing the important role of inflammation to be carried out [51]. This decrease in macrophages in the wound environment prevents them to carry out their function of phagocytosis - increasing the apoptotic burden in the wound and allowing the inflammatory signals present to linger while serving little functional purpose [52, 55, 56]. Beyond CCL2, other members of the 'CC-chemokine' family are expressed in the wound environment upon injury and impacted by the diabetic disease state. CCL3 and CCL4 also are known macrophage chemoattractants and their disruption could further contribute to the hindered macrophage infiltration seen in the diabetic wound [22]. 'CC-chemokines' are not the only signals that impact macrophage recruitment and development within the wound.

Another soluble signal of note is granulocyte-macrophage colony-stimulating factor (GM-CSF), which can act on both myeloids (monocytes/macrophages/granulocytes) as well as DCs, and has been shown to have decreased expression in diabetic skin [57, 58]. When externally supplemented GM-CSF has a positive effect on diabetic wound closure through increased re-epithelialization and collagen deposition [59, 60, 61]. These signals are crucial

for the initial recruitment of myeloid cells to the wound environment so that they can carry out their subsequent function of phagocytosis, ECM deposition and move the wound out of inflammation into the proliferative phase of healing. While this burst of recruitment to the wound is important - prolonged residence of these cells can also be problematic. It has been seen that while diabetic wounds show lower macrophage counts early on in the process, they are more abundant in late stage wounds - which could also contribute to prolonged ROS production and inflammatory cytokine signalling [62]. Additionally, the formation of blood and lymph vessels is hindered by this macrophage deregulation - further hindering the re-epithelialization of the tissue [56].

Macrophages are not the only cellular population that is impacted by the diabetic disease state, multiple myeloid cells are perturbed including dendritic cells. Prior to wounding, healthy skin shows significantly more DCs when compared to diabetic skin - setting the stage for an unbalanced response upon injury [62]. Within the subsets of DCs there are further differences between healthy and diabetic wounds - there are significantly fewer cDC1s and cDC2s from day 5 post injury onward in the diabetic skin. Dendritic cells are also professional phagocytes and seeing fewer of them could also impact the apoptotic load present in the wound environment. Their presence in the late stage of wound healing in healthy mice also point to a function in the proliferative and remodelling phases of tissue repair - though this branch of work is still in its infancy.

The immune cells discussed do not operate in a vacuum though and their presence and the signals they secrete impact other cellular populations present in the wound. The two cell types most closely tied with restoration of the cutaneous epithelial barrier, keratinocytes and fibroblasts, are responsive to the signals in the wound microenvironment produced by immune cells. Keratinocytes respond to many soluble factors and produce soluble factors as a result of the signals they receive - for example keratinocytes are producers of CCL2 [63]. One factor in particular associated with induction of keratinocyte proliferation is IL-6 [64]. IL-6

is seen to be increased in the plasma and wound tissue of diabetic patients and often viewed as an exacerbating factor in the non-healing diabetic wound setting; though its removal from *in vivo* knockout models show delayed healing [65]. Interestingly, looking immediately after injury the increase from baseline expression in IL-6 is significantly less in diabetic wounds when compared to non-diabetic wounds - again pointing to the delicate balance in magnitude and temporal control of the wound microenvironment milieu of soluble signals [66]. This finding further supports the notion of a numbed/blunted inflammatory response leading to prolonged non-productive inflammation in the diabetic wound as opposed to a hyper-inflamed stance.

These changes, while non-exhaustive, represent multiple points of potential intervention for the treatment of non-healing wounds. Additionally, these perturbations depict a complex web of cooperating signals that are highly context dependent, it is challenging to think about any one of these signals as 'good' or 'bad' or associate 'anti-inflammatory' with being strictly positive and 'pro-inflammatory' as strictly negative in the diabetic wound. In reality, these signals have functions that when diminished or prolonged in excess can be detrimental to the wound healing as a whole. As the paradigm towards the context-dependent nature of these signals and how these perturbations are related to one another and the cellular network that exists between them are better understood the opportunity for more innovative therapies become possible.

## **1.2 Current Standards of Care in Diabetic Wound Healing**

There has been minimal advancement in the standard of care for the treatment of chronic diabetic wounds [67]. The current standard of care relies mainly on nonspecific local wound care, not addressing the root causes underlying non-healing wounds. The treatments that do exist can be broken into three broad categories: physical measures, dressings, and growth factors. While some therapeutics cross the boundaries between these categories, most fall

squarely within one of these descriptions. All of these treatment, or the use of these treatments in concert, are addressing the six main areas of diabetic control: mechanical control, wound control, microbiological control, vascular control, metabolic control, and patient education [68]. The inadequacy of these treatments can be seen through the tremendously high lower-extremity amputation (LEA) rates of diabetic patients. This diabetic patient population constitutes 65% of the LEA patient population [69, 70]. This gap in clinical care presents the need for better treatment strategies and therapeutics for use in improving the healing of chronic diabetic wounds.

### *1.2.1 Physical Measures*

The primary 'physical measures' treatment strategies include surgical debridement and wound offloading. Surgical debridement consists of the removal of any callus which may surround the ulcer and any devitalised tissue within its margins [68]. The removal of this dead tissue is important to prevent infection and puts the wound back into an acutely injured state presenting the opportunity for improved healing allowing for new cellular migration and the formation of granulation tissue [71]. While surgical debridement is the primary form of this treatment there are other methods that have been used to clear the wound bed of necrotic tissue. For example, enzymatic debridement utilizes exogenous enzymes that digest the nonviable tissue is one example of this [72]. Debridement, while a central tenant of diabetic wound care, is invasive, painful, and must occur with frequency in order to be successful; all of these factors negatively impact the patient's quality of life. There are mixed analysis of the wound closure rate of any form of wound debridement over a control - demonstrating marginal success of debridement as a strategy for the closure of diabetic wounds and prevention of infection and amputation [73].

Often paired with debridement, or any treatment for the closure of diabetic foot ulcers, is wound offloading. Wound offloading is the practice of relieving pressure from the wound to

promote healing and prevent further damage from occurring [74]. Studies using total contact casts show compelling evidence of benefit of this strategy - depicting that neuropathic ulcers that had not healed for months or years healed within 6 weeks in a total contact cast [75]. Though healing in the general clinic is far less effective with the main cause being cited as poor patient compliance, especially with removable off-loading devices, where only 28% of patients wore their offloading device during daily activities [76].

Many other approaches have been implemented to aid healing of chronic diabetic wounds such as hyperbaric oxygen therapy (HBO) where there have been conflicting reports of efficacy [77, 78, 79]. When efficacy was seen with this therapeutic strategy, it was in the short-term and did not significantly improved major amputation rates patients with diabetic foot ulcers [79]. Low Level Laser Therapy (LLLT) is a newer means of treating DFUs that has more aligned results, showing that it can be an effective modality for treatment of non-healing wounds [80]. Ultimately, these treatment modalities have mixed results in terms of their efficacy and require consistent treatment at a specialized clinic, another factor impacting poor patient compliance [81]. Debridement and wound offloading will likely remain mainstays in the treatment strategy of DFUs and used in conjunction with emerging treatments and technologies.

### *1.2.2 Dressings*

Dressings are used to maintain a moist and clean environment for the wound and are considered another core component of the treatment of non-healing diabetic wounds [74, 82, 83]. There are many subclasses of dressing whose properties are intended to match the characteristics of the patient's ulcer [82]. The four main categories of wound dressing are hydrocolloids, hydrogels, foams, and films. Hydrocolloids are proficient at absorbing wound fluids and maintaining moisture in the wound bed while still being semi-permeable to water and oxygen. This dressing type is used on granulating and epithelializing wounds but not in wounds

that are potentially infected and highly exuding [84, 82]. Hydrogels are similar to hydrocolloids as they also are used predominately to maintain highly moist wound environments while still being permeable to water, oxygen and metabolites [85]. A particular advantage to hydrogels as a dressing is their flexibility and their ability to applied and removed with little interference to the wound bed [84, 82]. Foam dressings are used as an alternative to hydrogel and hydrocolloid dressings and used primarily in wounds with high levels of exudate. Lastly film dressings are an impermeable covering that are used on wounds of little exudate; whose function is primarily for protection instead of promotion of healing [84, 82]. In recent years dressing have been designed to deliver living cells or soluble signals to the wound environment, referred to as 'biologically active wound dressing', in an effort to further increase the benefit of dressing application [86].

### *1.2.3 Growth Factors*

Growth factors are another class of soluble mediators of cellular communication and function. Their development as therapeutics has provided the field with a new approach in treating DFUs. With this approach came new approved treatments for improving non-healing diabetic wounds, most notably becaplermin (Regranex) a recombinant human platelet-derived growth factor (rhPDGF) [87]. Yet, becaplermin's use in clinic is limited due to its moderate efficacy. Other growth factors have been used in clinical trials (e.g. VEGF and TGF- $\beta$ ) but have shown less success than rhPDGF [88, 89].

Topical cell therapy is another clinically relevant methodology for the treatment of non-healing diabetic wounds, though its successes are also convoluted and limited [89, 88]. Dermagraft and Apligraf are clinically approved cell based therapies composed of human fibroblasts or fibroblasts and keratinocytes, respectively [90, 91]. These therapeutics are expensive, and like many treatment strategies for non-healing diabetic wounds the proportion of non-responding patients and recurrence remains high - continuing to demonstrate the need for

new innovation in the field [89].

#### *1.2.4 Emerging Technologies for the Treatment of Non-Healing Diabetic Wounds*

Innovation in the treatment of non-healing diabetic wounds has remained a field of interest for decades, but with little clinical success, as previously discussed. As the pathophysiology of the diabetic wound environment continues to be better understood therapeutic intervention is able to better address the underlying causes of the non-healing wound (i.e. previously, inflammation in the diabetic wound was viewed only as harmful, now a short spike in acute inflammation is being considered beneficial to move the wound into the next phase of healing, as discussed previously). The basis for treatment of the diabetic wound will remain, but new approaches and targets can improve their efficacy. An example of this is the work being done in the field of cytokine and growth factor engineering. Cytokines and growth factors play crucial roles in the orchestration of the wound repair response, but as noted their success clinically is limited - thus engineering strategies have been applied to these soluble molecules (coined immunoengineering) to improve their delivery and pharmacologic profile to further their clinical impact [92, 93].

Polymeric materials have also gained notoriety over the years for the treatment of diabetic wounds, and like growth factor engineering new polymeric payloads have been developed based upon better understanding the nuances of the diabetic wound microenvironment. Even beyond direct payload delivery, polymers that modulate the microenvironment themselves have been designed. It has been shown that polymeric microparticles decorated with 'cell-instructive surface chemistry' were able to induce fibroblast proliferation and subsequently improve closure in the db/db mouse model [94]. This strategy is promising from a transnational perspective as biologic based therapeutics typically have more constraints surrounding them in terms of production, storage, and delivery; whereas polymers tend to

be more robust in these aspects.

In addition to new therapeutic innovations, continued steps must be taken to improve early detection and intervention of diabetic wounds. Additionally, the physical interventions that are currently used will likely not become obsolete upon approval of improved pharmacotherapies. Thus, improvement of efficacy and patient compliance should be of focus as well for the time being.

# CHAPTER 2

## TOPICALLY APPLIED COLLAGEN-BINDING SERUM ALBUMIN FUSED IL-4 FOR THE TREATMENT OF DIABETIC WOUNDS

### 2.1 Abstract

Non-healing wounds, often in the form of diabetic foot ulcers, have a negative impact on quality of life and account for many cases of amputation and even early death among diabetic patients. Despite the significant clinical demand, treatment with biologics has not broadly impacted clinical care. Interleukin-4 (IL-4) is a potent modulator of the immune system, capable of skewing macrophages towards a pro-regeneration phenotype (M2) and promoting angiogenesis but can be toxic after frequent administration and is limited by its short half-life and low bioavailability. Here, we demonstrate the design and characterization of an engineered recombinant interleukin-4 construct. We utilize this collagen-binding, serum albumin-fused IL-4 variant (CBD-SA-IL-4) delivered in a hyaluronic acid (HA)-based gel for localized application of IL-4 to dermal wounds in the type 2 diabetic mouse model, known for poor healing. Our studies indicate that CBD-SA-IL-4 is retained within the wound and can modulate the wound microenvironment through induction of M2 macrophages and angiogenesis. CBD-SA-IL-4 treatment significantly promoted wound healing compared to native IL-4 and HA vehicle treatment without inducing systemic side effects. This CBD-SA-IL-4 construct may be clinically useful by addressing the underlying immune dysfunction present in the chronic diabetic wound, leading to more effective tissue regeneration.

## 2.2 Introduction

Diabetes Mellitus (“diabetes”) is one of the leading causes of death in the United States [95]. Beyond mortality, there are many complications that are often associated with diabetes, one of which is an impaired ability to heal [96]. This most often manifests in wounds on the lower extremities (i.e., ulceration in the feet) and is often a result of loss of sensation in the extremities, known as diabetic peripheral neuropathy [97][98]. Incomplete wound healing, especially within the context of diabetes, is a problem that has substantial work surrounding it but lacks a satisfying solution due to low success rate of the current standard of care, such as wound offloading, surgical debridement, infection management, and revascularization therapy [67]. These non-healing wounds, if not cared for properly or if the ulcerations ultimately do not heal, can lead to amputation of lower extremities, a procedure for which diabetic patients make up 65% of the patient population [69, 70].

Healthy wound healing is a complex and well-orchestrated process that depends on the initiation and cessation of multiple signals as the wound environment moves through each phase of healing [22, 35, 49, 99]. The first phase includes initial coagulation to stop bleeding followed by inflammation which serves to clear invading bacteria via neutrophil infiltration and clearing subsequent apoptotic debris through macrophage-mediated phagocytosis [100][101]. After the wound bed is clear of debris, the wound can progress to the proliferative and remodeling phases, in which blood vessel formation and extracellular matrix (ECM) deposition occur [26]. Many components of the diabetic wound are highly dysfunctional and stray from this path in many ways, one of which is an altered immune profile [102] [103][104]. For example, non-healing diabetic wounds exhibit both decreased and delayed neutrophil and macrophage recruitment, creating a non-productive inflammatory environment, where the inflammatory signals in the wound bed are insufficient to serve out their function and ultimately halt healing and create a chronic inflammatory environment [51]. One way this immune dysfunction is actualized is through the dysregulation of soluble cytokine signals

present within the milieu when compared to healthy, healing wounds [51]. These differences present the opportunity to treat chronic diabetic wounds through immunotherapy, specifically therapeutically administered immune cytokines to modulate the immune microenvironment within the dysfunctional diabetic wound and improve therapeutic outcomes through restoration of the healthy healing environment.

Growth factor therapy has been studied as a promising strategy to treat chronic, non-healing diabetic wounds but showed limited clinical utility due to safety concerns and suboptimal efficacy [49][105]. For example, recombinant human VEGF-A was in Phase II clinical trials, but improvement of diabetic foot ulcer healing was marginal after topical application [106][107]. Recombinant PDGF-BB showed promise in efficacy but has concerns regarding risk of cancer associated with its use [108][109]. Engineering strategies have been used to target these growth factors to the extracellular matrix (ECM), to minimize adverse effects when used to treat diabetic wounds [92][110]. In this fashion, but with an immune cytokine rather than a growth factor, we designed an IL-4 variant targeted to ECM in the diabetic wound microenvironment.

Interleukin-4 (IL-4) is a potent cytokine that has many functions and has garnered interest as a cytokine that can facilitate regeneration of many tissue types [111][112][113]. Interleukin-4, signals through the phosphorylation of STAT6, leading to downstream changes in target cell phenotype. One example of this is the polarization of macrophages away from the pro-inflammatory associated phenotype (M1) and towards a phenotype that promotes tissue healing (M2) [114][115]. This shift in macrophage phenotype is crucial for a wound to move from the inflammatory phase of wound healing onward to the ECM deposition and regeneration phase [24]. In the diabetic wound, the ratio between M1 and M2 macrophages is skewed towards M1 compared to healthy, healing skin [116]. Though macrophage activation states are considered to be more of a spectrum than a clear-cut line[117][118] this general categorization strategy is suitable within this context. This M1/M2 imbalance has

been recapitulated in a murine type 2 diabetic model (db/db), as db/db mice demonstrate reduced expression of M2-related genes such as Ym1 and Arg-1 and elevated expression of M1-related genes such as iNOS [116]. M2 macrophages are thought to potentiate wound repair through their secretion of anti-inflammatory cytokines, facilitation of blood vessel formation, and deposition of ECM [119][120][121]. These activation states carry over into human biology. In samples of chronic wounds from type 2 diabetic patients macrophages present in the wound resemble the classically activated M1 phenotype rather than pro-regenerative M2 macrophages [122][123][124][125]. This imbalance serves as an interesting target to promote wound healing by driving the phenotypic shift towards M2 macrophages in the diabetic wound microenvironment using IL-4. This strategy has been used in other models of chronic inflammation and showed a therapeutic effect in these models, but to our knowledge has not been used for the treatment of non-healing wounds [126]. Still, current difficulties for unmodified cytokines as therapeutics are primarily related to lack of efficacy due to their short-lived bioavailability due to quick clearance from the bloodstream and their off-target effects as many cytokines are considered pleiotropic meaning their effect is highly dependent on what other signals are present [127]. These features have limited the clinical translation of cytokines as therapeutics [128]. A cytokine engineering strategy that can leverage spatiotemporal control of immune cytokine signaling to enhance desirable effects would be significant and beneficial for the utilization of cytokines in the therapeutic context.

To address these concerns, we hypothesized that exposed collagen within the wound bed would make a suitable target for cytokine binding after local administration. Collagen is highly abundant in the dermal tissue as a primary component of the ECM and is highly exposed in a wound, making it a practical target [11][129]; as a collagen-binding domain (CBD), we fused the A3 domain of von Willebrand factor, which binds both collagen I and collagen III [130][131]. Further, serum albumin (SA), a well characterized and abundant protein in the body, was added to increase the molecular weight of the final construct to

improve retention within the hydrogel composition. Here, we show that IL-4 fused to both SA and the A3 domain, creating a CBD-SA-IL-4 recombinant protein, exhibits the desired spatiotemporal control when topically administered in a hyaluronic acid (HA)-based hydrogel and thus improved closure of a chronic diabetic wound.

## 2.3 Results

### 2.3.1 *CBD-SA-IL-4 Binds to Collagen, Induces M2 Macrophages in vitro, and is Retained Within Wounds in vivo*

We produced and purified CBD-SA-IL-4 recombinant fusion protein in mammalian cells and characterized it *in vitro*.

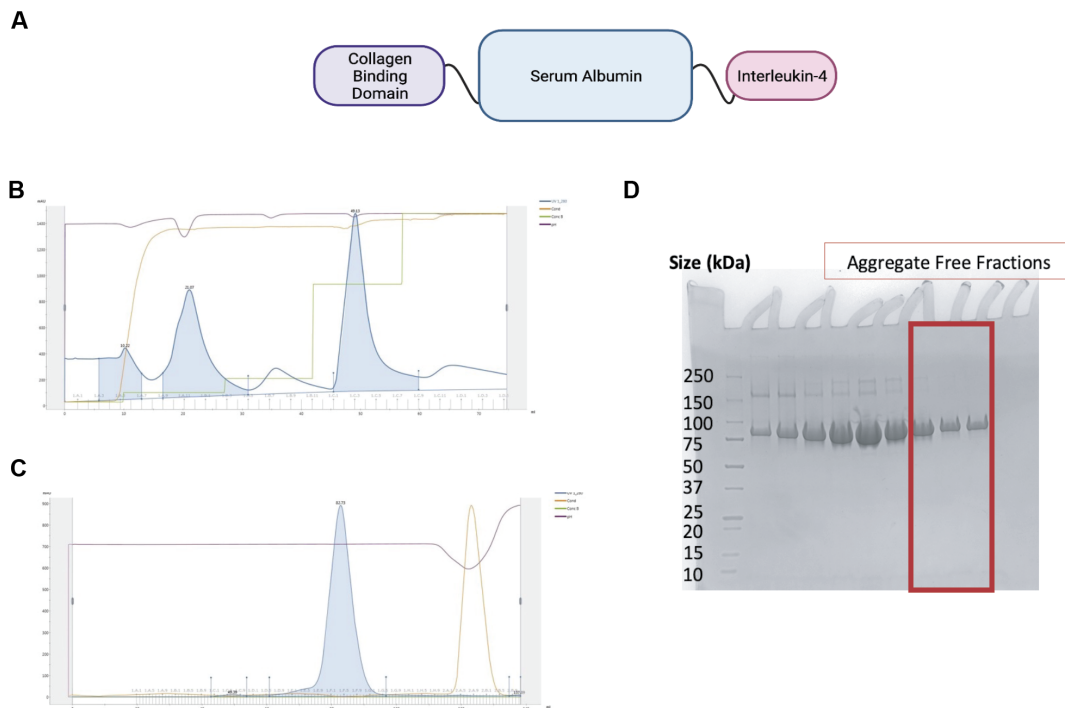


Figure 2.1: CBD-SA-IL-4 schematic and production. A) Schematic depicting composition of engineered IL-4 construct, flexible linkers are composed of (GGGS)<sub>2</sub> sequence. B) HIS-Trap purification trace. C) Size Exclusion Column (SEC) purification trace. D) SDS-Page demonstrating >90% purity in collected fractions.

Both WT IL-4 and the CBD-SA-IL-4 fusion protein bind the IL-4R $\alpha$  subunit with equal affinity. Additionally, like its wild type (WT) counterpart, CBD-SA-IL-4 induced phosphorylation of STAT6 in a dose-dependent manner, but with a resulting EC50 40-fold less than WT IL-4, likely due to steric effects (Fig. 2.2).

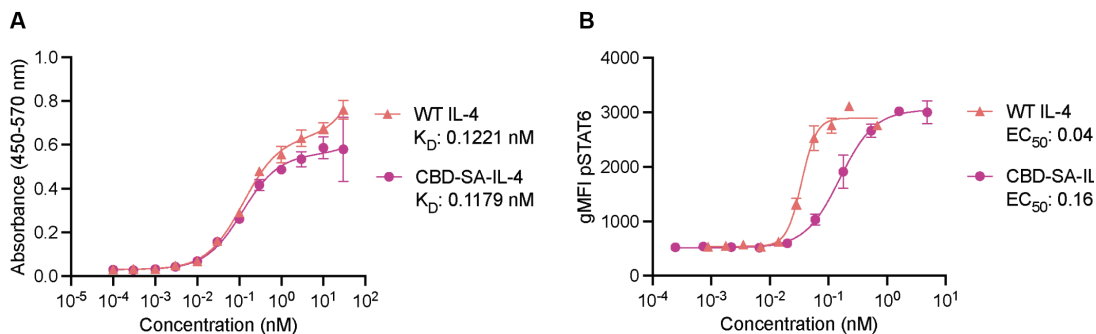


Figure 2.2: CBD-SA-IL-4 binds its receptor and signals through pSTAT6. A)ELISA using immobilized IL-4R $\alpha$ . KD values shown B)Dose-dependent signaling through STAT6 in RAW264.7 cell line with both WT IL-4 and engineered construct CBD-SA-IL-4. EC50 values shown.

Because IL-4 is known to induce an M2 phenotype in macrophages [132][133][134], we cultured RAW264.7 macrophage-like cells with CBD-SA-IL-4 and its wild type counterpart and found that CBD-SA-IL-4 and WT IL-4 similarly polarized macrophages toward the M2 phenotype, as demonstrated by an increase in Arg1+ cells. As a control for the M1 phenotype, we included lipopolysaccharide (LPS) in the experimental panel, which induced the upregulation of iNOS (Fig. 2.3).

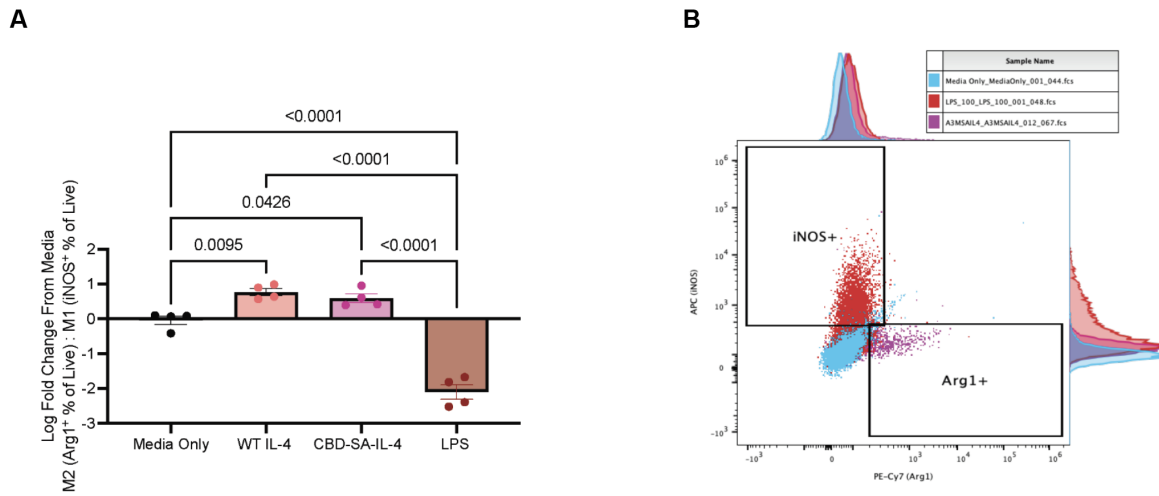


Figure 2.3: CBD-SA-IL-4 induces M2-like macrophage phenotype. A) Polarization of RAW264.7 macrophage-like cell line towards M2 phenotype (Arg1+) when treated with WT IL-4 or CBD-SA-IL-4 (65 ng/mL IL-4 equivalent) or M1 (iNOS+) when treated with LPS (50 ng/mL. B) Representative histogram for Arg1 and iNOS expression.

CBD-SA-IL-4 protein also demonstrated a high affinity for both collagen I and III, as quantified as the equilibrium dissociation constant determined via surface plasmon resonance (SPR), showing a  $K_d=8$  nM for collagen I and a  $K_d=37$  nM for collagen III (Fig. 2.4). The high binding affinity is on a similar order to that observed in our previous work with CBD fused to other cytokines.

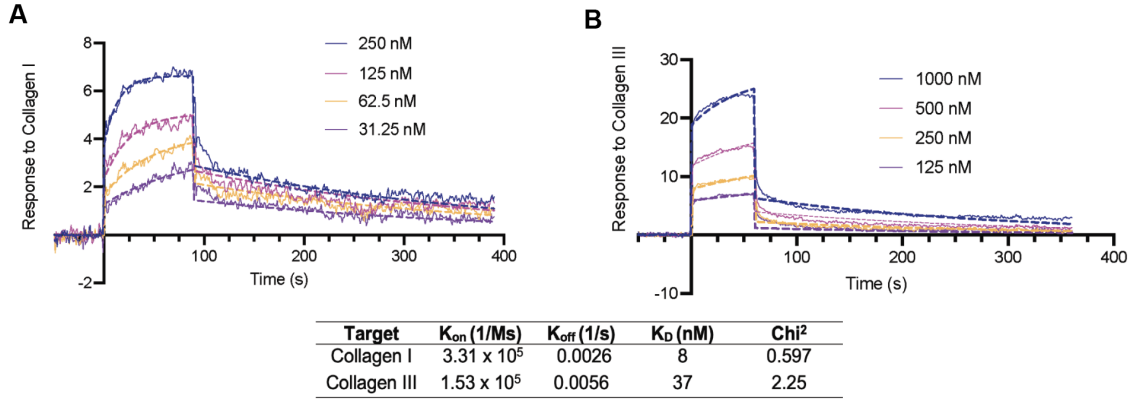


Figure 2.4: CBD-SA-IL-4 binds collagen I and collagen III. A,B) Affinities ( $K_D$  values are shown) of CBD-SA-IL-4 against collagen I and collagen III were measured by SPR. A SPR chip was functionalized with collagen I (A) or collagen III (B) and the engineered construct was flowed over the chip at indicated concentrations. Curves represent the specific responses in (RU) to each collagen observed. Experimental curves were fitted with Langmuir binding kinetics.

We then incorporated CBD-SA-IL-4 protein into a simple hydrogel that can be applied topically to the wound. HA is a well-studied, clinically used and biologically active polymer that has been shown to regulate tissue repair and is also considered safe; thus, we selected it to complement the effects of the CBD-SA-IL-4 [135][136][137][138]. We selected a 1% (w/v) composition of HA as our carrier based upon its desirable viscoelasticity that allowed easy topical application of the treatment without running out of the wound. Additionally, HA-based dressings have been used as carriers for cellular therapies such as autologous fibroblasts [139]. To understand the release of CBD-SA-IL-4 from the 1% HA gel in vivo, we wounded C57BL/6J mice and applied a 1% (w/v) HA gel containing either WT IL-4 or CBD-SA-IL-4. We collected blood at 0.5, 1, 4, 8, 12, and 24 hr to look for systemic IL-4, and we homogenized the wounds at 24 hr to look for IL-4 remaining in the treatment site (Fig. 2.5). We demonstrated that significantly less CBD-SA-IL-4 entered the systemic circulation when compared to the WT IL-4, as quantified by an IL-4 ELISA of the serum. Additionally, after 24 hr there was more IL-4 present in the wounds treated with CBD-SA-IL-4 when compared to the WT IL-4.

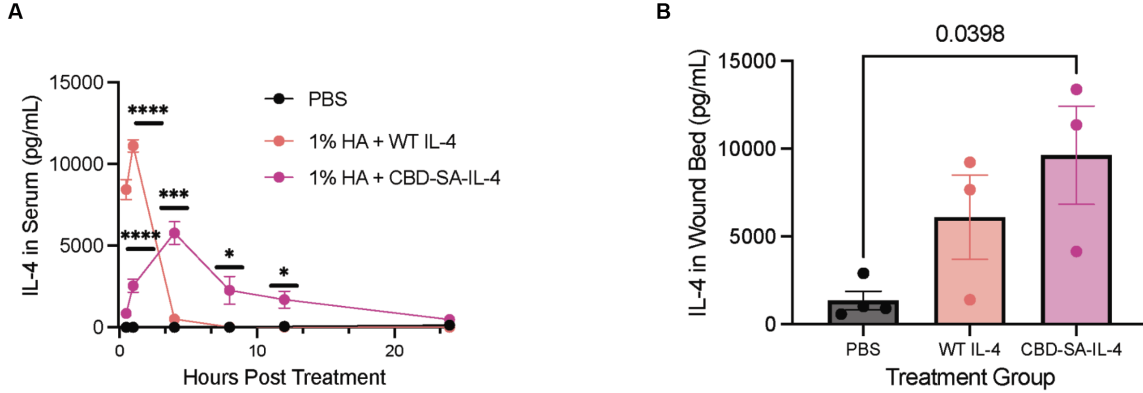


Figure 2.5: Pharmacokinetic of CBD-SA-IL-4. A) Release of CBD-SA-IL-4 or WT IL-4 (100  $\mu\text{g}/\text{mL}$  IL-4 equivalent) from 1% HA carrier after topical application in vivo, IL-4 concentration from serum timepoints quantified by IL-4 ELISA, using appropriate standard for each construct to account for binding differences. B) IL-4 content in the wound microenvironment quantified by IL-4 ELISA, using appropriate standard for each construct to account for binding differences 24 hr after treatment with IL-4 constructs containing HA gels in vivo.

These data show that the engineered CBD-SA-IL-4 construct displays slower systemic release kinetics compared to WT IL-4 (Fig. 2.5). The data also demonstrate that more CBD-SA-IL-4 is retained in the wound microenvironment as compared to WT IL-4, creating a localized effect while minimizing systemic exposure.

### 2.3.2 CBD-SA-IL-4 Therapy Promotes Diabetic Wound Healing

We tested a topically-delivered CBD-SA-IL-4 carried in a 1% (w/v) HA gel in PBS applied four days after surgically inflicted wounds in the type-2 diabetic db/db mouse, which is a well-established and clinically relevant model of impaired non-healing wound healing [92][140]. To more closely approximate human healing, we applied a silicone splint around each wound to prevent closure by skin contraction, the primary form of wound closure in mice but not humans. We compared four treatment groups: PBS, 1% HA, 1% HA + WT IL-4, and 1% HA + CBD-SA-IL-4. The PBS group represented an untreated wound, while the 1% HA group served as a carrier-only control, though due to its use in clinic already, we expected that it might help promote some healing due to the retention of moisture within the wound

environment. We also expected wounds treated with 1% HA + WT IL-4 to show improved healing, but due to its quick clearance and leakage into the periphery likely would be less clinically relevant than our localized engineered therapy. Wounds were excised and analyzed via H&E staining 11 days after wounding, thus 7 days after treatment. As a result, 1% HA + CBD-SA-IL-4 treatment significantly promoted reepithelialization when compared to the PBS-treated wounds (Fig. 2.6A). Strikingly, 56% of wounds treated with 1% HA + CBD-SA-IL-4 showed >90% reepithelialization. In contrast, only 18%, 32%, and 27% of PBS, 1% HA, and 1% HA + WT IL-4 treated wounds had reepithelialization above 90%, respectively (Fig. 2.6B). 1% HA or 1% HA + WT IL-4 did not enhance reepithelialization compared to PBS treatment.

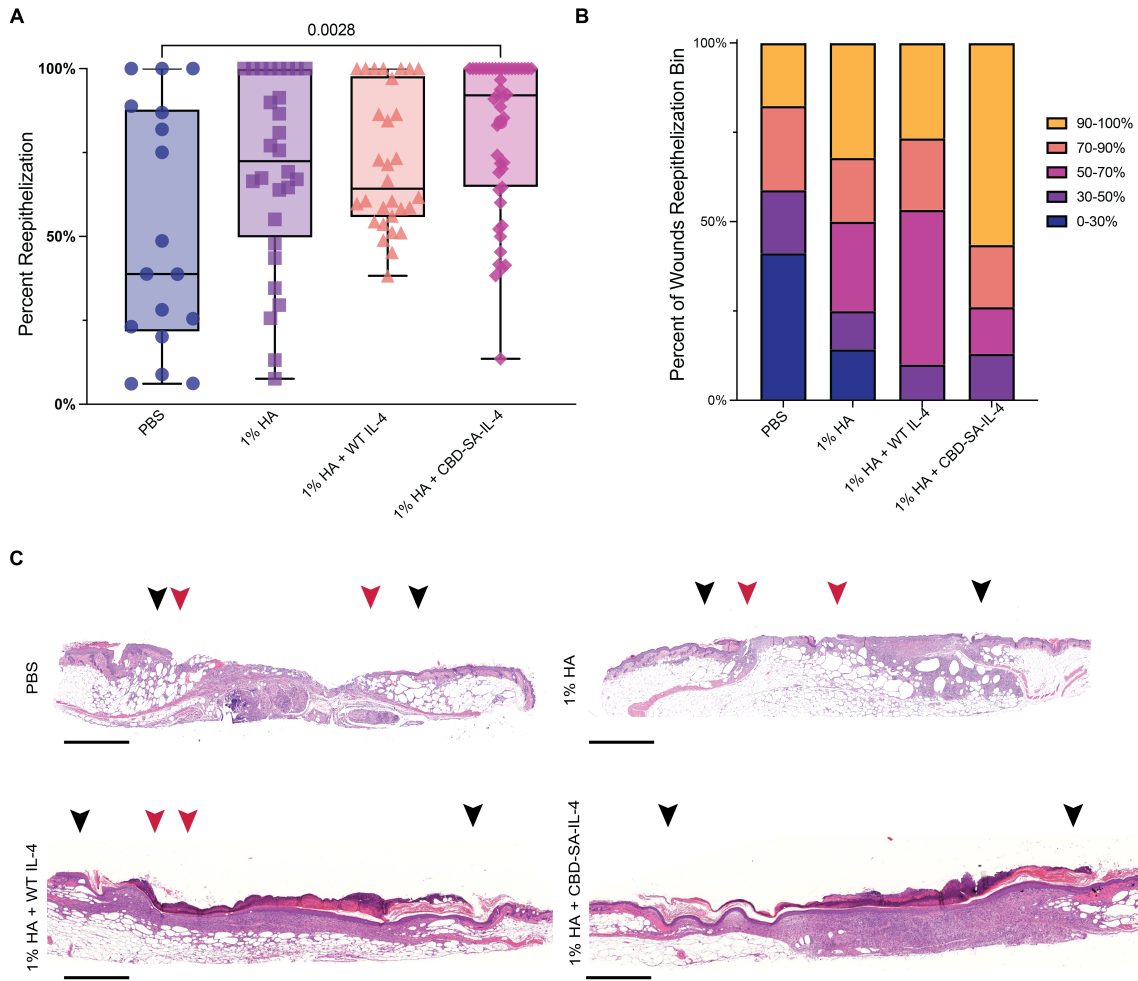


Figure 2.6: Topically applied 1% HA + CBD-SA-IL-4 enhances skin wound healing. Full-thickness back-skin wounds in 8-10-week-old C57BLKS/J-m/Lepr db (db/db) male mice treated with CBD-SA-IL-4 (100  $\mu\text{g}/\text{mL}$ ) or WT IL-4 (100  $\mu\text{g}/\text{mL}$ ). Four treatment groups were tested: PBS, 1% HA, 1% HA + WT IL-4, and 1% HA + CBD-SA-IL-4. After 11 days, A,B) extent of wound closure was evaluated by histology (PBS: n = 17, mean = 52.37%; 1% HA n = 28, mean = 69.90; 1% HA + WT IL-4 n = 30, mean = 71.87; 1% HA + CBD-SA-IL-4 n = 47, mean = 81.29). B) The wounds were binned based on percent closure after 11 days of healing (i.e. what percent of wounds were 90%-100% re-epithelized). C) Representative wound histology (hematoxylin and eosin staining) at day 11 (scale bar 800  $\mu\text{m}$ ). Black arrowheads indicate margin of wound and red arrowheads indicated the tips of epithelium tongue.

To further assess the degree of wound closure, granulation tissue area of these wounds was quantified. These results demonstrate increased granulation tissue formation in both IL-4 treated groups (Fig. 2.7A). Additionally, the reepithelialization seen in the H&E images was

recapitulated in cytokeratin 16 stained slides, further confirming the extent of reepithelialization (Fig. 2.7B-C)

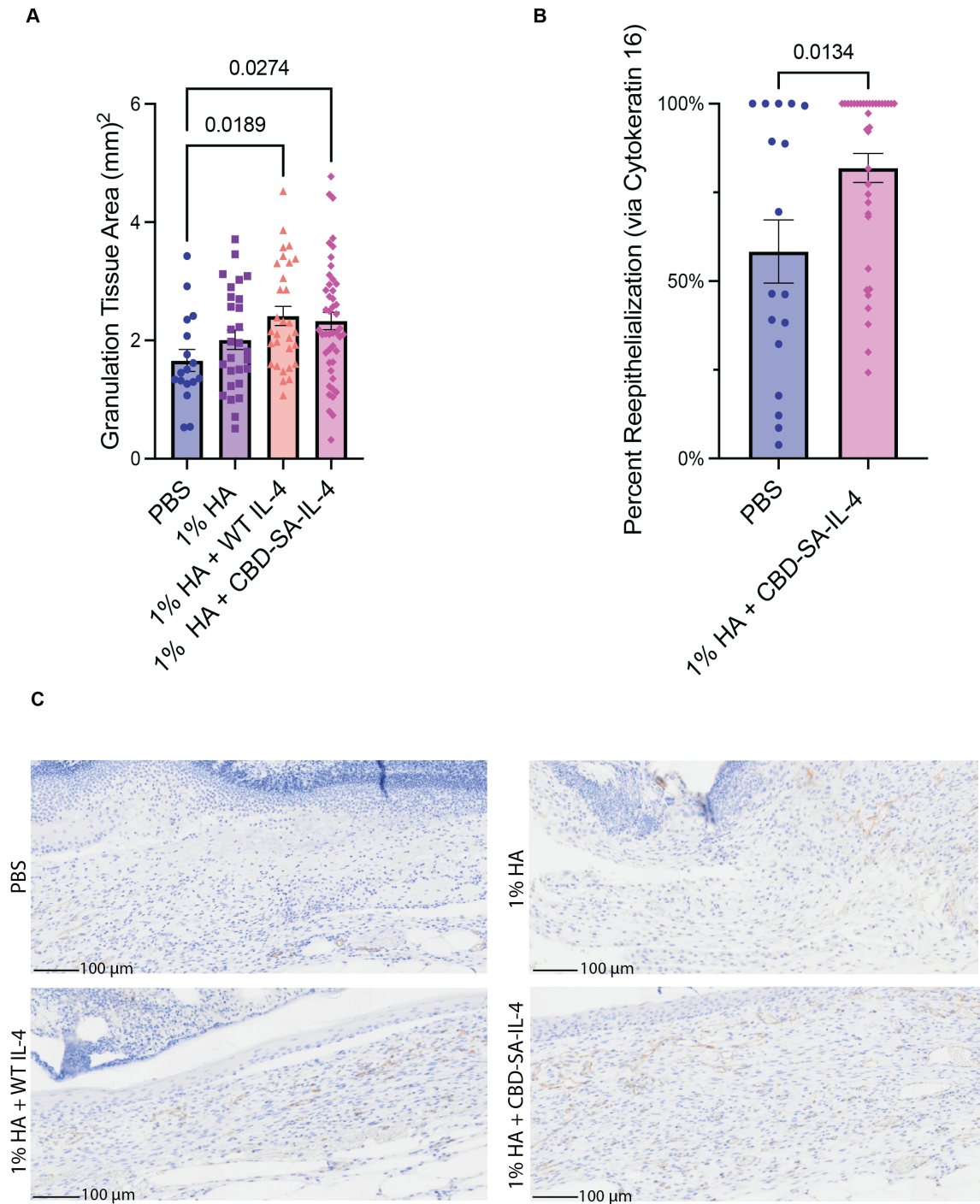


Figure 2.7: Topically applied 1% HA + CBD-SA-IL-4 enhances granulation tissue formation. A) Granulation tissue area quantification. B) Percent reepithelialization quantified through cytokeratin 16 IHC immunostaining. C) Representative cytokeratin 16 IHC immunostaining images for PBS and 1% HA + CBD-SA-IL-4.

These data indicate that the topical treatment of 1% HA + CBD-SA-IL-4 improves wound reepithelization when compared to the non-treated control, demonstrating that by modulating the signals present in the immune microenvironment of the wound, the dysregulation caused by the diabetic disease state can be modulated and therapeutic outcomes can be improved.

### *2.3.3 CBD-SA-IL-4 Induces Macrophage Recruitment to the Wound*

#### *Microenvironment Through Soluble Signals*

We next assessed the downstream mechanisms of action of CBD-SA-IL-4 on wound healing. We treated diabetic wounds following the same treatment timeline as above, excising wounds 24, 48, 72 and 96 hr post-treatment. After 24 hr, the wounds treated with either 1% HA and 1% HA + CBD-SA-IL-4 displayed significant decreases in both IFN- $\alpha$  and IFN- $\gamma$ , indicating lower levels of inflammation within the wound microenvironment (Fig. 2.8A-B). Moreover, only wounds treated with CBD-SA-IL-4 showed significantly increased levels of granulocyte-macrophage colony stimulating factor (GM-CSF) when compared to both PBS-treated wounds and 1% HA-treated wounds (Fig. 2.8C). GM-CSF is a crucial regulator of granulocyte and macrophage lineage populations [141] and promotes wounds healing [60]. Finally, CCL2, a chemoattractant for macrophages, demonstrated stark changes throughout all four timepoints, showing an initial increase at 24 and 48 hr (Fig. 2.8D) post-treatment, peaking at 72 hr, and finally returning to comparable levels to PBS-treated and 1% HA-treated wounds by 96 hr post-treatment (Fig. 2.8E). This marked difference in CCL2 secretion follows the dynamic process we would expect with healthy healing, where macrophage recruitment occurs initially but quickly subsides [142].

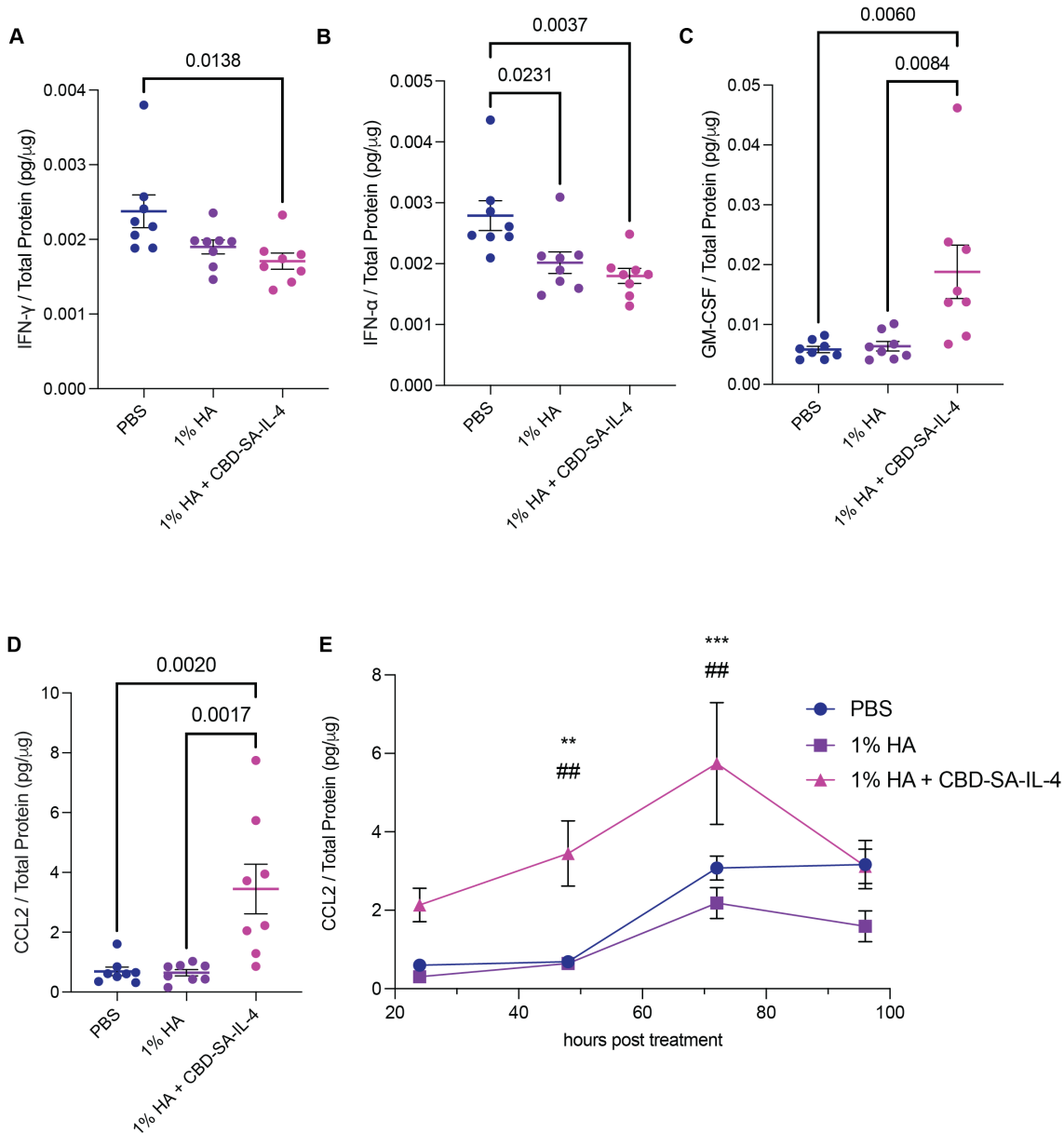


Figure 2.8: CBD-SA-IL-4 reduced inflammatory cytokines and induced regenerative cytokines/chemokines in the wounds. A)IFN- $\gamma$  concentration in the wound 24 hr post-treatment. B)IFN- $\alpha$  concentration in the wound 24 hr post-treatment. C)GM-CSF concentration in the wound 48 post-treatment. D)CCL2 concentration in the wound 48 hr post-treatment. E)Kinetics of CCL2 concentration from 24, 48, 72 and 96 hr post-treatment.

These data show that 1% HA + CBD-SA-IL-4 induces signals to recruit macrophages to the wound.

### *2.3.4 CBD-SA-IL-4 Treatment Increases M2 Macrophages and Pro-angiogenic Cell Populations in the Wound*

Because chemokine CCL2 expression was changed, we hypothesized that immune cell populations may have been altered by CBD-SA-IL-4 application. To understand how CBD-SA-IL-4 influences the cellular populations intra-wound, we treated diabetic wounds following the same treatment timeline as used previously, excising wounds 48 hr post-treatment and digesting them to create single cell suspensions for flow cytometric analysis. Through this, we saw that there was a marked decrease in surface IL-4R $\alpha$  expression on both CD45+ immune cells (Fig. 2.9A) and CD45- non-immune cells (Fig. 2.9B) cell populations in the 1% HA + CBD-SA-IL-4 treated group as compared to the control groups, suggesting internalization of the receptor after IL-4 binding, which is a well-documented step of IL-4 signaling [143][144]. 1% HA + CBD-SA-IL-4 increased Arg1+ expression on macrophages (F480+ CD11b+), indicating their M2 phenotypic polarization, which was not seen in either the PBS- or 1% HA-treated groups (Fig. 2.9C). These M2 macrophages showed increased Ki67+ expression, a marker of cellular proliferation, when treated with 1% HA + CBD-SA-IL-4 compared to PBS-treated wounds, supporting M2 macrophage proliferation in the wounds (Fig. 2.9D). Furthermore, these M2 macrophages were associated with formation of new blood vasculature within the wound, as demonstrated by the increase in CD31+ cells in wounds treated with 1% HA + CBD-SA-IL-4 (Fig. 2.9E).

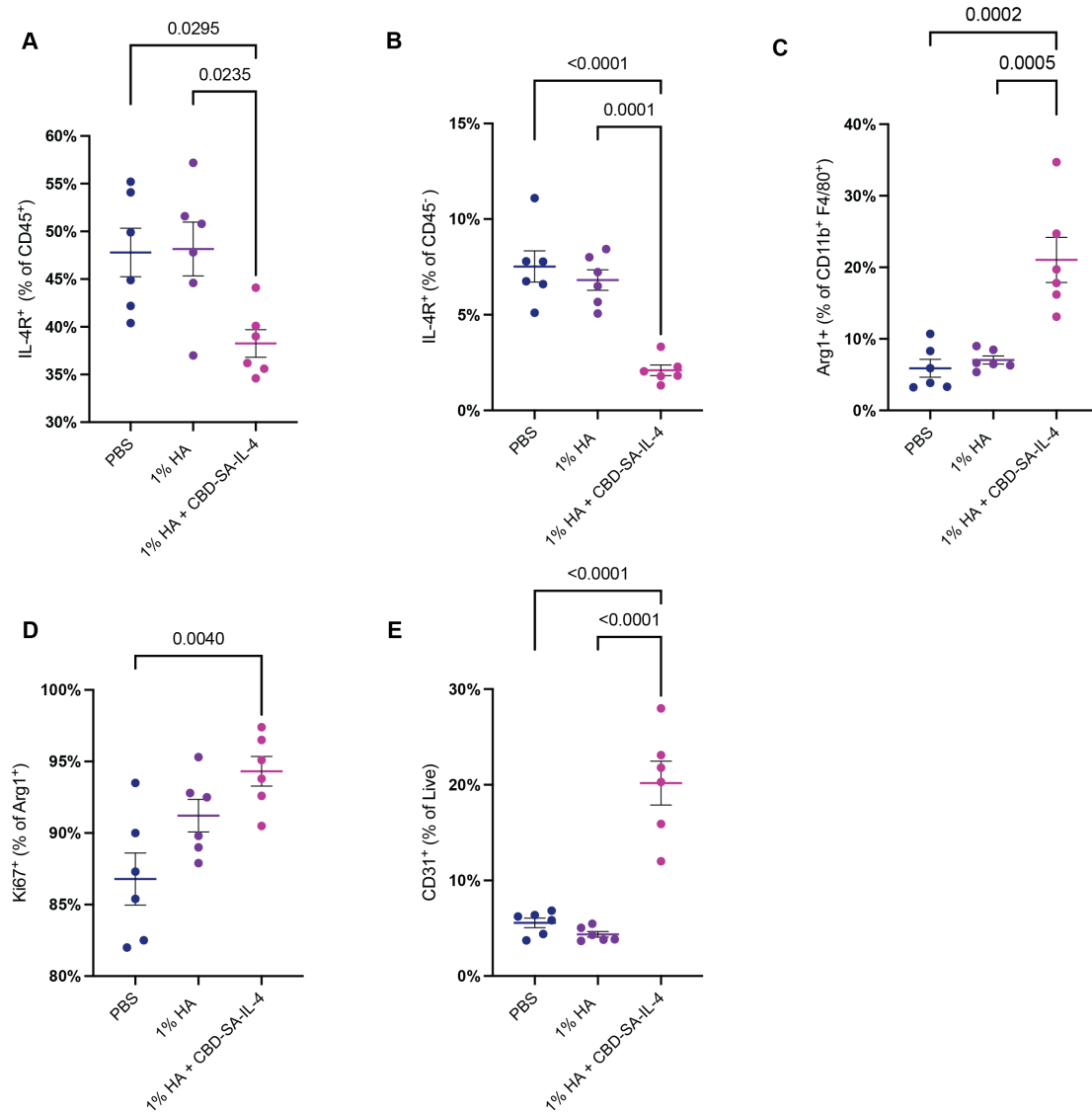


Figure 2.9: CBD-SA-IL-4 (100  $\mu\text{g}/\text{mL}$ ) induces M2 macrophage proliferation and angiogenesis in the wounds. A) IL-4R $\alpha$ <sup>+</sup> cells as a percent of CD45<sup>+</sup> cells. B) IL-4R $\alpha$ <sup>+</sup> cells as a percent of CD45<sup>-</sup> cells. C) M2 macrophages (Arg1<sup>+</sup>) as a percentage of total macrophages (CD11b<sup>+</sup> F4/80<sup>+</sup>). D) Proliferative (Ki67<sup>+</sup>) M2 macrophages as a percentage of total M2 macrophages. E) Angiogenic cells (CD31<sup>+</sup>) as a percentage of live cells.

These data show that 1% HA + CBD-SA-IL-4 modulates the cellular populations present within the wound environment and potentiates a more regenerative cellular phenotype.

### *2.3.5 Single Systemic Administration of CBD-SA-IL-4 did not Upregulate Toxicity Markers*

Due to concerns of toxicity associated with cytokine therapy, we sought to explore toxicity of the locally administered CBD-SA-IL-4. While based on our measurements, we do not expect the entire dose to be systemically exposure after topical administration, to ensure a lack of toxicity in this worst case we administered a full dose subcutaneously. After subcutaneous administration of CBD-SA-IL-4 and WT IL-4 we monitored the body weight of healthy, wild-type mice for 4 days and demonstrated no changes in body weight (Fig. 2.10A). We analyzed organ damage markers in serum using a biochemistry analyzer to test whether CBD-SA-IL-4 induced any adverse effects in the blood two days post treatment. Treatment with CBD-SA-IL-4 did not change levels of organ-damage markers (Fig. 2.10B-G). Treatment with CBD-SA-IL-4 and WT IL-4 did increase spleen weight (Fig. 2.10H). Neither treatment induced a change in B cell counts in the blood, a documented phenomenon associated with prolonged IL-4 administration [145].

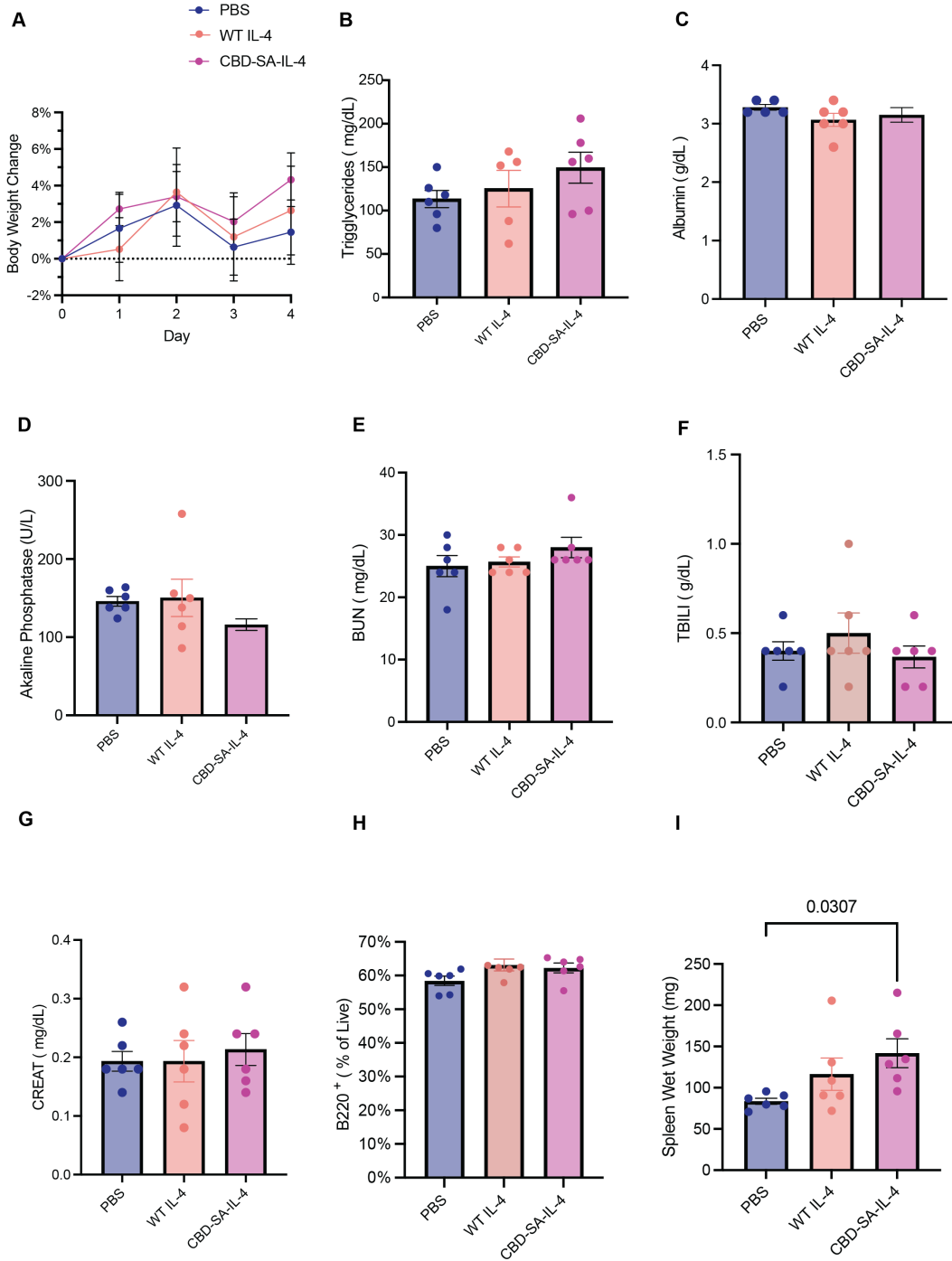


Figure 2.10: CBD-SA-IL-4 (100  $\mu$ g/ mL IL-4 equivalent) does not show toxicity after a single subcutaneous administration. A) Percent change in body weight. Measurements two days post administration (B-G) B) Serum triglyceride levels. C) Serum albumin levels. D) Serum alkaline phosphatase level. E) Serum blood urea nitrogen (BUN) levels. F) serum total bilirubin (TBILI) levels. G) Serum creatinine (CREAT) levels. H) B Cells (B220+) in blood. i) Spleen wet weight four days post-treatment.

These data suggest that CBD-SA-IL-4 is well-tolerated after a single, systemic dose of 32  $\mu\text{g}$ , reinforcing the safety of use at this concentration when applied topically to an open wound and systemic exposure is much less.

## 2.4 Discussion

Diabetic wound healing is a difficult clinical problem that lacks a satisfactory solution. Current treatments for non-healing diabetic wounds primarily focus on management strategies and do not address the underlying dysfunctional and poorly regulated signaling milieu of the immune system [146][147]. The continued release of proinflammatory cytokines within the wound stagnates its repair and keeps the environment in a non-productive inflammatory stage, preventing progression to proliferation and remodeling [148][149]. In normal wound tissue, there is an initial influx of immune cells, predominantly neutrophils and macrophages, and a subsequent resolution of these cells after debris has been cleared from the environment marked by a transition from M1 macrophages to M2 macrophages [150]. In the diabetic wound, the influx of these immune cells does not peak but rather plateaus, and inflammation remains insufficient to progress towards resolution [51][151][152].

CCL2 reportedly promotes healing in the diabetic wound through the restoration of the macrophage response. By pushing the wound environment out of the stagnant plateau of nonproductive inflammation it otherwise displays and by recruiting immune cells to the wound to clear debris and signal, the commencement of the subsequent phases [54]. The clear peak in CCL2 concentration within the wound microenvironment exhibited in the 1% HA + CBD-SA-IL-4 group indicates its ability to restore the influx of immune cells to achieve productive clearance of debris from the wound bed. Its subsequent decrease shows that this recruitment is resolved and does not continue, indicating the beginning of the resolution phase. Additionally, CCL2 has been shown to have angiogenic effects, and blocking CCL2 diminishes angiogenesis [153], further supporting the benefits of the induced CCL2 peak.

It has been demonstrated in diabetic patients that their chronic wounds displayed significantly less GM-CSF when compared to healthy controls [60]. Additionally, GM-CSF knockout mice demonstrate delayed wound healing, and it has been suggested that GM-CSF acts as keratinocyte proliferation inducer [59][154]. The significant increase of GM-CSF displayed in the 1% HA + CBD-SA-IL-4 further indicates that our treatment is acting to restore the healthy healing environment through recruitment and biasing of the M2 macrophage population to the wound.

The wounds treated with 1% HA + CBD-SA-IL-4 also had significantly less IFN- $\alpha$  and IFN- $\gamma$  when compared to the PBS treated wounds, demonstrating a suppression of general inflammation in the environment at 24-hr post treatment. The signals present in the 1% HA + CBD-SA-IL-4 thus demonstrate a molecular shift that could potentiate wound healing when compared to both the PBS and 1% HA treated groups.

The differences in molecular signals described above influence the changes in cellular phenotype we see between treatment groups, as demonstrated through flow cytometry of the wound tissue early in the healing trajectory. It has been shown in the literature that cytokine receptors are internalized after binding of their ligand, and this is the case for IL-4R $\alpha$  and IL-4. With this considered, our data show that IL-4 treatment is active and is acting on both CD45+ and CD45- cell populations. The wounds treated with 1% HA + CBD-SA-IL-4 also showed a striking increase in the frequency of M2 macrophages when compared to both the PBS-treated and 1% HA-treated groups. This strong increase in M2 macrophages indicates a shift caused by the 1% HA + CBD-SA-IL-4 towards a regenerative cellular phenotype. Additionally, 1% HA + CBD-SA-IL-4 treatment induces an increase in CD31+ cells within the wound, a population that has demonstrated the ability to induce blood vessel formation in disease models such as ischemic vascular disease [155]. This is especially pertinent in the healing of diabetic wounds where blood vessel formation is stunted, which is thought to be a main contributor to dysregulated healing [156]. It has also been shown that IL-4R $\alpha$  signaling

in myeloid cells directly controls collagen fibril assembly in the skin [119]. Overall, our data indicate that IL-4 treatment induces cellular changes that strongly indicate a pro-regenerative environment through polarization of macrophages and formation of blood vasculature, which ultimately result in improved collagen deposition and reepithelization.

Our design of CBD-SA-IL-4 is a novel approach for the topical treatment of non-healing diabetic wounds, utilizing the exposed collagen within a dermal wound as a target to potentiate a localized therapeutic effect. This therapy differs from other strategies previously used in the field by targeting immune cells directly, with the intention of modulating the dysregulated immune profile present in the diabetic disease state. Previous attempts in development of a topical therapy have focused on growth factor-based treatment, which are a downstream result of earlier signals present at large within the diabetic wound microenvironment [157]. Additionally, growth factor therapies have been associated with higher risk of cancer induction and have seen limited clinical success due to such safety and toxicity concerns [108][109]. Through the protein engineering strategies previously discussed, CBD-SA-IL-4 allows for a localized immunotherapy that minimizes off-target, systemic effects. Our toxicity analyses showed that treatment with CBD-SA-IL-4 is well-tolerated. Although we observed modest splenomegaly, this is typically transient and not considered as a critical toxicity; moreover, this was observed with subcutaneous administration as a surrogate for the worst-case of topical administration. Our topical IL-4 based therapy can thus potentially address a highly unmet clinical need of non-healing diabetic wounds, most commonly diabetic foot ulcers, where currently 30% of diabetic patients undergo amputation due to these non-healing wounds and, the 5-year overall survival rate following an amputation in diabetic patients is only 43% [158][159][160]. The therapy we describe here has the potential to address this large problem and prevent both the loss of limb and loss of life. In conclusion, here we show that our engineered IL-4 construct, CBD-SA-IL-4, can bind collagen in the diabetic wound microenvironment and, through the polarization of macrophages towards a

pro-regenerative M2 phenotype, can facilitate closure of a skin wound in the db/db mouse model of Type 2 diabetes.

## 2.5 Materials and Methods

**Cytokine Production and Purification** The sequence encoding for CBD-SA-IL-4 was synthesized and subcloned into the mammalian expression vector pcDNA3.1(+) by Genescript. A sequence encoding for 6 His was added at the N-terminus for affinity purification of the recombinant protein. Suspension-adapted HEK-293F cells were routinely maintained in serum-free FreeStyle 293 Medium (Gibco). On the day of the transfection, cells were inoculated into fresh media at a density of  $1 \times 10^6$  cells/mL. A total of  $1 \mu\text{g/mL}$  plasmid DNA,  $2 \mu\text{g/mL}$  linear 25-kDa polyethylenimine (Polysciences), and OptiPRO SFM media (4% final concentration, ThermoFischer) were sequentially added. The culture flask was agitated by orbital shaking at 135 rpm at  $37^\circ\text{C}$  in the presence of 5%  $\text{CO}_2$ . Six days after transfection, the cell culture medium was collected by centrifugation and filtered through a  $0.22 \mu\text{m}$  filter. Culture media was loaded into a HisTrap HP 5-mL column (GE Healthcare), using and ÄKTA Pure 25 instrument (GE Healthcare) as done previously<sup>47</sup>. After binding of the protein with binding buffer (20 nM  $\text{NaH}_2\text{PO}_4$ , 0.5 M NaCl, pH 7.4) protein was eluted with stepwise increases of 500 mM imidazole (in 20 nM  $\text{NaH}_2\text{PO}_4$ , 0.5 M NaCl, pH 7.4). The elution solution was further purified with size-exclusion chromatography using a HiLoad Superdex 200PG column (GE Healthcare). All purification steps were carried out at  $4^\circ\text{C}$ . The expression of cytokines was determined by a Nanodrop 2000 spectrophotometer. The proteins were verified as  $>90\%$  pure by SDS-PAGE and images acquired with ChemiDoc XRS+ system (Bio-Rad). Constructs were confirmed to be free of endotoxin via a TLR4-Blue reporter cell line (Invitrogen).

**Bioactivity** RAW264.7 macrophage cell line (ATCC) were plated in 96 well non-tissue treated U-bottom plates at a concentration of  $2 \times 10^6$  cell/mL and allowed to adhere

overnight. Stimulating media containing cytokine the construct was added in a serial dilution to the plate and incubated at 37°C for 15 min. Cells were dissociated from the plate using an ice-cold solution containing PBS, 1 mM EDTA, and 1 mM EGTA. Phosflow Lyse/Fix Buffer (BD Biosciences) was added to the plate and incubated at 37 °C for 10 min. The plate was centrifuged and washed with PBS before adding Perm III Buffer (BD Biosciences) and incubating on ice for 30 min. The plate was centrifuged and washed with a 2% FBS solution in PBS. To block non-selective binding, anti-CD16/32 antibody (BioLegend) was applied and incubated for 15 min at room temperature. In a solution of 2% FBS in PBS PE anti-pSTAT6 antibody (BD Biosciences, pY641) was added and incubated for 1 hr at room temperature. Cells were analyzed using a Fortessa (BD Biosciences) flow cytometer and FlowJo software (FlowJo, LLC). Gating strategies are shown in the Supplementary Fig 2.

**SPR** SPR measurements were performed as previously described[131] using a Biacore X100 SPR system (GE Healthcare). Collagen I or collagen III (EMD Millipore) was immobilized by amine coupling on a CM5 chip (GE Healthcare) for around 1,000 resonance units according to the manufacturer’s instructions. CBD–SA-IL-4 was flowed for 90 s (for collagen I) and 30 s (for collagen III) at increasing concentrations in the running buffer at 30  $\mu\text{l min}^{-1}$ . The sensor chip was regenerated with 50 mM NaOH for every cycle. Specific binding of CBD–SA-IL-4 to collagen was calculated automatically using the response to a non-functionalized channel as a reference. The binding curves were fitted using BIAevaluation (GE Healthcare). The binding results were fitted with Langmuir binding kinetics (1:1 binding with drifting baseline Rmax local).

**Macrophage Polarization** RAW 264.7 cells were plated at a concentration of  $2 \times 10^6$  cells/mL in a 96-well U-bottom plate and allowed to adhere overnight at 37°C. Cytokine-containing media was applied to the cells at a concentration of 65 ng/mL relative to IL-4 content and incubated for 24 hr at 37°C. Cells were dissociated using 1 mM EDTA and 1 mM

EGTA in PBS. Nonspecific binding was blocked using anti-CD16/32 antibody (BioLegend). Cells were stained intracellularly for iNOS (Invitrogen, APC,) and Arg1 (Invitrogen, PE-Cy7). The eBioscience Foxp3/Transcription Factor Staining Buffer Set kit was used and followed according to manufacturer's instructions (Invitrogen). Cells were analyzed using a Fortessa (BD Biosciences) flow cytometer and FlowJo software (FlowJo, LLC). Gating strategies are shown in the Supplementary Fig 3.

**Mouse skin chronic wound-healing model** Male C57BLKS/J-m/Lepr db (db/db) 8-10-week-old mice (The Jackson Laboratory) were used. Their backs were shaved and cleaned and four full-thickness punch-biopsy wounds (6 mm diameter) were created in each mouse. Each wound was splinted open using a silicone ring (inner diameter 8 mm, outer diameter 12 mm) to prevent contraction. Four days post-surgery, PBS, hydrogel only, or cytokine containing hydrogels (80  $\mu$ L in total, 100  $\mu$ g / mL IL-4 based concentration) were topically applied to the wounds. The wounds were covered with Adaptic dressing and sealed with adhesive film. Mice were single caged after the wounding surgery. After 11 days, mice were euthanized, and the skin wounds were carefully excised for histological analysis. All experiments using mice received approval from the Institutional Animal Use Committee of the University of Chicago under ACUP 72450. The animals' care was in accordance with institutional guidelines. This experiment was repeated a total of three times for a final sample size of PBS(n=17), 1% HA (n=28), 1% HA + WT IL-4 (n=30), 1% HA + CBD-SA-IL-4 (n=47).

**Histomorphometric analysis of wound tissue sections** Wounds were fixed overnight in 2% PFA and cut down the center into two and embedded into paraffin for histological analysis on 5- $\mu$ m serial sections. The extent of reepithelization was measured blindly by histomorphometric analysis of tissue sections (H&E stain) using QuPath software (University of Edinburgh). For analysis of reepithelization, the distance that the epithelium had traveled across the wound was measured; the muscle edges of the panniculus carnosus were used as

an indicator for the wound boundary; and reepithelization was calculated as the percentage of the distance between the edges of the panniculus carnosus muscle.

**Pharmacokinetics** Nine C57BL/6J male mice aged 9-10 weeks (The Jackson Laboratory) were wounded using a 6 mm diameter biopsy punch to make a full thickness wound. Cytokine- containing hydrogels at IL-4 equivalent concentrations of 100  $\mu\text{g} / \text{mL}$  were immediately applied, and the wound was covered as described above. Blood was collected via submandibular draw at relevant time points. Upon euthanasia, the wound tissue was excised in uniform area, 6mm, and homogenized using T-Per Buffer (ThermoFisher) and Matrix D lysing tubes (MP Biomedical). Plasma was harvested in Heparin coated tubes and used for detection with pre-coated interleukin-4 ELISA kits (Invitrogen). An additional standard using recombinant CBD-SA-IL-4 to measure CBD-SA-IL-4 in plasma.

**Cytokine profile of wound tissue** Male C57BLKS/J-m/Lepr db (db/db) 8-10-week-old mice (The Jackson Laboratory) were used. Skin wounds were treated with hydrogels as described above. After 24, 48, 72 and 96 hr, the wounded skin was removed as described above and transferred to T-Per Solution (ThermoFisher) in Lysing Matrix D containing tubes (MP Biomedical) and homogenized (MP Biomedical). Then, the solution was centrifuged, and the supernatant was retained for analysis using LegendPlex Mouse Cytokine Release Syndrome Multiplex Kit (BioLegend) carried out according to manufacturer's instruction.

**Flow cytometric analysis of the wounds** Male C57BLKS/J-m/Lepr db (db/db) 8-10-week-old mice (The Jackson Laboratory) were used. Skin wounds were treated with hydrogels as described above. 48 hr post treatment application, wounded skin was removed as described above and cut into small pieces ( $<5 \text{ mm}^2$ ) and transferred to 4 mL of an enzyme solution (Liberase TL (0.4 mg/mL) Roche, DNase I (13.7 pU/mL) MP Biomedicals)), and incubated for 2 hr at 37°C. Then, the cells from the digested wounds were resuspended in 25 mL of media, passed through a 70  $\mu\text{m}$  cell strainer, and centrifuged. The single cell suspension was counted, and  $2 \times 10^6$  cells/mL were plated and stained for 15 min in 50  $\mu\text{L}$

| Marker    | Fluorophore     | Catalog Number  | Clone       | Dilution |
|-----------|-----------------|-----------------|-------------|----------|
| CD86      | BUV 395         | 564199          | GL1         | 50       |
| CD31      | BUV 563         | 741251          | MEC13.3     | 100      |
| CD124     | BUV 661         | 741557          | mIL4R-M1    | 50       |
| CD45      | BUV 805         | 752415          | 13/2.3      | 200      |
| CD206     | BV 421          | 141717          | C068C2      | 200      |
| CD11b     | BV 650          | 563402          | M1/70       | 400      |
| CD11c     | BV 711          | 117349          | N418        | 100      |
| F4/80     | FITC            | 123108          | BM8         | 400      |
| Ly-6G     | PerCP-Cy5.5     | 56060           | IA8         | 200      |
| IA/IE     | APC             | 107614          | M51114.15.2 | 800      |
| Ly-6C     | APC-Fire 750    | 128045          | HK1.4       | 400      |
| SMA       | Alexa Fluor 700 | MBP2-34522AF700 | 1A4/asm-1   | 100      |
| Ki67      | BV 605          | 652413          | 16A8        | 200      |
| iNOS      | Alexa Fluor 532 | 58-5920-80      | CXNFT       | 200      |
| Arg1      | PE-Cy7          | 25-3697-82      | AlexF5      | 200      |
| Live Dead | Zombie NIR      | 423105          | N/A         | 800      |

Table 2.1: CBD-SA-IL-4 Treated Wound Characterization Panel Details

live/dead fixable dye and anti CD16/32 (BioLegend). After one wash. cells were stained for 30 min in 50  $\mu$ L of 2% FBS in PBS-containing antibodies (see table below). Intracellular staining was performed using the eBioscience Foxp3/Transcription Factor Staining Buffer Set according to the manufacturer’s instructions (Invitrogen). Cells were analyzed using an Aurora (Cytek) spectral flow cytometer and FlowJo software (FlowJo, LLC). Gating strategies are shown in Supplementary Fig.4.

**Toxicological Studies** Female C57BL/6J 8-week-old mice (The Jackson Laboratory) were used. A single dose of either PBS, WT IL-4, or CBD-SA-IL-4 was administered subcutaneously at an equivalent concentration to that applied topically in previous wounding studies on all four wounds (32  $\mu$ g). Body weight was monitored daily, and two days post dose administration blood was collected for analysis using a blood chemistry analyzer (Alfa Wassermann VetAxcel) and flow cytometric readouts.

**Statistical Analysis** Statistical methods were not used to predetermine the necessary sample size, rather sample sizes were chosen based on estimates from pilot experiments and previously published results such that appropriate statistical tests could yield significant results.

## 2.6 Author Contributions

A.L.L., J.I., and J.A.H. designed the project. A.L.L., R.P.W., A.T.A., A.I., T.N.B., A.J.S., K.C.R., A.M., S.G., and J.I. performed the experiments. A.L.L., J.I., and J.A.H. analyzed the data. A.L.L., J.I., and J.A.H. wrote the manuscript.

## 2.7 Funding

We thank the Chicago Immunoengineering Innovation Center (CIIC) for the funding for this project.

## 2.8 Acknowledgements

We thank the Human Tissue Resource Center of the University of Chicago for histology analysis, the Light Microscopy Core for their slide scanning services, and the Cytometry and Antibody Technology Core of the University of Chicago for flow cytometry panel design.

## 2.9 Conflicts of Interest

The University of Chicago has filed for patent protection on the technology described herein, upon which J.A.H., J.I., A.I., and A.L.L. are inventors. HeioThera, Inc., has licensed these patents, and J.A.H., J.I. and A.I. hold equity therein.

# CHAPTER 3

## SYSTEMICALLY ADMINISTERED FLT3L FOR THE TREATMENT OF DIABETIC WOUNDS

### 3.1 Abstract

Therapeutic options remain limited for treatment of non-healing chronic wounds and consist of physical measures and topical ointments. Here, we describe the use of Flt3L and an engineered counterpart Flt3L serum albumin fusion construct (Flt3L-SA) for the systemic based treatment of diabetic wounds. Flt3L treatment is capable of modulating the dendritic cell composition in the diabetic wound recapitulating it towards that of a healthy wound, potentiating more effective tissue regeneration.

### 3.2 Introduction

The treatment of non-healing diabetic wounds has been a clinical challenge for decades [96, 98]. Current treatments are limited to physical measures such as debridement and topical ointments that have mixed results [87, 88, 89]. It has become more recognized that there is an immune dysfunction that underlies the impaired healing ability of diabetic patients [28, 48, 49]. This immune dysfunction has served as a target for therapeutic development, though the primary immune cell of focus has been macrophages. Recently, more work has been done characterizing other immune cell populations within the temporal wound healing process [62].

One cellular population that showed meaningful differences between healthy and diabetic wounds was dendritic cells. Prior to wounding, intact diabetic skin had less dendritic cells when compared to intact healthy skin. Following wounding, diabetic skin consistently had less dendritic cells both in the bulk compartment and also when considering DC subtypes,

cDC1s and cDC2s, when compared to healthy wounds. [62]. Though the precise function of these dendritic cells within wound healing is not parsed out yet, the striking differences elude to impactful purpose. When dendritic cells were depleted in a mouse wounding model, healing was impaired [161]. Furthermore, enhancing the dendritic cell population enhanced early stage wound healing. This could be due to their role as "professional phagocytes" [162]. With this function of clearing the apoptotic debris from the wound bed dendritic cells could play an important role in moving the wound out of the inflammation phase into the proliferative phase. Recent work has depicted that this benefit could be related to the efferocytic capacity of dendritic cells within the wound, especially cDC1s [18]. Furthermore, these enhanced efferocytic DCs displayed differentiated metabolism and increased expression of GDF15, a member of the TGFB family [163]. These findings present the opportunity to utilize DC expanding Flt3L and engineered Flt3L constructs for the treatment of non-healing diabetic wounds, providing the potential for systemically administered treatment.

### 3.3 Results

#### *3.3.1 Systemically Administered Flt3L Enhances Wound Healing in Type 2 Diabetic Mouse Model*

We tested the efficacy of systemically administered Flt3L for the treatment of surgically inflicted wounds in the type-2 diabetic (db/db) mouse model, a well-established and clinically relevant model of impaired wound healing [92, 140]. The PBS group represented an untreated wound and was the main comparison for efficacy of the Flt3L treatment. We expected wounds treated with Flt3L to show improved healing when compared to PBS controls. Wound were excised and analyzed via H&E staining 10 days after wounding and treatment (day 0). As a result, systemic Flt3L therapy significantly promoted reepithelialization when compared to PBS treated controls (Fig. 3.1A-B). Furthermore, we were able to show that efficacy be

maintained with a 20-fold lower dose using an engineered version of Flt3L, fused to serum albumin (SA), likely by the extension of the half-life of the construct. Strikingly, 45.8% of wounds treated with WT Flt3L showed >90% reepithelialization, while only 17.4% of wounds treated with saline showed reepithelialization >90% (Fig. 3.2A). Representative H&E images depict full reepithelialization (Fig. 3.2B). These data indicate that systemic administration of Flt3L or its engineered counterpart, Flt3L-SA, improves wound closure when compared to the non-treated control.

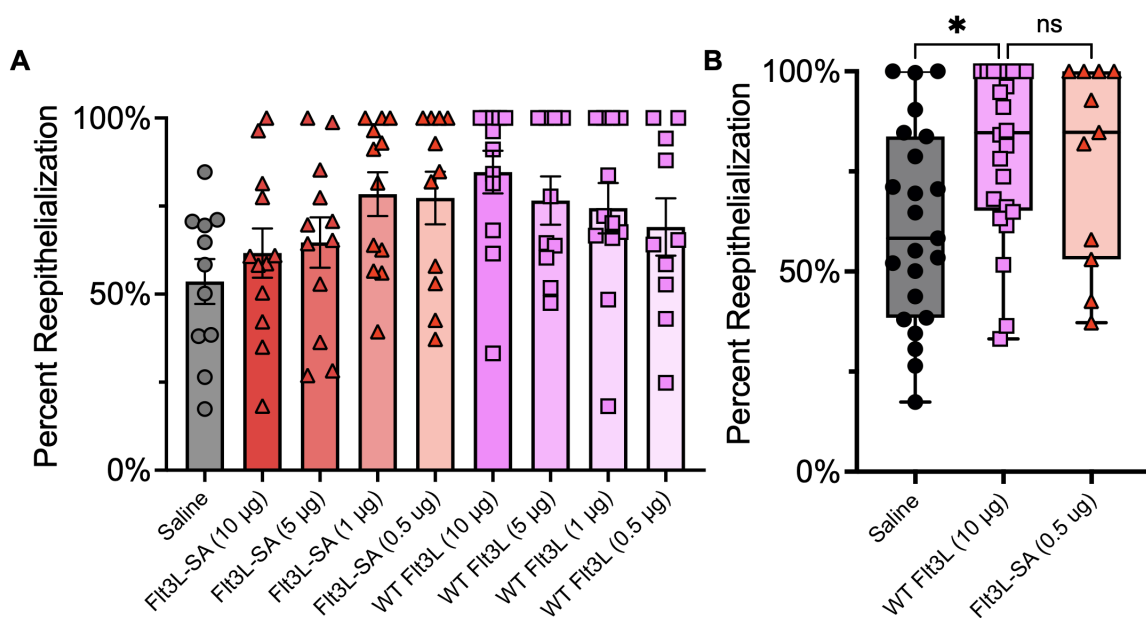


Figure 3.1: Flt3L treatment promotes reepithelialization. A) Multidose study of Flt3L-SA and WT Flt3L ranging from 10  $\mu\text{g}$  - 0.5 $\mu\text{g}$  B) Comparison of WT Flt3L (0.5 $\mu\text{g}$ ) and Flt3L-SA (10 $\mu\text{g}$ ) reepithelialization.

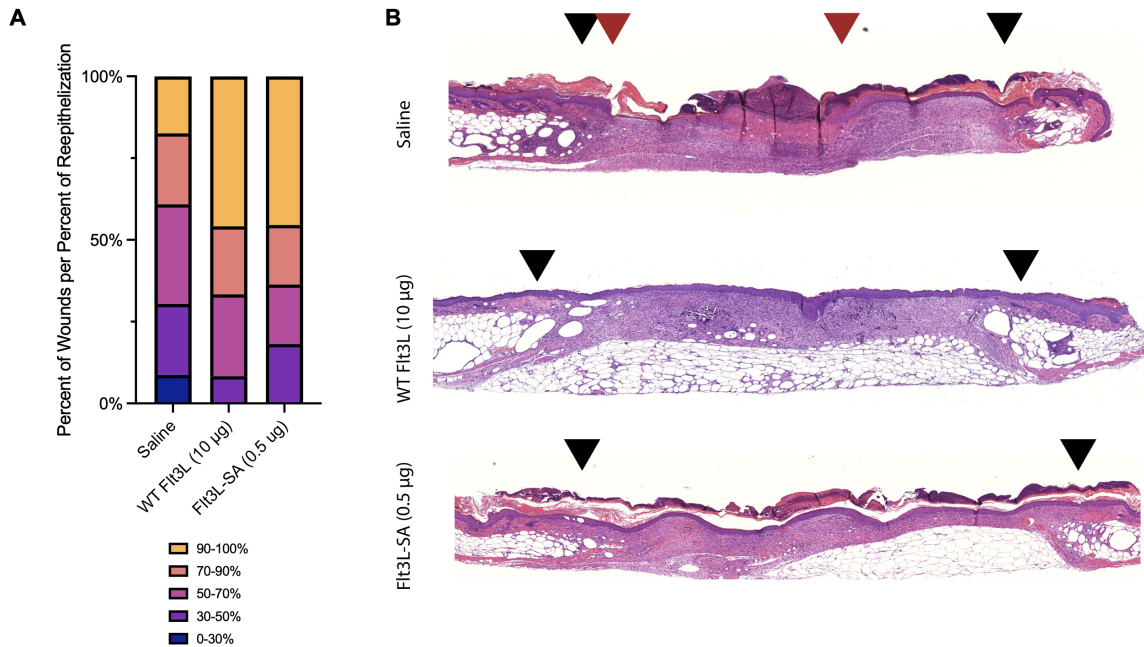


Figure 3.2: Flt3L treatment representative histology images. A) The wounds were binned based on percent closure after 10 days of healing (i.e what percent of wounds were 90%-100% reepithelialized). B) H&E stained slides representative of each group's degree of reepithelialization.

### 3.3.2 Flow Cytometric Analysis of Wound Tissue Following Flt3L treatment

Because Flt3L is well known to expand the dendritic cell compartment in the bone marrow, in a relatively selective manner [164]. we hypothesized that there would be increased dendritic cell infiltration in the wound bed following Flt3L administration. To test this hypothesis, we treated db/db wounds following the same treatment timeline as used previously, excising wounds 4 days post-treatment and digesting to create single cell suspensions for flow cytometric analysis. Through this, we first noted that the overall immune cell infiltration was unchanged across all three groups (Fig. 3.3A). Additionally, there were no differences in the macrophage population between groups (Fig. 3.3B). However, we did see increased bulk dendritic cell infiltration into the wound bed (Fig. 3.3C). This shift in the Flt3L treated wounds shows a bulk dendritic cell composition. Additionally, we observed significant increases in both cDC1 and cDC2 compartments after Flt3L treatment (Fig. 3.3D-E). These

results indicate that following Flt3L treatment the wound more closely recapitulates the healthy wound tissue in the dendritic cell compartment when compared the PBS treated diabetic wounds.

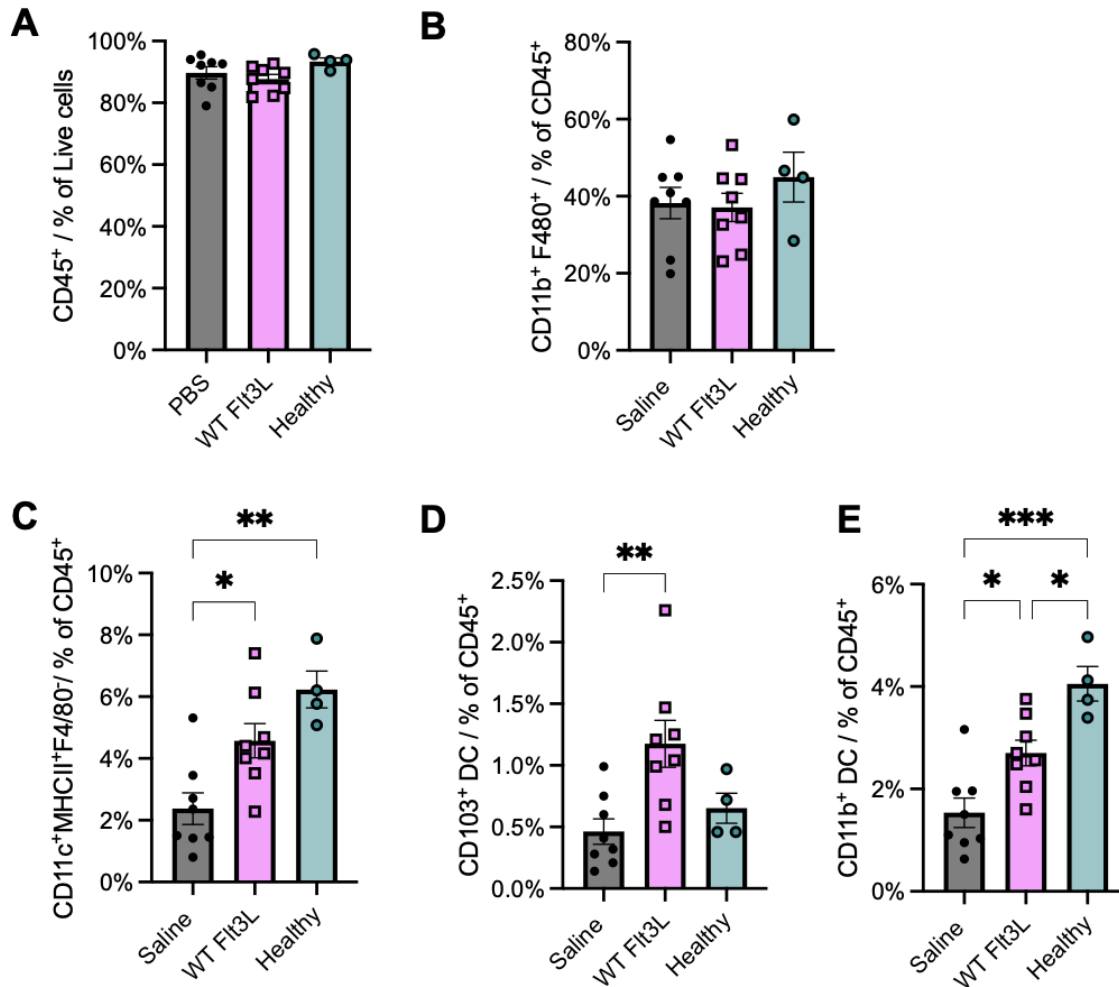


Figure 3.3: Flt3L treatment modulates immune cell compartments in the wound bed. A) Immune cells (CD45<sup>+</sup> cells as a percent of live cells) in the wound bed. B) Macrophages (CD11b<sup>+</sup> F4/80<sup>+</sup> cells as a percent of CD45<sup>+</sup> cells) in the wound bed. C) Dendritic cells (CD11c<sup>+</sup> MHCII<sup>+</sup> F4/80<sup>-</sup> cells as a percent of CD45<sup>+</sup> cells) in the wound bed. D) cDC1s (CD103<sup>+</sup> DCs as a percent of CD45<sup>+</sup> cells) in the wound bed. E) cDC2s (CD11b<sup>+</sup> DCs as a percent of CD45<sup>+</sup> cells) in the wound bed. Statistical analysis was performed using ordinary one-way analysis of variance with Tukey multiple comparisons with respect to media control. \*p < 0.05, \*\*p < 0.01, \*\*\*p < 0.001, \*\*\*\*p < 0.0001, ns = not significant.

### 3.4 Discussion

Wound healing is a tightly regulated process composed of many cellular players with specific functions. While dendritic cells have not been of primary focus for their role in wound healing, with recent work it is becoming clear that they serve a critical role. As proficient phagocytes, dendritic cells within the wound bed help clear the high burden of debris present after injury. Current treatment options fall short of addressing the large clinical gap that exists, leading to high rates of amputation [146, 147]. The work depicted here demonstrates potential in closing the clinical gap, through the expansion of dendritic cells via systemic administration of Flt3L or its engineered counterpart. The efficacy data depicted here depicts the first use of a systemic based therapy for the treatment of non-healing chronic wounds. This therapy is potentiated through the expansion of dendritic cells, which have recently been shown to aid healing due to their efferocytic capacity. With the possibility to maintain efficacy while reducing the dose 20-fold with the fusion of Flt3L to serum albumin, this treatment

### 3.5 Materials and Methods

**Mouse skin chronic wound-healing model** Male C57BLKS/J-m/Lepr db (db/db) 8-10-week-old mice (The Jackson Laboratory) were used. Their backs were shaved and cleaned and four full-thickness punch-biopsy wounds (6 mm diameter) were created in each mouse. Each wound was splinted open using a silicone ring (inner diameter 8 mm, outer diameter 12 mm) to prevent contraction. Immediately following the procedure treatments were administered. The wounds were covered with Adaptic dressing and sealed with adhesive film. Mice were single caged after the wounding surgery. After 10 days, mice were euthanized, and the skin wounds were carefully excised for histological analysis. All experiments using mice received approval from the Institutional Animal Use Committee of the University of Chicago under ACUP 72450. The animals' care was in accordance with institutional guidelines.

**Histomorphometric analysis of wound tissue sections** Wounds were fixed overnight in 2% PFA and cut down the center into two and embedded into paraffin for histological analysis on 5- $\mu$ m serial sections. The extent of reepithelization was measured blindly by histomorphometric analysis of tissue sections (H&E stain) using QuPath software (University of Edinburgh). For analysis of reepithelization, the distance that the epithelium had traveled across the wound was measured; the muscle edges of the panniculus carnosus were used as an indicator for the wound boundary; and reepithelization was calculated as the percentage of the distance between the edges of the panniculus carnosus muscle.

**Flow cytometric analysis of the wounds** Male C57BLKS/J-m/Lepr db (db/db) 8-10-week-old mice (The Jackson Laboratory) were used. Skin wounds were treated with hydrogels as described above. Four days post treatment application, wounded skin was removed as described above and cut into small pieces ( $<5\text{ mm}^2$ ) and transferred to 4 mL of an enzyme solution (Liberase TL (0.4 mg/mL) Roche, DNase I (13.7 pU/mL) MP Biomedicals)), and incubated for 2 hr at 37°C. Then, the cells from the digested wounds were resuspended in 25 mL of media, passed through a 70  $\mu$ m cell strainer, and centrifuged. The single cell suspension was counted, and  $2 \times 10^6$  cells/mL were plated and stained for 15 min in 50  $\mu$ L live/dead fixable dye and anti CD16/32 (BioLegend). After one wash. cells were stained for 30 min in 50  $\mu$ L of 2% FBS in PBS-containing antibodies (Table 2). Intracellular staining was performed using the eBioscience Foxp3/Transcription Factor Staining Buffer Set according to the manufacturer’s instructions (Invitrogen). Cells were analyzed using an Fortessa flow cytometer (BDSciences) and FlowJo software (FlowJo, LLC).

### 3.6 Author Contributions

A.L.L., A.T.A., and J.A.H. designed the project. A.T.A. and K.C.R. produced material. A.L.L., A.T.A., J.B., K.C.R., and A.J.S. performed experiments. A.L.L., A.T.A., and J.A.H.

| Marker    | Fluorophore | Catalog Number | Supplier     | Clone       | Dilution |
|-----------|-------------|----------------|--------------|-------------|----------|
| CD45      | BUV 395     | 564279         | BD Horizon   | 30-F11      | 200      |
| CD31      | BV786       | 740870         | BD OptiBuild | MEC13.3     | 200      |
| CD11c     | BV605       | 117333         | Biolegend    | N418        | 200      |
| MHCII     | PerCP       | 107626         | Biolegend    | M5/114.15.2 | 200      |
| CD207     | APC         | 144206         | BioLegend    | 4C7         | 200      |
| CD013     | PE          | 561043         | BD Horizon   | M290        | 200      |
| CD11b     | PE-Cy7      | 101216         | BioLegend    | M1/70       | 200      |
| CD8       | BUV737      | 612759         | BD Horizon   | 53-6.7      | 200      |
| LAP       | BV421       | 141408         | Biolegend    | TW7-16B4    | 200      |
| F4/80     | FITC        | 123108         | BioLegend    | BM8         | 200      |
| Live Dead | APC-Cy7     | L34994         | Invitrogen   | N/A         | 500      |

Table 3.1: Flt3L Treated Wound Characterization Panel Details

analyzed the data. A.L.L., A.T.A., and J.A.H. wrote the manuscript

### 3.7 Funding

We thank the Chicago Immunoengineering Innovation Center (CIIC) for the funding for this project.

### 3.8 Acknowledgements

We thank the Human Tissue Resource Center of the University of Chicago for histology analysis and the Light Microscopy Core for slide scanning services.

### 3.9 Conflicts of Interest

The University of Chicago has filed for patent protection on the technology described herein, upon which J.A.H., A.L.L., and A.T.A. are inventors.

# CHAPTER 4

## MANNOSE-DECORATED CO-POLYMER FACILITATES CONTROLLED RELEASE OF BUTYRATE TO ACCELERATE CHRONIC WOUND HEALING

### 4.1 Abstract

Butyrate is a key bacterial metabolite that plays an important and complex role in modulation of immunity and maintenance of epithelial barriers, but its translation to clinic has been limited by ineffective delivery strategies. Here we report a novel polymeric delivery platform for tunable and sustainable release of butyrate, which is also applicable to other therapeutically-relevant metabolites. This butyrate-containing material modulated immune cell activation *in vitro* and induced striking changes in the milieu of soluble cytokine and chemokine signals present *in vivo*. These results motivated the use of our platform in a murine model of chronic, non-healing diabetic wounds, where we demonstrated robust efficacy in the promotion of healing. This novel therapy shows promise in the treatment of non-healing wounds, where there are few existing therapies and limited efficacy. Treated with the current standard-of-care, these wounds often lead to infection and subsequent amputation, and our novel platform is positioned to address this large unmet clinical need.

### 4.2 Introduction

Wound healing is a critical but complex process in which every cellular player and soluble signal is tightly controlled [165]. Dysfunction in the wound is associated with many disease states and can disrupt and inhibit wound closure through perturbations in these signaling pathways and cellular interactions. It is well known that the diabetic disease state causes dysfunction in many aspects of the wound, ultimately leaving the diabetic wound chroni-

cally inflamed and unable to mount the classical tissue damage response, leaving the wound chronically open and susceptible to infection [166, 89]. Due to this high risk of infection in non-healing wounds, diabetic patients make up 65% of amputees in the United States[167]. Despite decades of efforts to improve the outcomes of chronic wounds, few treatment strategies have shown efficacy in large-scale, well-controlled clinical studies, leaving clinicians with few reliable options for treatment[168]. For this reason, it is of strong clinical interest to develop novel inducers of healing for chronic wounds.

Butyrate is a short chain fatty acid produced through bacterial fermentation of dietary fiber in the intestinal lumen. It has been proposed that butyrate production offers protection against colonic inflammation and oxidative stress and increases epithelial barrier integrity[169]. While these mechanisms are not entirely understood, data suggests that butyrate exerts anti-inflammatory effects through inhibition of NF $\kappa$ B signaling[170, 171]. Separately, butyrate modulates barrier function by promoting cell migration[172] and increasing production of mucins[173] and heat shock proteins[174, 175]. Clearly, butyrate plays important roles in regulating cellular function and could offer unique promise in modulating the wound environment in the case of chronic wounds, where the immune and metabolic phenotype is dysregulated.

Given the clear clinical need to alter the disrupted immune phenotype of non-healing wounds, we hypothesized that butyrate's immunosuppressive and barrier promoting activity could be beneficial to promote an exit from the chronic, inflammatory phase of wound healing into a pro-regenerative state[176]. However, butyrate has a notoriously pungent smell, even in solution, that limits its potential as a topical therapy. Consequently, we developed a delivery platform from which butyrate is in an inactive, esterified form and is released over time via esterases, with the release rate being tunable based on the ester chemistry employed. The material is a co-polymer with pendant mannose groups that increase solubility and promote receptor mediated endocytosis on mannose receptor-expressing cells[177, 178]. Here, we

evaluate the *in vitro* and *in vivo* immunological bioactivity of our butyrate co-polymers and demonstrate their promise in a murine model of diabetic wound healing.

## 4.3 Results

### 4.3.1 Tunable, Sustained Release of Butyrate from Mannose Co-Polymer

To vary release kinetics of butyrate from the co-polymer, we synthesized methacrylamide monomers with either an aliphatic ester or a phenyl ester as described in Methods. Either of two monomers were co-polymerized with a mannose-functionalized methacrylamide monomer and with water-soluble spacer monomer hydroxyethyl methacrylamide (HEMA) via RAFT polymerization to produce pMan-But (Fig. 4.1A) or pMan-PhBut (Fig. 4.1B). Monomers were incorporated at a ratio of mannose:HEMA:butyrate of 3:5:4 to balance water solubility and high butyrate payload. GPC analysis of both polymers revealed a single, broad elution profile (Fig. 4.1C) corresponding to a similar number-averaged molecular weight around 11 kDa (Fig. 4.1D). We also characterized the polymers via  $^1H$ -NMR (Fig. 4.2A-B).

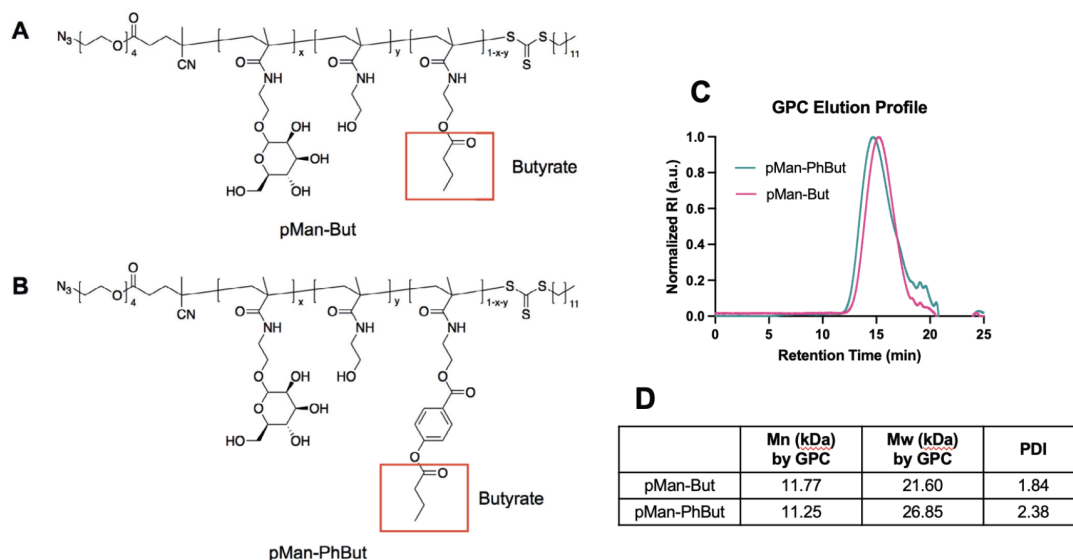


Figure 4.1: Structure and characterization of pMan-But and pMan-PhBut. Structures of random co-polymers A) pMan-But and B) pMan-PhBut, with butyrate highlighted in a red box – the terminal carboxyl alcohol of the released butyrate is incorporated during ester hydrolysis from surrounding water, and the oxygen here is left as a free primary alcohol on the polymer chain. C) GPC elution profiles of both polymers and D) resulting molecular weight characterization as compared to PMMA standards.

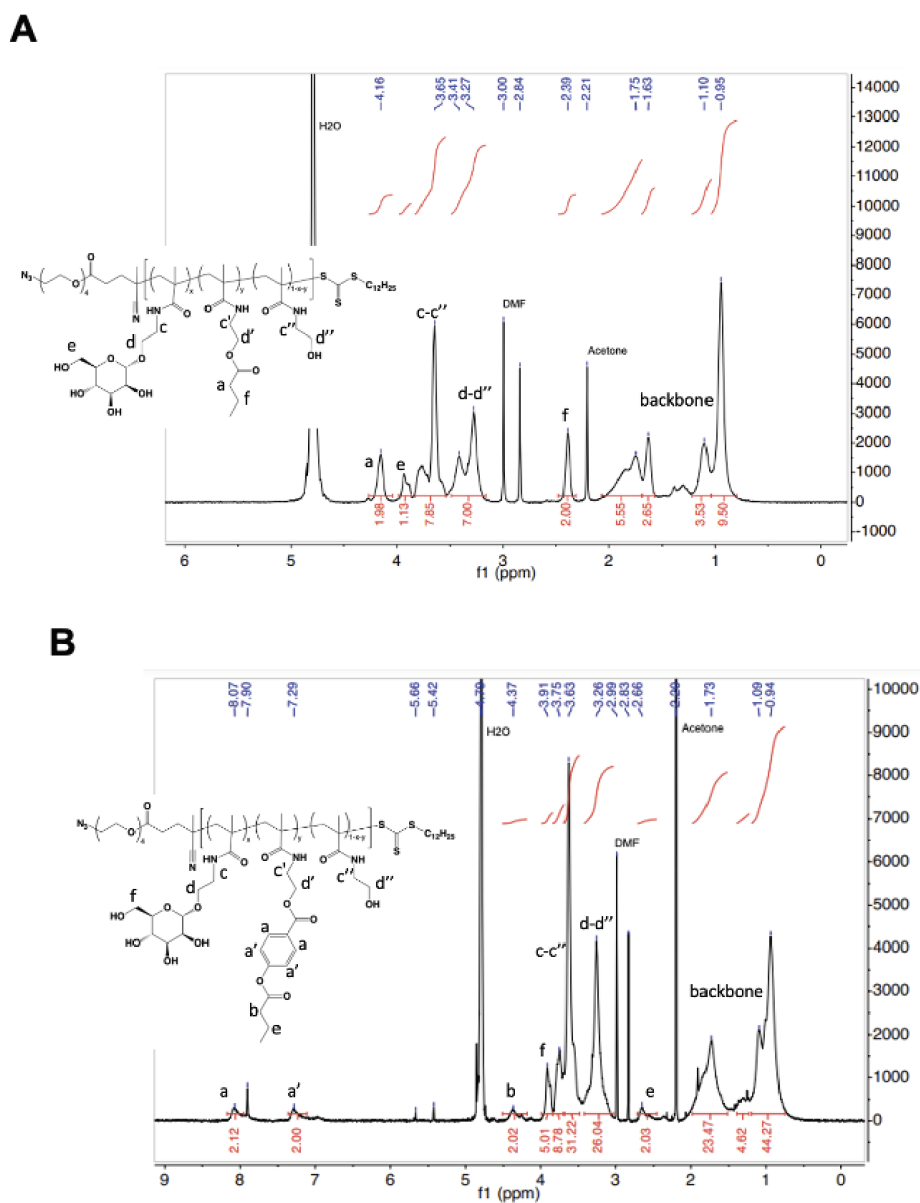


Figure 4.2: Proton NMR characterization of butyrate-containing copolymers. NMR spectra of purified (A) pMan-but and (B) pMan-PhBut in  $\text{CDCl}_3$  using a 400 MHz spectrometer.

With the resulting materials, we analyzed butyrate release kinetics in a variety of solutions. We found that negligible butyrate was released from either polymer in phosphate-buffered saline, regardless of pH within the physiological range (Fig. 4.3A-C). It was only in

complete media, which contained 5% v/v fetal bovine serum (FBS), that butyrate released from the polymer backbone, demonstrating release dependency on esterase enzymes, found in FBS, rather than simply acid-catalyzed hydrolysis. When directly comparing the two polymers, we found that butyrate released faster from pMan-PhBut than from pMan-But, with half-lives of 8.0 and 56.9 hours, respectively (Fig. 4.3C). We also found that total butyrate released was equivalent to a mass ratio of approximately 10% w/w.

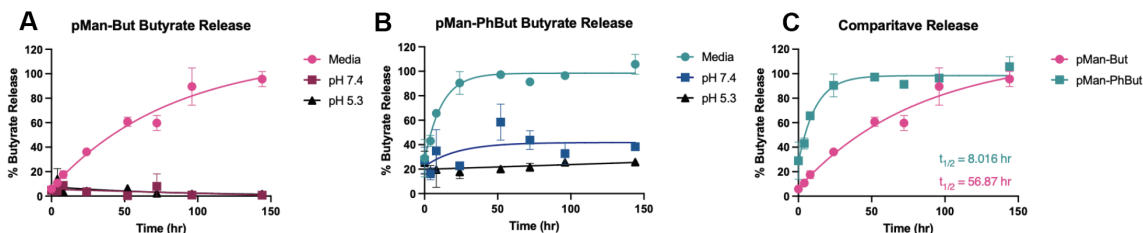


Figure 4.3: Butyrate release from pMan-But and pMan-PhBut. Solvent-dependent kinetics of butyrate were measured via LC-MS from (A) pMan-But and (B) pMan-PhBut in complete RPMI cell culture media, PBS as pH 7.4, and PBS at pH 5.3. (C) Comparative release rates of butyrate from pMan-But and pMan-PhBut in cell culture media. Data are presented as mean  $\pm$  SEM. Release curves were fit based on a one-phase decay model, and half-lives were calculated from fit curves.

#### 4.3.2 pMan-But and pMan-PhBut Modulate Inflammation *In Vitro*

To assess the bioactivity of our constructs in comparison to unmodified sodium butyrate (NaBut), we turned to an *in vitro* model of prophylactic immune suppression in response to lipopolysaccharide (LPS) stimulation using murine bone-marrow derived dendritic cells (BMDCs) (Fig. 4.5A). We first confirmed that doses used were non-toxic to cells by measuring cell viability (Fig. 4.4).

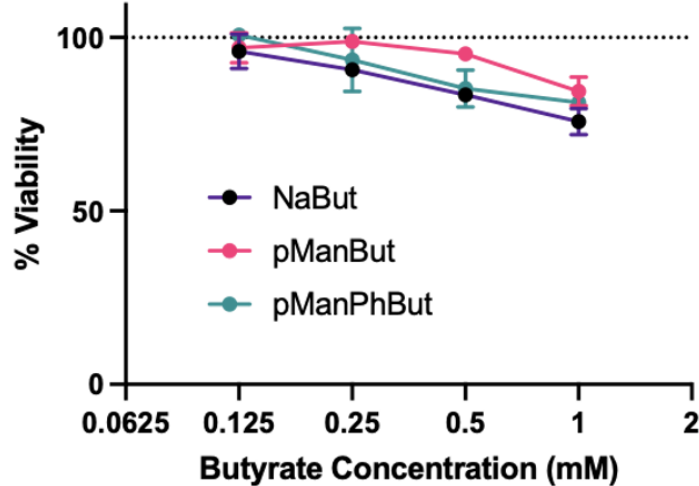


Figure 4.4: pMan-But and pMan-PhBut are non-toxic to mBMDCs. BMDCs ( $n = 4$ ) were plated and treated with butyrate constructs and LPS, as stated in Figure 2 and methods. Cells were stained with violet fixable live/dead stain (Fisher) and collected via flow cytometry. Data are plotted as mean  $\pm$  SEM. The experiment was repeated twice with similar results.

In response to pre-treatment of BMDCs by the butyrate-containing co-polymers, we broadly observed changes in cell-surface receptor expression and suppression of pro-inflammatory signaling similar to those mediated by unmodified NaBut. Levels of both T cell costimulatory factors CD80 and CD86 were upregulated as compared to cells without butyrate pre-treatment (Fig. 4.5B-C), which is consistent with other reports of butyrate bioactivity *in vitro*[179]. Levels of CD40, a marker of activated DCs, were decreased with all types of butyrate pre-treatment (Fig. 4.5D); precise modulation of CD40-CD40L interactions has been implicated at various stages of wound healing[180, 181]. Next, we observed a significant upregulation in histone H4 staining, indicating a characteristic inhibition of histone deacetylase 4 (HDAC4) (Fig. 4.5E)[182, 183], which may also have implications on keratinocyte differentiation[184]. Interestingly, we saw an increase in retinaldehyde dehydrogenase 1 (RALDH1) (Fig. 4.5F), which is activated by butyrate downstream of both GPCR109A activation and HDAC inhibition[185], in only pMan-But and NaBut, but not in pMan-PhBut. These markers together indicate phenotypic butyrate bioactivity of our

polymers and potential for pro-regenerative signaling in the wound.

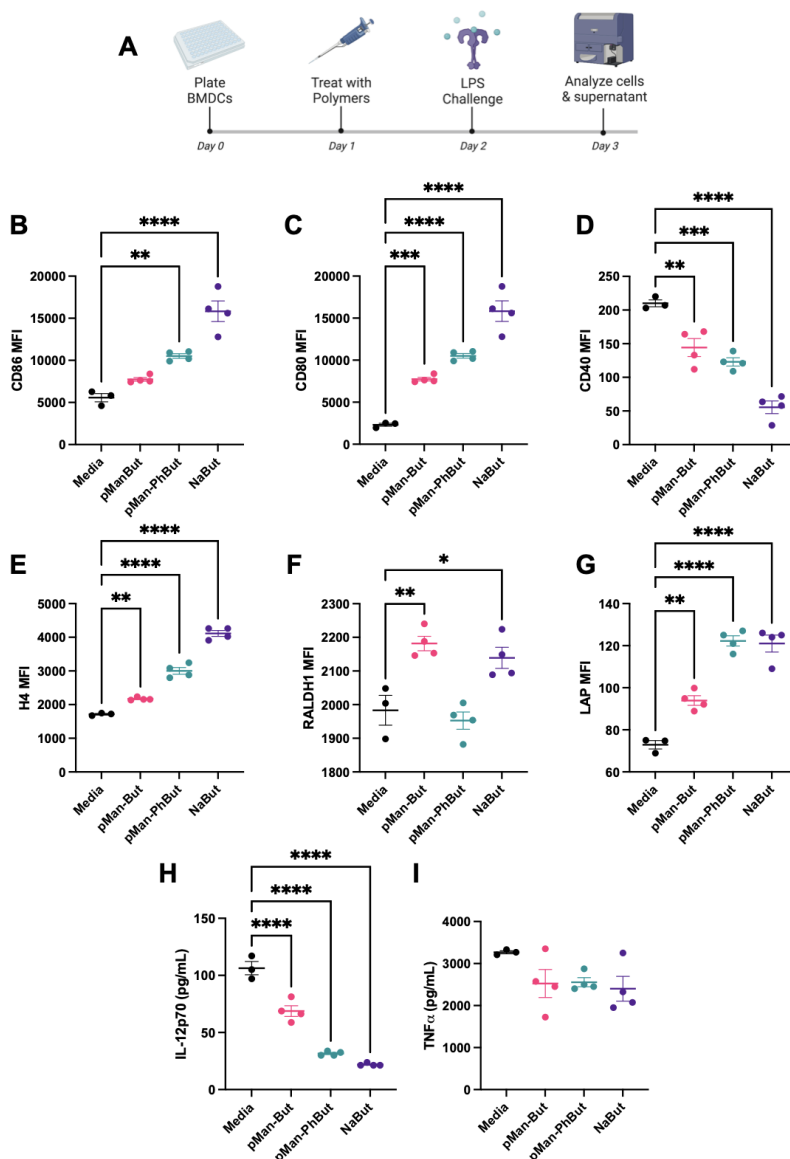


Figure 4.5: In vitro characterization of butyrate polymer bioactivity. (A) A schematic of the experimental timeline. Murine BMDCs were treated with pMan-But, pMan-PhBut, or unmodified sodium butyrate (NaBut) at a concentration of 1 mM butyrate equivalent. After 18 hr, endotoxic lipopolysaccharide (LPS) was added at 100 ng/mL, and cells and supernatant were analyzed 24 hr later. Flow cytometric analysis of the cells themselves included quantification of (B) CD86, (C) CD80, (D) CD40, (E) H4, (F) RALDH1, and (G) LAP expression. Analysis of the supernatant via ELISA allowed for quantification of secreted (H) IL-12p70 and (H) TNF $\alpha$ . Statistical analysis was performed using ordinary one-way analysis of variance with multiple comparisons with respect to media control. \* $p < 0.05$ , \*\* $p < 0.01$ , \*\*\* $p < 0.001$ , \*\*\*\* $p < 0.0001$ , ns = not significant.

As for cytokine profiles, the latency-associated peptide (LAP) of TGF- $\beta$  is upregulated (Fig. 4.5G), corresponding to an increase in precursor TGF- $\beta$  that could be activated to yield the anti-inflammatory cytokine by integrin signaling[186]. LPS-induced secretion of the pro-inflammatory cytokine IL-12p70 was markedly reduced with all butyrate pre-treatments (Fig. 4.5H), however, we did not observe a change in TNF $\alpha$  production (Fig. 4.5I). We further characterized BMDC and RAW-264.7 phenotypes in response to pMan-But stimulation (Fig. 4.6 - 4.7) Together, these results suggest that pMan-But and pMan-PhBut modulate cellular immune phenotypes similarly to NaBut in a way that could be beneficial for wound healing.

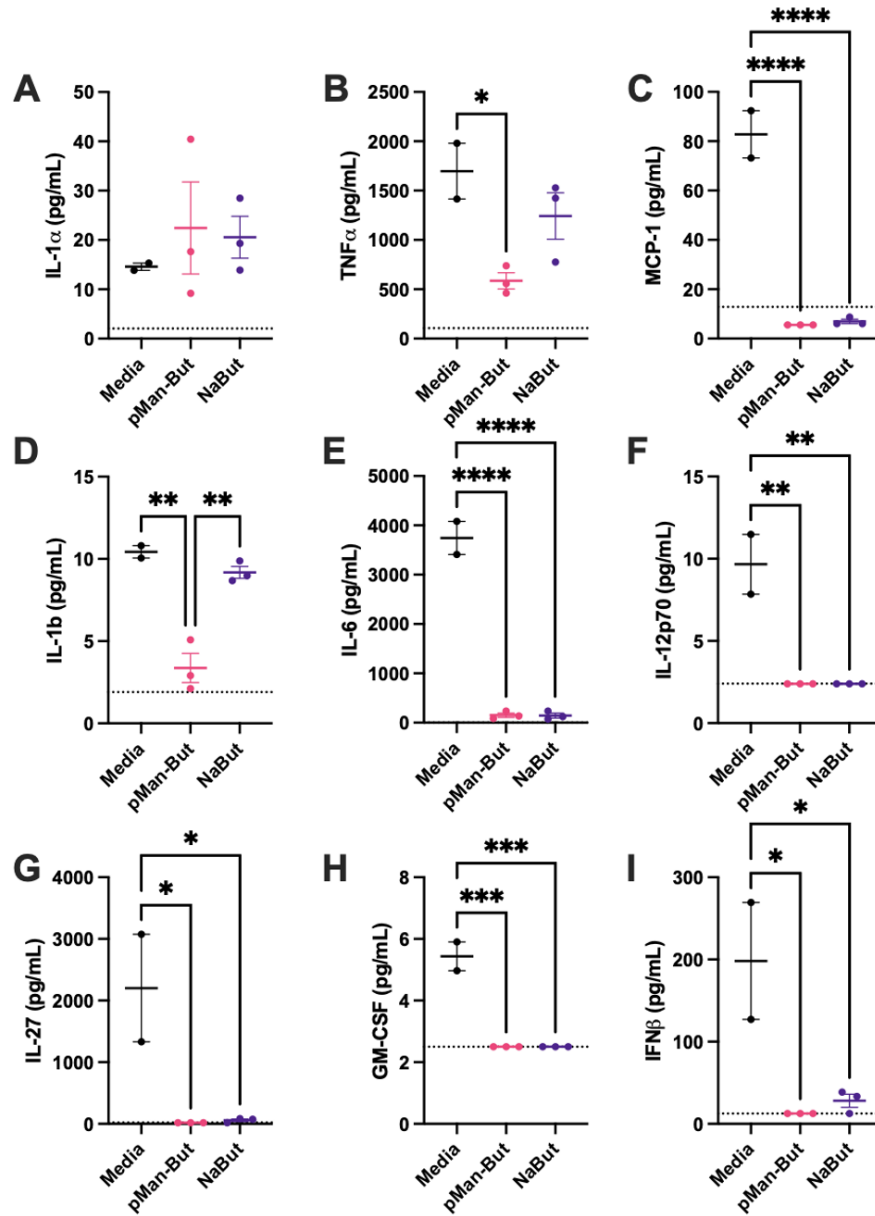


Figure 4.6: pMan-But suppresses pro-inflammatory cytokine and chemokine signaling from mBMDCs. The *in vitro* experiment from Figure 2 was repeated with slight differences. Briefly, cells were plated, pre-treated with 0.5 mM butyrate equivalent of pMan-But or NaBut, and, after 24 hours, challenged with LPS. The supernatant was analyzed using LegendPlex mouse inflammation panel. Suppression of pro-inflammatory cytokine and chemokine signaling was observed in all analytes except (A) IL-1a. These included (B) TNF $\alpha$ , (C) MCP-1, (D) IL-1b, (E) IL-6, (F) IL-12p70, (G) IL027, (H) GM-CSF, and (I) IFN $\beta$ . Interestingly, the butyrate-induced suppression was stronger than that of free NaBut in TNF $\alpha$  (B) and (D) IL-1b. Statistical analysis was performed using ordinary one-way analysis of variance with multiple comparisons between each group. Data are plotted as mean  $\pm$  SEM.

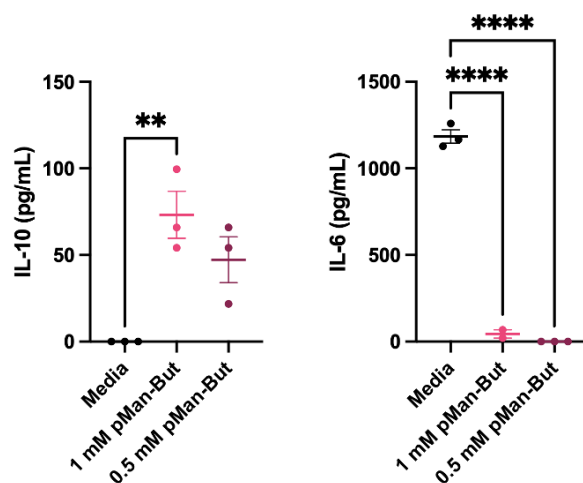


Figure 4.7: pMan-But alters cytokine signals from RAW 246.7 cells. The *in vitro* experiment from Figure 2 was repeated using RAW 264.7 macrophage-like cells. Briefly, cells were plated, pre-treated with two concentrations of pMan-But, and, after 24 hours, challenged with LPS. ELISA analysis of the cell culture supernatant revealed a dose-dependent increase in the anti-inflammatory cytokine IL-10 and similar dose-dependent suppression of LPS-induced, pro-inflammatory cytokine IL-6. Statistical analysis was performed using ordinary one-way analysis of variance with multiple comparisons between each group. Data are shown as mean  $\pm$  SEM. \*\* $p < 0.01$ ; \*\*\*\* $p < 0.0001$ .

#### 4.3.3 pMan-But but not pMan-PhBut Modulate Soluble Signals *In Vivo*

After demonstrating that our constructs induced changes in immune activation *in vitro*, we moved toward assessing the changes in soluble signals induced through treatment *in vivo*. We utilized the type 2 diabetic (db/db) excisional wound murine model, treating the wounds at the time of incision and measuring cytokines and chemokines after 2 or 7 days (Fig. 4.8A). To provide viscosity for the purpose of retention of the polymers at the site of application, they were dissolved in a 1% hyaluronic acid (HA) carrier, and the carrier was studied as a treatment as well. Broadly, we saw that pMan-But induced significant pro-regenerative shifts in the milieu of the wound microenvironment. Levels of the chemokines CCL3, a macrophage chemotactic recruitment factor, were significantly higher after treatment with pMan-But when compared to all other treatment groups 2 days post treatment, but decreased

by day 7 (Fig. 4.8B). The temporal profile indicates a healthy recruitment and phagocytic response with subsequent resolution, which is reported to be dysregulated in the untreated diabetic wound[22, 187]. A similar trend can be seen in the chemokine CCL4 profile, another macrophage chemotactic factor[188], which showed an initial increase in expression followed by its gradual decrease (Fig. 4.8C). Treatment of the wound with pMan-But also induced early elevation of  $\text{TNF}\alpha$  followed by a slight decrease in expression over time, while other treatment groups had the opposite trend with gradual increases in  $\text{TNF}\alpha$  levels by day 7 (Fig. 4.8D). Early induction of  $\text{TNF}\alpha$  has been shown to be a crucial component of complete closure of a cutaneous wound [189].

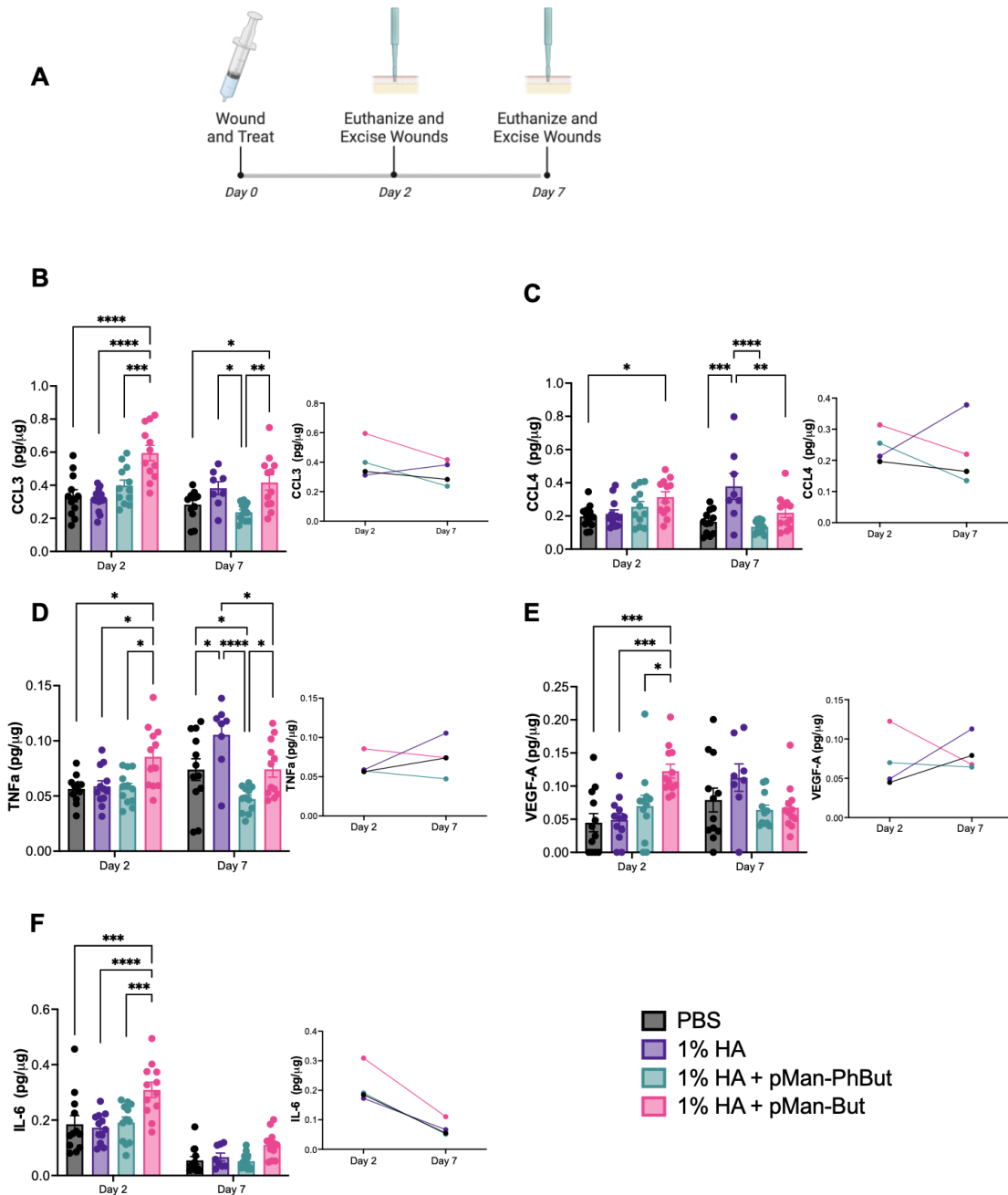


Figure 4.8: In vivo characterization of butyrate polymer immune milieu modulation. (A) A schematic of the experimental timeline. Male db/db mice had four 6 mm wounds excised from dorsal cutaneous tissue and were subsequently treated with PBS, 1% HA, 1% HA + pMan-But, or 1% HA + pMan-PhBut at a concentration of 12.5 mg/mL butyrate equivalent. After 2 or 7 days mice were sacrificed and their wounds harvested and homogenized. Multiplexed soluble signal analysis of the homogenate was collected quantifying wound content of (B) CCL3, (C) CCL4, (D) TNF $\alpha$ , (E) VEGF-A, (F) IL-6. Statistical analysis was performed using ordinary two-way analysis of variance with Tukey's multiple comparison test against all groups. \* $p < 0.05$ , \*\* $p < 0.01$ , \*\*\* $p < 0.001$ , \*\*\*\* $p < 0.0001$ , ns = not significant.

Angiogenic factors are known to play a critical role in wound healing and are found to be diminished in the chronic wound [190]. Treatment with pMan-But induced a strong increase in VEGF-A expression, the most prominent angiogenic factor, on day 2. This strong induction was resolved by day 7, while all other groups displayed the opposite trend (Fig. 4.8E). This striking temporal trend indicates a transition between wound healing phases, where blood vasculature is no longer being produced but rather pruned and substantiated[191]. Lastly, pMan-But, but not pMan-PhBut, induced a profound increase in the expression of IL-6 on day 2 that was resolved by day 7 (Fig. 4.8F). IL-6 has been implicated in the migration of fibroblasts and keratinocytes to sites of injury and promotes deposition of the extracellular matrix components that are required for re-epithelization [192, 38]. These results suggest that pMan-But, but not pMan-PhBut, administered in 1% HA favorably modulates the soluble signal profile in the wound microenvironment to a milieu more conducive to regeneration of the wound. In the *in vivo* experiments, we did not study free NaBut administered in 1% HA since it is not a relevant formulation due to its unacceptable odor.

#### *4.3.4 pMan-But Treatment Accelerates Wound Healing in Type 2 Diabetic Murine Model*

Due to the favorable shift we saw in the soluble signals present in the wound microenvironment after treatment with pMan-But, we tested its efficacy in a db/db cutaneous excisional model. To better understand the material properties of the therapeutically applied gels, we performed rheometric analysis (Fig. 4.9).

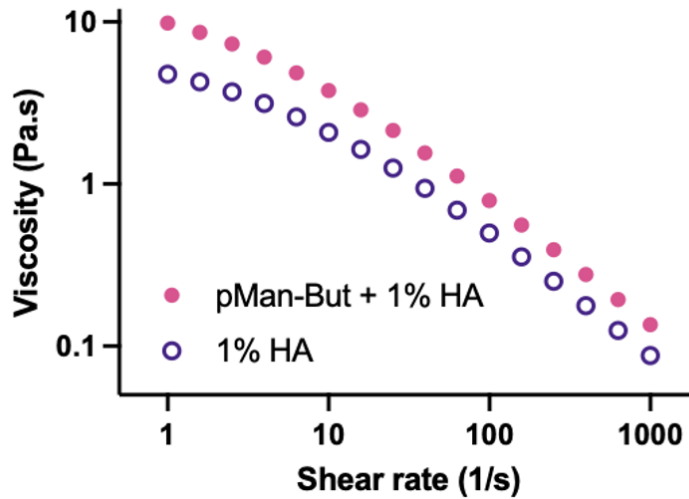


Figure 4.9: Polymer addition increases the viscosity of HA gel. Shear rheology characterization of pMan-But using torsional rheometry. Steady shear viscosity of 1% HA in PBS as a function of shear rate exhibits shear thinning response. Addition of pMan-But increases the low-rate viscosity with analogous degree of shear thinning behavior. Rheological measurements were conducted using a TA Instruments Discovery HR-30 shear rheometer with a smooth parallel plate geometry ( $d = 40$  mm) using a gap size of 0.3 mm. Measurements were performed at room temperature ( $22$  °C). Steady shear viscosity values were measurable in the shear rates in the range of  $1$ – $10^3$  1/s.

After the wounds were created in the dorsal cutaneous tissue, they were treated with either PBS, 1% HA (carrier), or pMan-But in 1% HA carrier. After 7 days pMan-But had significantly improved healing when compared to both the PBS and carrier controls (Fig. 4.10A-B). This 7 day time point depicted an acceleration of wound closure after pMan-But treatment, but a majority of the wound remained open. We then extended the length of time allowed for healing. After 11 days, the pMan-But-treated wounds showed significantly more healing compared to the PBS treatment group (Fig. 4.10C-D), whereas the carrier group did not, although pMan-But was not statistically different from the carrier control. Still, only pMan-But in 1% HA showed a statistically significant increase in closure relative to the PBS-treated group.

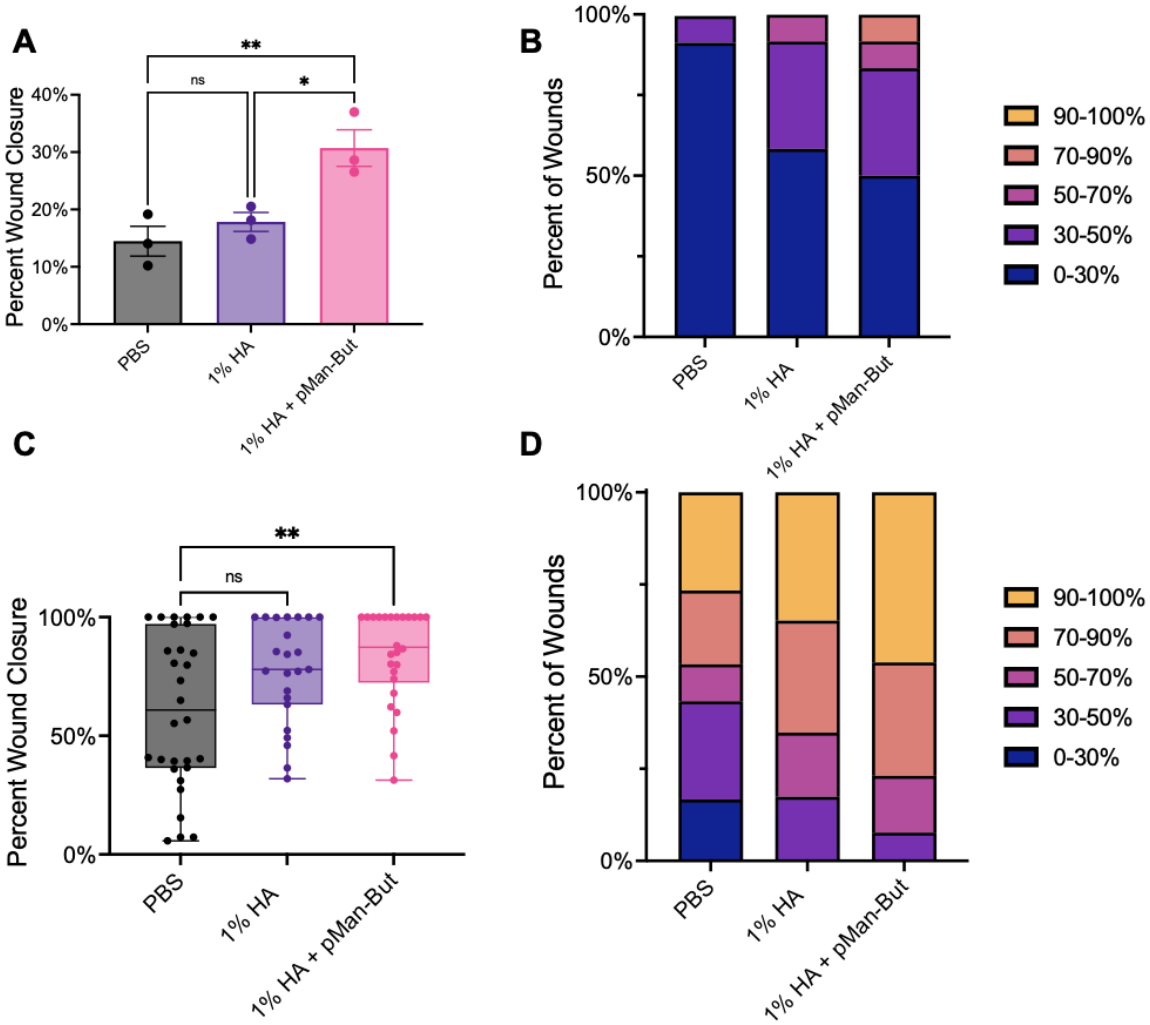


Figure 4.10: In vivo wound closure efficacy of butyrate polymer. Male db/db mice had four 6 mm wounds excised from dorsal cutaneous tissue and were subsequently treated with PBS, 1% HA, or 1% HA + pManBut at a concentration of 12.5 mg/mL butyrate equivalent. After 7 or 11 days mice were sacrificed and their wounds excised for histological analysis. (A) Percent wound closure after 7 days. (B) Percent of wounds within each bin of closure after 7 days. (C) Percent wound closure after 11 days, experiment was repeated a total of two times and pooled. (D) Percent of wounds within each bin of closure after 11 days. Statistical analysis was performed using (A) ordinary one-way analysis of variance with Tukey's multiple comparison test against all groups or (C) Kruskal-Wallis test with Dunn's multiple comparison with respect to PBS control. \* $p < 0.05$ , \*\* $p < 0.01$ , ns = not significant.

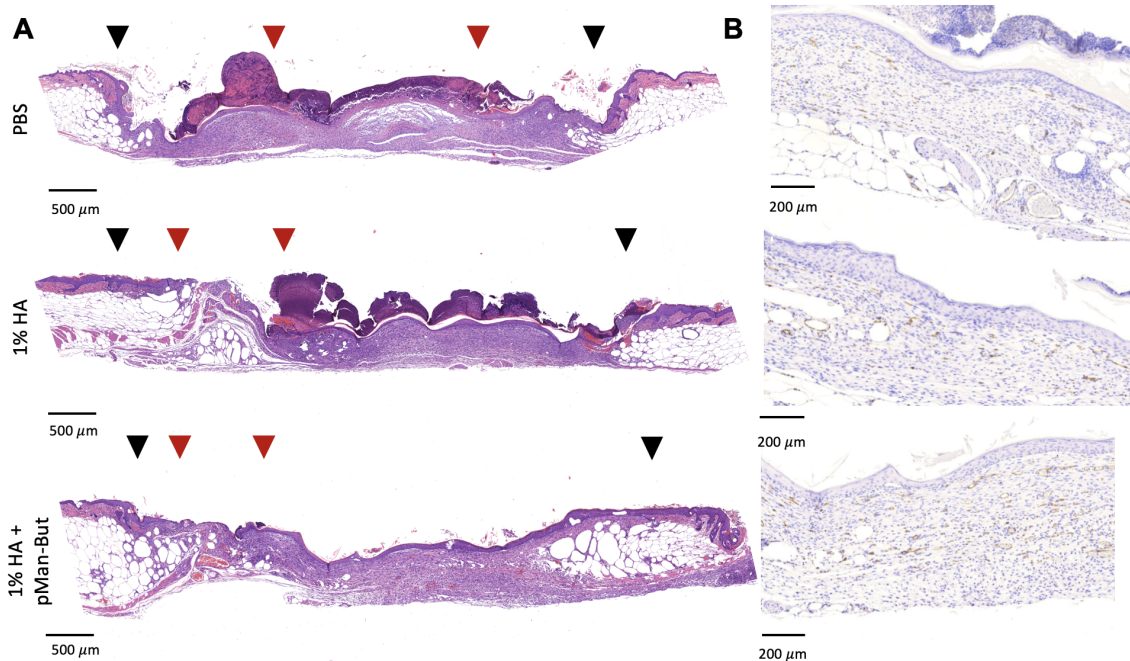


Figure 4.11: In Vivo wound closure with butyrate polymer representative images.(A) Representative H&E images after 11 days. The black arrowheads indicate the margin of the original wound and red arrowheads indicate the tips of epithelium tongue. (B) Representative  $CD31^+$  IHC images after 11 days.

Representative H&E images (Fig. 4.11) visualize the improved re-epithelialization after pMan-But treatment at the 11 day time point. We also visualized blood vessel development indicated by  $CD31^+$  staining via immunohistochemistry, which suggested that pMan-But treatment induces potent vasculature formation (Fig. 4.11). These results taken together indicate that pMan-But can accelerate the healing of chronic type 2 diabetic wounds. It should also be noted that a molecular weight-matched HEMA-only control polymer, without mannose and butyrate, showed a hindrance to closure of these wounds at day 11, indicating the relevance of our functional co-monomers (Fig. 4.12).

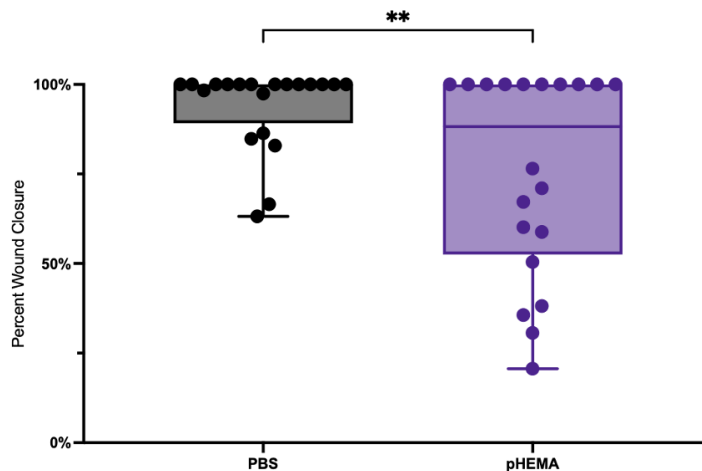


Figure 4.12: PBS vs. pHEMA healing efficacy. This experiment was conducted as described in Methods. The endpoint is on Day 11 post-treatment. Statistical analysis was performed using an unpaired t-test.  $**p < 0.01$

## 4.4 Discussion

The results laid out above demonstrate a platform material that is capable of dynamically delivering its payload, in this context butyrate, in a manner that is targeted to cells expressing the mannose receptor for ligand scavenging. The different release kinetics of the two constructs allow for a tunable delivery. In a prophylactic context, i.e. preventing response to an inflammatory signal, both pMan-But and pMan-PhBut are capable of preventing signature markers of inflammation on LPS-stimulated BMDCs. For wound healing, a slower release of butyrate was thought to be beneficial as to not blunt the important spike in inflammation that facilitates the clearance of debris in the wound[51]. The initial peak of the cytokine and chemokine signals seen, followed by their gradual decrease by day 7 suggests a rebalancing of the milieu present in the wound microenvironment after treatment with pMan-But. This result is corroborated with the enhanced morphological healing seen after pMan-But treatment. These results taken together depict a versatile and novel polymer-based approach to treating chronic wounds.

The pMan-But and pMan-PhBut polymers are implementations of a broader platform that could be extended to the delivery other interesting small molecules and metabolites for wound healing[193, 194, 195, 196]. We demonstrate an implementation of the material using both an aliphatic hydroxyl butyric ester and a phenyl butyric ester, which have differing release kinetics. Because the wound healing process is so dynamic, the exact timing of therapeutic release must be considered for each drug delivered[197]. Furthermore, as mentioned above, the pendant mannose groups serve to enhance solubility and promote internalization, but could further promote an immunosuppressive, anti-inflammatory environment via mannose receptor crosslinking[198]. Finally, the high molecular weight polymers, relative to small molecules like butyrate, increase viscosity and thus promote hydration in the wound[199].

The therapeutic potential of butyrate is especially promising due to its established role in maintaining barrier integrity in the gut[200, 201]. To date, most therapeutic efforts using butyrate have involved delivery to the gut to modulate disease states therein, including inflammatory bowel disease[202], Crohn's Disease[203], diabetic inflammation[204], and even colorectal cancer[200]. Butyrate's topical administration has been considered and attempted in various murine wound models[205, 206, 207, 208], but its translational potential is limited due to its particularly foul smell[209] and common need for co-delivery with another therapeutic agent. However, these accounts point to key mechanistic steps in butyrate's therapeutic efficacy, including inhibition of histone deacetylase, NLRP3 inflammasome, and pro-inflammatory cytokine production[210].

There have been many attempts to solve the large clinical problem of non-healing diabetic wounds with few clinically impactful outcomes, leaving the current standard of care to rely primarily on physical measures such as surgical debridement and wound offloading[166, 211, 212]. Outside of these methods, the many attempts made to improve chronic wound healing outcomes can be categorized into three broad approaches. First, dressings and hydrogels which act to keep the wound clean and moist[166]. These dressings cover a wide array of com-

positions, but only provide moisture regulation and in some cases antimicrobial activity[213]. Even with improvements made in the field, there remains to be seen high-quality evidence that suggests any significant differences in wound healing outcomes when comparing various types of dressing[168, 214, 215]. Second, delivery of growth factors and cytokines which aim to modulate the wound microenvironment. This approach has shown some promise, with the clinical approval of Becaplermin, a topically-applied PDGF-BB-containing gel[216]. Many other growth factors have been tested, with limited clinical success due to both their short half-life and their widespread effects if introduced into systemic circulation[108, 217]. The pleiotropic nature of protein based therapeutics is a clear pitfall and proves to be a continued difficulty when ensuring their targeted effects, though engineering attempts have been made to counter such unwanted activity[110, 93, 127, 92]. Third, cell based therapies attempt to repopulate the wound with cells directly involved in healing. This approach has shown some small scale success with little consensus on optimal cell types [218]. However, regardless of efficacy, cell based treatments are troubled with the problem of scale-up, making this approach translationally challenging within the current production workflow and its constraints[219, 220].

The work detailed here provides insight into the characterization of a new bioactive material that has utility in the treatment of chronic wounds. The efficacy is promising and there are some clear mechanistic signals on how our new material pro-drug modulates the wound microenvironment. Subsequent work should be focused on the mechanistic underpinnings of how this therapeutic is potentiating the healing efficacy it demonstrates. Our data clearly demonstrate induction of immunological chemokines and cytokines thought to be beneficial for wound healing. An additional explanation for the improved healing could be HIF-1 $\alpha$  induction, which is closely tied to improved wound healing outcomes [193, 221]. It has been established that butyrate can induce the expression of HIF-1 $\alpha$  [222, 223]. Further, our data demonstrates increased VEGF-A expression, a downstream factor induced through HIF-1 $\alpha$

activity, following pMan-But treatment [224, 225]. Another mechanistic explanation could be butyrate’s direct activity on keratinocytes, the main cellular population responsible for re-epithelization[36]. Butyrate has been shown to induce keratinocyte differentiation and improved wound closure in vitro [226, 227]. Furthermore, it has recently been shown that butyrate promotes and accelerates the differentiation of epidermal keratinocytes by directly altering their metabolism, enhancing skin barrier function [228]. pMan-But treatment may induce keratinocyte differentiation and migration through a butyrate-mediated metabolic shift, ultimately improving wound closure.

In conclusion, we have demonstrated the utility of a mannose-decorated co-polymer for the sustained and appropriately timed release of butyrate to the diabetic wound microenvironment. The controlled release of our butyrate delivery form enabled the rebalancing of the soluble cytokine and chemokine signals present and subsequently promoted the re-epithelialization of the wound in a type 2 diabetes model of delayed wound healing. Our novel and versatile constructs have the potential to fill a clinical gap for the treatment of chronic wounds, a pressing clinical need.

## 4.5 Materials and Methods

### 4.5.1 *Small Molecule Synthesis*

Unless otherwise stated, chemicals were reagent grade and purchased from Sigma–Aldrich. All NMR spectra were collected on a Bruker Avance-II 400 MHz NMR and analyzed with MnovaNMR (Mestrelab). Mannose monomer and azide-terminated RAFT chain transfer agent were synthesized as previously described[178]. Full synthesis schema with structures provided in the supplementary information.

**N-(2-butanoyloxyethyl) methacrylamide (BMA):** N-(2-hydroxyethyl) methacrylamide (3.30 mL, 25.6 mmol, 1.0 eq), triethylamine (7.15 mL, 251.2 mmol, 2.0 eq) and 50

mL DCM were added into a 250 mL flask. After the reaction system was cooled down by an ice bath, butyric anhydride (5.00 mL, 30.7 mmol, 1.2 eq) was added dropwise under the protection of nitrogen and was allowed to react overnight. The reaction mixture was filtered and washed sequentially by ammonium chloride solution, sodium bicarbonate solution, then water. After drying by anhydrous magnesium sulfate, the organic layer was concentrated by rotary evaporation, pure product was isolated on a silica column using DCM/MeOH (MeOH fraction v/v from 0% to 5%). The product was obtained as pale yellow oil (4.56 g, 89.6%). MS(ESI).  $C_{10}H_{17}NO_3$ , m/z calculated for  $[M+H]^+$ : 199.12, found: 199.1.  $^1H$ -NMR (400 MHz, d-Chloroform)  $\delta$  0.95 (t, 3H), 1.66 (m, 2H), 1.97 (s, 3H), 2.32 (t, 2H), 3.59 (dt, 2H), 4.23 (t, 2H), 5.35 (s, 1H), 5.71 (s, 1H), 6.19 (br s, 1H).

**4-butanoyloxybenzoic acid:** 4-hydroxybenzoic acid (1 g, 7.2 mmol, 1 eq) and triethylamine (4.04 mL, 28.8 mmol, 4 eq) were dissolved in dry DCM. To that solution, butanoic anhydride (1.42 mL, 8.6 mmol, 1.2 eq) was added. After 8 h, the solvent was removed by rotary evaporation and the crude product was purified on a silica column using DCM/MeOH (MeOH fraction v/v 0% to 2%). The product was white solid (0.92 g, yield 61%). MS (ESI).  $C_{11}H_{12}O_4$ , m/z calculated for  $[M+H]^+$ : 208.07, found: 208.0.  $^1H$ -NMR (400 MHz, d-Chloroform)  $\delta$  8.12 (d, 2H), 7.16 (d, 2H), 2.56 (t, 2H), 1.82 (m, 2H), 1.05 (t, 3H).

**N-[2-(4-butanoyloxybenzoyloxy)ethyl] methacrylamide (PhBMA):** Synthesized 4-butanoyloxybenzoic acid (0.67 g, 3.2 mmol, 1.0 eq), N-(2-hydroxyethyl) methacrylamide (HEMA, 0.62 g, 4.8 mmol, 1.5 eq), and DCC (0.99 g, 4.8 mmol, 1.5 eq) were dissolved in dry DCM. The reaction mixture was stirred at 0 °C for 30 min. After that time, 4-dimethylaminopyridine (19 mg, 0.15 mmol, 0.05 eq) dissolved in dry DCM was added to the reaction mixture dropwise. The reaction was allowed to rise to room temperature overnight. The reaction mixture was filtered and solvent was removed by rotary evaporation. The crude product was purified on a silica column using ethyl acetate:hexanes 1:1 v/v. The product was white solid (0.98 g, yield 96%). MS (ESI).  $C_{17}H_{21}NO_5$ , m/z calculated for  $[M+H]^+$ :

319.14, found: 319.1.  $^1\text{H-NMR}$  (400 MHz, d-Chloroform)  $\delta$  8.07 (d, 2H), 7.18 (d, 2H), 6.24 (br, 1H), 5.71 (s, 1H), 5.35 (s, 1H), 4.48 (m, 2H), 3.72 (m, 2H), 2.57 (t, 2H), 1.97 (s, 3H), 1.79 (m, 2H), 1.05 (t, 3H).

#### 4.5.2 *Polymer Synthesis and Characterization*

The polymerizations of pMan-But or pMan-PhBut were similar as described in a previous paper regarding other side-chain glycopolymers[178]. Briefly, mannose monomer (300 mg, 1.03 mmol), HEMA (Combi Blocks, 500 mg, 3.50 mmol), and butyrate monomer (for pMan-But: BMA, 400 mg, 2.00 mmol; for pMan-PhBut: PhBMA, 400 mg, 1.26 mmol) were dissolved in dry DMF in a Schlenk tube. To that solution, azide CTA (30 mg, 0.05 mmol) and free radical initiator AIBN (2 mg, 0.01 mmol) were added. The reaction vessel was degassed via four freeze-pump-thaw cycles and then heated to 70 °C to initiate polymerization. After 14 h, the reaction vessel was immersed in liquid nitrogen to stop the reaction. The polymer was precipitated in cold acetone three times. The final product was dried under reduced pressure. The product was white powder (360 mg, yield 72%). The polymer was characterized by  $^1\text{H-NMR}$  and GPC.

GPC characterizations of pMan-But or pMan-PhBut were performed on Tosoh EcoSEC size exclusion chromatography System using Tosoh SuperAW3000 column. Samples were dissolved in eluent DMF with 0.01 M LiBr at 1 mg/mL. The temperature of the column was set to 50 °C. Refractive index (RI) detector was used to detect polymers. Number averaged molecular weight, weight averaged molecular weight, and polydispersity index were determined via the column calibration using PMMA as standards.

Both the pMan-But and pMan-PhBut used in the biological studies had a number average molecular weight of 11 kDa. The butyrate content of pMan-But or pMan-PhBut was determined by LC-MS/MS after the complete hydrolysis catalyzed by NaOH.

### 4.5.3 Butyrate Release Kinetic Characterization

**Sample preparation:** Samples were prepared and derivatized as described elsewhere[229]. Briefly, pMan-But or pMan-PhBut was dissolved in RPMI complete cell culture media (pH 7.4), PBS buffer, or pH 5.3 acetate buffer at a concentration of 10 mg/mL. 20  $\mu\text{L}$  of the solution was transferred into 500  $\mu\text{L}$  of water:acetonitrile 1:1 v/v at 0, 4, 8, 24, 52, 72, 96, and 144 h. The sample was centrifuged using Amicon Ultra (Merck, 3 kDa molecular mass cutoff) at  $13,000 \times g$  for 15 min, to remove polymers. The filtrate was stored at  $-80\text{ }^{\circ}\text{C}$  before derivatization.

**Sample derivatization:** 3-nitrophenylhydrazine (NPH) stock solution was prepared at 0.02 M in water:acetonitrile 1:1 v/v. EDC stock solution was prepared at 0.25 M in water:acetonitrile 1:1 v/v. 4-methylvaleric acid was added as internal standard. Samples were mixed with NPH stock and EDC stock at 1:1:1 ratio by volume. The mixture was placed in a heating block at  $60\text{ }^{\circ}\text{C}$  for 30 min. Samples were transferred into HPLC vials and stored at  $4\text{ }^{\circ}\text{C}$  before analysis.

**LC conditions:** The instrument used for quantification of butyrate was Agilent 1290 UHPLC. The column used was Thermo Scientific C18  $4.6 \times 50\text{ mm}$ , 1.8  $\mu\text{m}$  particle size, at room temperature. Mobile phase A: water with 0.1% v/v formic acid. Mobile phase B: acetonitrile with 0.1% v/v formic acid. The injection volume was 5.0  $\mu\text{L}$  and the flow rate was 0.5 mL/min. Gradient of solvent: 15% mobile phase B at 0.0 min; 100% mobile phase B at 3.5 min; 100% mobile phase B at 6.0 min; 15% mobile phase B at 6.5 min.

**ESI-MS/MS method:** The instrument used to detect butyrate was Agilent 6460 Triple Quad MS-MS. Both derivatized butyrate-NPH and 4-methylvaleric-NPH were detected in negative mode. The MS conditions were optimized on pure butyrate-NPH or 4-methylvaleric-NPH at 1 mM. The fragment voltage was 135 V and collision energy was set to 18 V. Multiple reaction monitoring (MRM) of  $222 \rightarrow 137$  was assigned to butyrate, and MRM of  $250 \rightarrow 137$  was assigned to 4-methylvaleric acid as internal standard. The ratio between MRM of

butyrate and 4-methylvaleric acid was used to quantify the concentration of butyrate. For butyrate releasing study, the results were plotted by Prism software (GraphPad) and fitted by exponential plateau model to calculate first order reaction constant.

#### 4.5.4 *In Vitro Bioactivity Characterization*

Murine BMDCs were prepared from C57Bl/6 mice (Charles River) as previously described[230]. Day 9 BMDCs were seeded at a density of 200,000 cells/well in a round bottom 96-well plate in IMDM with 10% FBS and 2% penicillin/streptomycin and incubated at 37°C. After 1 day, cells were treated with pMan-But, pMan-PhBut, or unmodified sodium butyrate (NaBut) at a concentration of 1 mM butyrate equivalent. After 18 hours, LPS was added to a final concentration on 100 ng/mL. 24 hours after LPS stimulation, cells and supernatant were analyzed. ELISA kits were used for IL-12p70 (Invitrogen #88-7121-88) and TNF $\alpha$  (Invitrogen #88-7324-88) quantification.

Prior to flow cytometry, anti-RALDH1 (ALDH1A1, Invitrogen #PIPA511537, Polyclonal) and anti-Histone 4 (H4, Abcam #ab177790, clone EPR16606) antibodies were conjugated to fluorophores using Alexa Fluor antibody labeling kits (A20181) according to manufacturer's protocol. Other antibodies used included PE-Cy7 conjugated anti-LAP (Fisher Scientific #50-112-3461, clone TW7-16B4), PerCP-Cy5.5 conjugated anti-CD40 (BioLegend #124623, clone 3/23), BUV737 conjugated anti-CD80 (BD #612773, clone 16-10A1), and APC-eFluor780 conjugated anti-CD86 (Invitrogen #47-0862-82, clone GL1). BMDCs were stained for flow cytometry. Cells were washed once in PBS and stained with LD Violet (Invitrogen #L23105) (1:500) and Fc-block (1:200) for 15 minutes at 4°C. Cells were washed in PBS + 2% FBS and surface stain was added in PBS + 2% FBS for 30 mins at 4°C. Cells were washed, fixed, and permeabilized with Foxp3 transcription factor kit (eBioscience #00-5521-00). Intracellular antibodies, including H4 and RALDH1, were added in permeabilization buffer for 1 hour at RT. Cells were washed per manufacturer's protocol and resuspended in

PBS + 2% FBS and collected on a BD LSRFortessa, with data analysis in FlowJo.

#### *4.5.5 Mouse skin chronic wound healing model*

Male C57BLKS/J-m/Lepr db (db/db) 8-10-week-old mice (The Jackson Laboratory) were used. Their backs were shaved and cleaned and four full-thickness punch-biopsy wounds (6 mm diameter) were created in each mouse. Each wound was splinted open using a silicone ring (inner diameter 8 mm, outer diameter 12 mm) to prevent contraction. Immediately following wound induction, PBS, 1% HA, or 1% HA + pMan-But were topically applied to the wounds. The butyrate constructs contained 10% w/w butyrate equivalent. The wounds were covered with Adaptic dressing and sealed with adhesive film. Mice were single caged after the wounding surgery. After 7 and 11 days, mice were euthanized, and the skin wounds were carefully excised for histological analysis. All experiments using mice received approval from the Institutional Animal Use Committee of the University of Chicago under ACUP 72450. The animals' care was in accordance with institutional guidelines. The 11 day time point experiment was replicated a total of two times for a final sample size of PBS (n = 30), 1% HA (n = 23), pMan-But (n = 26).

#### *4.5.6 Cytokine profile in wound tissue*

Male C57BLKS/J-m/Lepr db (db/db) 8-10-week-old mice (The Jackson Laboratory) were used. Skin wounds were treated with formulations as described above. After 2 days and 7 days, the wounded skin was removed as described above and transferred to T-Per Solution (ThermoFisher) in Lysing Matrix D containing tubes (MP Biomedical) and homogenized (MP Biomedical). Then, the solution was centrifuged, and the supernatant was retained for analysis using LegendPlex Mouse Cytokine Release Syndrome Multiplex Kit (BioLegend) carried out according to manufacturer's instruction. Cytokine normals were normalized to total protein content per BCA assay (ThermoFisher).

#### *4.5.7 Histomorphometric analysis of wound sections*

Wounds were fixed overnight in 2% PFA and cut down the center into two and embedded into paraffin for histological analysis on 5  $\mu\text{m}$  serial sections. The extent of reepithelization was measured blindly by histomorphometric analysis of tissue sections (H&E stain) using QuPath software (University of Edinburgh). For analysis of re-epithelization, the distance that the epithelium had traveled across the wound was measured; the muscle edges of the panniculus carnosus were used as an indicator for the wound boundary; and reepithelization was calculated as the percentage of the distance between the edges of the panniculus carnosus muscle.

### **4.6 Author Contributions**

A.L.L., A.J.S., R.W., and J.A.H. designed the project. R.W., A.J.S., M.M.R. synthesized materials. A.L.L., A.J.S., E.A.W., and S.C. performed the experiments. A.L.L., A.J.S., R.W., M.M.R., E.A.W and J.A.H. analyzed the data. A.L.L., A.J.S., and J.A.H. wrote the manuscript. All authors edited and approved the final manuscript.

### **4.7 Funding**

We thank the Chicago Immunoengineering Innovation Center (CIIC) for the funding for this project.

### **4.8 Acknowledgements**

We thank the University of Chicago Nuclear Magnetic Resonance Spectroscopy Core Facility, Mass Spectrometry Core Facility, Human Tissue Resource Center, and Light Microscopy Core for respective services. Parts of this work were carried out at the Soft Matter Characterization Facility of the University of Chicago, a shared facility at the University of

Chicago Materials Research Science and Engineering Center, supported by National Science Foundation under award number DMR-2011854. Parts of these figures were created on BioRender.com.

## **4.9 Conflicts of Interest**

J.A.H., A.L.L., A.J.S., R.W., and M.M.R. are inventors on a provisional patent application on this technology. All other authors declare no conflict of interest.

## CHAPTER 5

# DISCUSSION, LIMITATIONS, FUTURE DIRECTIONS, AND CONCLUSIONS

The main objective of this thesis was to develop novel therapeutic interventions for the treatment of non-healing diabetic wounds. The dysfunctional wound microenvironment caused by the diabetic disease state creates both an interesting but complex target to modulate and subsequently improve healing. We pursued this modulation through two main approaches: cytokine engineering and materials science approaches. However, it should be acknowledged that other approaches such as virus-mediated delivery strategies for transient expression of cytokines are also being pursued. Additionally, cellular based therapeutic development remains of strong interest for treatment of non-healing wounds. Our work demonstrates the nuances of the perturbed wound healing process by demonstrating that there are multiple cellular targets that can be pursued to improve healing in the diabetic wound. In this chapter, we provide conclusions of the three projects encompassed by our dual pronged strategy and describe their limitations and future directions.

### 5.1 Discussion, Limitations, and Future Directions in Cytokine Engineering

In Chapters 2 and 3, we demonstrate the development and delivery of cytokine based therapies, upon either topical or systemic delivery actively alter the cellular composition within the diabetic wound. One overarching limitation to this body of work is the mouse model used. While the db/db mouse model is the 'gold standard' for diabetic-type non-healing wounds, mice heal through different mechanisms (primarily contraction) when compared to humans, while steps were taken to mitigate these differences, the model itself is an imperfect tool and the results herein-above should be regarded with this in mind.

In Chapter 2 we show that topical application of CBD-SA-IL-4 is better localized to the wound environment through collagen affinity and subsequently enhances macrophage recruitment and polarization towards pro-regenerative (M2) phenotypes both *in vitro* and *in vivo*. One potential limitation of this strategy is that it relies on the modulation of a particular cellular subset and human diabetic wounds tend to be heterogeneous - perhaps making the IL-4 directed modulation less relevant or effective in human disease. Though the recruitment of immune cells to the wound does seem to be universally required in human diabetic wounds, perhaps alleviating some of this concern as our approach did result in more immune infiltration. In Chapter 3 we also improved immune cell in Flt3L treated wounds - with particular regard to the dendritic cell compartment. This is striking because it has been previously reported, in mice, that DCs are limited in the diabetic wound - something our therapeutic approach addresses [62]. Again, a limitation with this approach is that DCs have been poorly characterized in the human diabetic wound.

The route of administration in the clinical setting is another important consideration. In Chapter 2 we utilize topical application, while in Chapter 3 we test systemic administration through subcutaneous (s.c.) injection. We believe that both approaches allow for sustained release of the cytokine therapeutic; topical application being retained in the wound environment and s.c. administration draining to the lymph node and causing a subsequent increase in cellular recruitment to the wound environment. Ultimately, we believe that systemic administration, in particular s.c. injection would be transitionally favored as it provides the opportunity for patient directed treatment and potentially the ability to target deep tissue wounds, something that topically therapies cannot address.

The above mentioned conclusion provides the interesting future direction for the systemically delivered Flt3L therapy and its application in radiation induced oral mucositis (RIOM) - an example of deep tissue lesions that topically based therapies cannot adequately address. This complication is common when patients with head and neck cancers undergo focused

radiation therapy, and despite its name, can also occur following chemotherapy as well - though less common. This complication is considered a dose limiting toxicity leading to the pausing or total cessation of treatment, which in turn causes a lose in tumor control [231]. Currently the primary approaches to managing RIOM include two factors, prevention and symptomatic treatment, neither of which address the underlying causes of the complication [232]. Furthermore, these management strategies (i.e. management of good oral hygiene and Palifermin - recombinant keratinocyte growth factor for prevention) are limited in their success. Beyond these treatment, management of pain is the primary goal of treatment (i.e. use of NSAIDs, analgesics, and opioids). One hurdles for development of treatment for RIOM is the location of the wounds. The lesions formed in the oral cavity are not conducive to treatment via topical therapy, a formulation commonly used for non-healing wounds.

The pathogenesis of RIOM is initiated by oral mucosa injury and then is potentiated through both DNA and non-DNA damage including: reactive oxygen species (ROS), induction of  $\text{NF}\kappa\text{B}$ , and release of proinflammatory soluble signals, further propagating cellular damage and apoptosis in a positive feedback loop [232]. Like diabetic wounds, this immune mediated focused pathogenesis lends itself to modulation through other immune signals that could direct regeneration of the mucosal barrier, without compromising tumor control. Flt3L and its engineered constructs lend themselves well to this purpose [233]. As we saw in Chapter 3, these therapies can be delivered systemically - a requirement of this indication, and these constructs are capable of modulating the wound microenvironment through the expansion of DCs, which are known as professional phagocytes, a cell type that could lower the apoptotic load within the oral mucosa upon radiation or chemotherapy induced insult. An additional benefit to the use of Flt3L mediated prevention of RIOM is that Flt3L has already been well documented in human subjects to enhance the effects of radiation for tumor control, and its concurrent safety data in humans is favorable.

We tested the pre-treatment of multiple Flt3L constructs in a single-dose head irra-

diation model for the prevention of RIOM. The study consisted of five groups; healthy (non-irradiated), no treatment control (saline + irradiation), wild type (WT) Flt3L and irradiation and serum albumin fused Flt3L (Flt3L-SA). The saline or Flt3L constructs were administered three days prior to radiation therapy in otherwise healthy mice. Upon euthanasia nine days post irradiation we harvested the tongues for macroscopic analysis via toluidine blue stain as well as microscopic analysis via H&E histology. It was seen that Flt3L-SA significantly decreased the ulcerated area on the tongues when compared to the no treatment control. This result provides exciting support for the pursuit of the development of Flt3L treatment for non-healing wounds outside of exclusively the diabetic disease state.

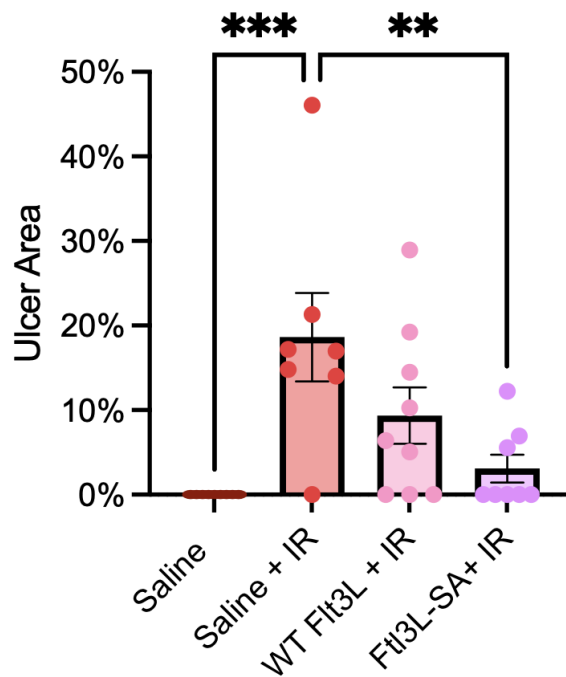


Figure 5.1: In vivo RIOM ulceration area. Quantification via H&E images of tongue mucosal structure. Statistical analysis was performed using ordinary two-way analysis of variance with Dunnett's multiple comparison test against Saline + IR. \* $p < 0.05$ , \*\* $p < 0.01$ , \*\*\* $p < 0.001$ , \*\*\*\* $p < 0.0001$ , ns = not significant.

## 5.2 Discussion, Limitations, and Future Directions in Polymer Based Therapeutics

In Chapter 4 we discuss the use of a mannose-decorated co-polymer for the controlled release of the microbial metabolite butyrate (pMan-But). One clinical limitation to the use of polymer based therapies is their manufacturing processes, while less expensive when compared to biologic therapeutics, polymer production is plagued with the batch-to-batch variability causing concern for their clinical development. When compared to previous chapters, this approach targets a different aspect of the dysfunctional diabetic wound environment, what we propose to be fibroblasts and keratinocytes instead of the immune cells seen to be targeted in Chapters 2 and 3. The primary future direction of this project could be focused on teasing out the mechanism that is implicated in the improved healing seen after pMan-But treatment. While we have detailed the soluble mediator at play it would be useful to confirm the cellular compartments mediating these positive changes. Furthermore, it would be interesting to investigate if pMan-But induces any functional change in the biomechanics of the healed wound (i.e. the strength of the healed area following closure). If it were to be found that pMan-But results in improved functional wound closure it could be utilized in other forms of topically accessible non-healing wounds outside of the diabetic disease state such as pressure ulcers.

## 5.3 Conclusions

In conclusion, this body of work describes three fundamentally different approaches to treat non-healing diabetic wounds, depicting the multiple lens and the complex balances at play within the healing wound. Additionally, we propose promising future directions beyond the scope of the diabetic disease state. These treatments all have the potential to be moved forward toward clinical development and benefit patients with non-healing wounds.

## REFERENCES

- [1] Erika Maria Tottoli, Rossella Dorati, Ida Genta, Enrica Chiesa, Silvia Pisani, and Bice Conti. Skin wound healing process and new emerging technologies for skin wound care and regeneration. *Pharmaceutics*, 12(8):735, 2020.
- [2] Madeleine Flanagan. *Wound healing and skin integrity: principles and practice*. John Wiley & Sons, 2013.
- [3] Michael S Hu, Mimi R Borrelli, H Peter Lorenz, Michael T Longaker, and Derrick C Wan. Mesenchymal stromal cells and cutaneous wound healing: a comprehensive review of the background, role, and therapeutic potential. *Stem cells international*, 2018, 2018.
- [4] Shah Jumaat Mohd Yussof, Effat Omar, Dinker R Pai, and Suneet Sood. Cellular events and biomarkers of wound healing. *Indian Journal of Plastic Surgery*, 45(02):220–228, 2012.
- [5] II George Broughton, Jeffrey E Janis, and Christopher E Attinger. The basic science of wound healing. *Plastic and reconstructive surgery*, 117(7S):12S–34S, 2006.
- [6] Henri H Versteeg, Johan WM Heemskerk, Marcel Levi, and Pieter H Reitsma. New fundamentals in hemostasis. *Physiological reviews*, 93(1):327–358, 2013.
- [7] Dougald M Monroe and Maureane Hoffman. What does it take to make the perfect clot? *Arteriosclerosis, thrombosis, and vascular biology*, 26(1):41–48, 2006.
- [8] Raheel Chaudhry, Syed Muhammad Usama, and Hani M Babiker. Physiology, coagulation pathways. *StatPearls*, 2018.
- [9] Robert AS Ariëns, Thung-Shenq Lai, John W Weisel, Charles S Greenberg, and Peter J Grant. Role of factor xiii in fibrin clot formation and effects of genetic polymorphisms. *Blood, The Journal of the American Society of Hematology*, 100(3):743–754, 2002.
- [10] JG Pool. Normal hemostatic mechanisms: a review. *The American journal of medical technology*, 43(8):776–780, 1977.
- [11] Melanie Rodrigues, Nina Kosaric, Clark A Bonham, and Geoffrey C Gurtner. Wound healing: a cellular perspective. *Physiological reviews*, 99(1):665–706, 2019.
- [12] Moritz Peiseler, Paul Kubes, et al. More friend than foe: the emerging role of neutrophils in tissue repair. *The Journal of clinical investigation*, 129(7):2629–2639, 2019.
- [13] Yingjun Su and Ann Richmond. Chemokine regulation of neutrophil infiltration of skin wounds. *Advances in wound care*, 4(11):631–640, 2015.
- [14] Chao Shi and Eric G Pamer. Monocyte recruitment during infection and inflammation. *Nature reviews immunology*, 11(11):762–774, 2011.

- [15] Simon Yona, Ki-Wook Kim, Yochai Wolf, Alexander Mildner, Diana Varol, Michal Breker, Dalit Strauss-Ayali, Sergey Viukov, Martin Williams, Alexander Misharin, et al. Fate mapping reveals origins and dynamics of monocytes and tissue macrophages under homeostasis. *Immunity*, 38(1):79–91, 2013.
- [16] Ralph van Furth and Zanvil A Cohn. The origin and kinetics of mononuclear phagocytes. *The Journal of experimental medicine*, 128(3):415–435, 1968.
- [17] Donna L Bratton and Peter M Henson. Neutrophil clearance: when the party is over, clean-up begins. *Trends in immunology*, 32(8):350–357, 2011.
- [18] Sophia Maschalidi, Parul Mehrotra, Burcu N Keçeli, Hannah KL De Cleene, Kim Lecomte, Renée Van der Cruyssen, Pauline Janssen, Jonathan Pinney, Geert van Loo, Dirk Elewaut, et al. Targeting slc7a11 improves efferocytosis by dendritic cells and wound healing in diabetes. *Nature*, 606(7915):776–784, 2022.
- [19] Paulina Krzyszczyk, Rene Schloss, Andre Palmer, and François Berthiaume. The role of macrophages in acute and chronic wound healing and interventions to promote pro-wound healing phenotypes. *Frontiers in physiology*, 9:419, 2018.
- [20] Derek S Whelan, Noel M Caplice, and Anthony JP Clover. Mesenchymal stromal cell derived ccl2 is required for accelerated wound healing. *Scientific reports*, 10(1):1–12, 2020.
- [21] Yuko Ishida, Yumi Kuninaka, Mizuho Nosaka, Machi Furuta, Akihiko Kimura, Akira Taruya, Hiroki Yamamoto, Emi Shimada, Mariko Akiyama, Naofumi Mukaida, et al. Ccl2-mediated reversal of impaired skin wound healing in diabetic mice by normalization of neovascularization and collagen accumulation. *Journal of Investigative Dermatology*, 139(12):2517–2527, 2019.
- [22] Anisyah Ridiandries, Joanne TM Tan, and Christina A Bursill. The role of chemokines in wound healing. *International journal of molecular sciences*, 19(10):3217, 2018.
- [23] Timothy J Koh and Luisa Ann DiPietro. Inflammation and wound healing: the role of the macrophage. *Expert reviews in molecular medicine*, 13, 2011.
- [24] Christopher J Ferrante and Samuel Joseph Leibovich. Regulation of macrophage polarization and wound healing. *Advances in wound care*, 1(1):10–16, 2012.
- [25] Margaret L Novak and Timothy J Koh. Macrophage phenotypes during tissue repair. *Journal of leukocyte biology*, 93(6):875–881, 2013.
- [26] Ning Xu Landén, Dongqing Li, and Mona Ståhle. Transition from inflammation to proliferation: a critical step during wound healing. *Cellular and Molecular Life Sciences*, 73(20):3861–3885, 2016.

- [27] Diana A Yanez, Richard K Lacher, Aurobind Vidyarthi, and Oscar R Colegio. The role of macrophages in skin homeostasis. *Pflügers Archiv-European Journal of Physiology*, 469(3):455–463, 2017.
- [28] Jacqueline Larouche, Sumit Sheoran, Kenta Maruyama, and Mikael M Martino. Immune regulation of skin wound healing: mechanisms and novel therapeutic targets. *Advances in wound care*, 7(7):209–231, 2018.
- [29] Gaëtan Juban and Bénédicte Chazaud. Dcs unchained: Whetting dendritic-cell appetite boosts wound healing. *Immunity*, 55(7):1156–1158, 2022.
- [30] Gregory S Schultz, Gloria A Chin, Lyle Moldawer, and Robert F Diegelmann. 23 principles of wound healing. *Mechanisms of vascular disease: a reference book for vascular specialists*, page 423, 2011.
- [31] Marcia G Tonnesen, Xiaodong Feng, and Richard AF Clark. Angiogenesis in wound healing. In *Journal of investigative dermatology symposium proceedings*, volume 5, pages 40–46. Elsevier, 2000.
- [32] Samielle K Brancato and Jorge E Albina. Wound macrophages as key regulators of repair: origin, phenotype, and function. *The American journal of pathology*, 178(1):19–25, 2011.
- [33] Alessandro Fantin, Joaquim M Vieira, Gaia Gestri, Laura Denti, Quenten Schwarz, Sergey Prykhozhiy, Francesca Peri, Stephen W Wilson, and Christiana Ruhrberg. Tissue macrophages act as cellular chaperones for vascular anastomosis downstream of vegf-mediated endothelial tip cell induction. *Blood, The Journal of the American Society of Hematology*, 116(5):829–840, 2010.
- [34] Markus Affolter, Rolf Zeller, and Emmanuel Caussinus. Tissue remodelling through branching morphogenesis. *Nature reviews Molecular cell biology*, 10(12):831–842, 2009.
- [35] JM Reinke and H Sorg. Wound repair and regeneration. *European surgical research*, 49(1):35–43, 2012.
- [36] Irena Pastar, Olivera Stojadinovic, Natalie C Yin, Horacio Ramirez, Aron G Nusbaum, Andrew Sawaya, Shailee B Patel, Laiqua Khalid, Rivkah R Isseroff, and Marjana Tomic-Canic. Epithelialization in wound healing: a comprehensive review. *Advances in wound care*, 3(7):445–464, 2014.
- [37] Pierre A Coulombe. Towards a molecular definition of keratinocyte activation after acute injury to stratified epithelia. *Biochemical and biophysical research communications*, 236(2):231–238, 1997.
- [38] Randle M Gallucci, Dusti K Sloan, Julie M Heck, Anne R Murray, and Sijy J O’Dell. Interleukin 6 indirectly induces keratinocyte migration. *Journal of Investigative Dermatology*, 122(3):764–772, 2004.

- [39] Sabine Werner, Thomas Krieg, and Hans Smola. Keratinocyte–fibroblast interactions in wound healing. *Journal of investigative dermatology*, 127(5):998–1008, 2007.
- [40] Zi-Qing Lin, Toshikazu Kondo, Yuko Ishida, Tatsunori Takayasu, and Naofumi Mukaida. Essential involvement of il-6 in the skin wound-healing process as evidenced by delayed wound healing in il-6-deficient mice. *Journal of leukocyte biology*, 73(6):713–721, 2003.
- [41] Meilang Xue and Christopher J Jackson. Extracellular matrix reorganization during wound healing and its impact on abnormal scarring. *Advances in wound care*, 4(3):119–136, 2015.
- [42] Richard Maynes. *Structure and function of collagen types*. Elsevier, 2012.
- [43] S Dimmeler. Zeiher am. *Akt takes center stage in angiogenesis signaling*. *Circ Res*, 86:4–5, 2000.
- [44] Miguel A Cabrita and Gerhard Christofori. Sprouty proteins, masterminds of receptor tyrosine kinase signaling. *Angiogenesis*, 11:53–62, 2008.
- [45] Mateusz S Wietecha, Wendy L Cerny, and Luisa A DiPietro. Mechanisms of vessel regression: toward an understanding of the resolution of angiogenesis. *New perspectives in regeneration*, pages 3–32, 2013.
- [46] Cecelia C Yates, Priya Krishna, Diana Whaley, Richard Bodnar, Timothy Turner, and Alan Wells. Lack of cxc chemokine receptor 3 signaling leads to hypertrophic and hypercellular scarring. *The American journal of pathology*, 176(4):1743–1755, 2010.
- [47] Thomas Wild, Arastoo Rahbarnia, Martina Kellner, Luboš Sobotka, and Thomas Eberlein. Basics in nutrition and wound healing. *Nutrition*, 26(9):862–866, 2010.
- [48] Afiat Berbudi, Nofri Rahmadika, Adi Imam Tjahjadi, and Rovina Ruslami. Type 2 diabetes and its impact on the immune system. *Current diabetes reviews*, 16(5):442, 2020.
- [49] Vincent Falanga. Wound healing and its impairment in the diabetic foot. *The Lancet*, 366(9498):1736–1743, 2005.
- [50] Frank M Davis, Andrew Kimball, Anna Boniakowski, and Katherine Gallagher. Dysfunctional wound healing in diabetic foot ulcers: new crossroads. *Current Diabetes Reports*, 18(1):1–8, 2018.
- [51] Andrew P Sawaya, Rivka C Stone, Stephen R Brooks, Irena Pastar, Ivan Jozic, Kowser Hasneen, Katelyn O’Neill, Spencer Mehdizadeh, Cheyanne R Head, Natasa Strbo, et al. Deregulated immune cell recruitment orchestrated by foxm1 impairs human diabetic wound healing. *Nature communications*, 11(1):1–14, 2020.

- [52] Savita Khanna, Sabyasachi Biswas, Yingli Shang, Eric Collard, Ali Azad, Courtney Kauh, Vineet Bhasker, Gayle M Gordillo, Chandan K Sen, and Sashwati Roy. Macrophage dysfunction impairs resolution of inflammation in the wounds of diabetic mice. *PloS one*, 5(3):e9539, 2010.
- [53] Sabine A Eming, Paul Martin, and Marjana Tomic-Canic. Wound repair and regeneration: mechanisms, signaling, and translation. *Science translational medicine*, 6(265):265sr6–265sr6, 2014.
- [54] Stephen Wood, Vijayakumar Jayaraman, Erica J Huelsmann, Brian Bonish, Derick Burgad, Gayathri Sivaramakrishnan, Shanshan Qin, Luisa A DiPietro, Andrew Zloza, Chunxiang Zhang, et al. Pro-inflammatory chemokine ccl2 (mcp-1) promotes healing in diabetic wounds by restoring the macrophage response. *PloS one*, 9(3):e91574, 2014.
- [55] Sofia Pavlou, Jaime Lindsay, Rebecca Ingram, Heping Xu, and Mei Chen. Sustained high glucose exposure sensitizes macrophage responses to cytokine stimuli but reduces their phagocytic activity. *BMC immunology*, 19(1):1–13, 2018.
- [56] Kazuichi Maruyama, Jun Asai, Masaaki Ii, Tina Thorne, Douglas W Losordo, and Patricia A D’Amore. Decreased macrophage number and activation lead to reduced lymphatic vessel formation and contribute to impaired diabetic wound healing. *The American journal of pathology*, 170(4):1178–1191, 2007.
- [57] John A Hamilton. Gm-csf in inflammation and autoimmunity. *Trends in immunology*, 23(8):403–408, 2002.
- [58] Nuh Zafer Cantürk, Birol Vural, NilÜFer Esen, Zeynep Cantürk, GÜLgÜN Oktay, GÜLdal Kirkali, and Seyhun Solakoglu. Effects of granulocyte-macrophage colony-stimulating factor on incisional wound healing in an experimental diabetic rat model. *Endocrine research*, 25(1):105–116, 1999.
- [59] Y Fang, S-J Gong, Y-H Xu, BD Hambly, and S Bao. Impaired cutaneous wound healing in granulocyte/macrophage colony-stimulating factor knockout mice. *British Journal of Dermatology*, 157(3):458–465, 2007.
- [60] Y Fang, J Shen, M Yao, KW Beagley, BD Hambly, and Shisan Bao. Granulocyte-macrophage colony-stimulating factor enhances wound healing in diabetes via upregulation of proinflammatory cytokines. *British Journal of Dermatology*, 162(3):478–486, 2010.
- [61] Ricardo Marques Da Costa, Fernando Miguel Ribeiro Jesus, Cristina Aniceto, and Mateus Mendes. Randomized, double-blind, placebo-controlled, dose-ranging study of granulocyte-macrophage colony stimulating factor in patients with chronic venous leg ulcers. *Wound Repair and Regeneration*, 7(1):17–25, 1999.
- [62] Natasha Joshi, Lea Pohlmeier, Maya Ben-Yehuda Greenwald, Eric Haertel, Paul Hiebert, Manfred Kopf, and Sabine Werner. Comprehensive characterization of myeloid

- cells during wound healing in healthy and healing-impaired diabetic mice. *European journal of immunology*, 50(9):1335–1349, 2020.
- [63] Minna Piipponen, Dongqing Li, and Ning Xu Landén. The immune functions of keratinocytes in skin wound healing. *International journal of molecular sciences*, 21(22):8790, 2020.
- [64] Amanda S MacLeod and Jonathan N Mansbridge. The innate immune system in acute and chronic wounds. *Advances in wound care*, 5(2):65–78, 2016.
- [65] Thomas J Fahey III, Anita Sadaty, William G Jones II, Annabel Barber, Bruce Smoller, and G Tom Shires. Diabetes impairs the late inflammatory response to wound healing. *Journal of Surgical Research*, 50(4):308–313, 1991.
- [66] Leena Pradhan, Xuemei Cai, Szuhuei Wu, Nicholas D Andersen, Michelle Martin, Junaid Malek, Patrick Guthrie, Aristidis Veves, and Frank W LoGerfo. Gene expression of pro-inflammatory cytokines and neuropeptides in diabetic wound healing. *Journal of Surgical Research*, 167(2):336–342, 2011.
- [67] G Frykberg Robert et al. Challenges in the treatment of chronic wounds. *Advances in wound care*, 2015.
- [68] Jude Edwards and Sally Stapley. Debridement of diabetic foot ulcers. *Cochrane Database of systematic reviews*, 21(1), 2010.
- [69] Maria Narres, Tatjana Kvitkina, Heiner Claessen, Sigrid Droste, Bjoern Schuster, Stephan Morbach, Gerhard Ruemenapf, Kristien Van Acker, and Andrea Icks. Incidence of lower extremity amputations in the diabetic compared with the non-diabetic population: a systematic review. *PloS one*, 12(8):e0182081, 2017.
- [70] Patricia Price. The diabetic foot: quality of life. *Clinical Infectious Diseases*, 39(Supplement\_2):S129–S131, 2004.
- [71] David Dayya, Owen J O’Neill, Tania B Huedo-Medina, Nusrat Habib, Joanna Moore, and Kartik Iyer. Debridement of diabetic foot ulcers. *Advances in Wound Care*, 11(12):666–686, 2022.
- [72] Robert Strohal, J Dissemond, J Jordan O’Brien, A Piaggese, R Rimdeika, T Young, and J Apelqvist. Ewma document: Debridement: An updated overview and clarification of the principle role of debridement. *Journal of wound care*, 22(Sup1):S1–S49, 2013.
- [73] David Dayya, Owen O’Neill, Nusrat Habib, Joanna Moore, Kartik Iyer, and Tania B Huedo-Medina. Debridement of diabetic foot ulcers: public health and clinical implications—a systematic review, meta-analysis, and meta-regression. *BMJ Surgery, Interventions, & Health Technologies*, 4(1), 2022.
- [74] Peter R Cavanagh, Benjamin A Lipsky, Andrew W Bradbury, and Georgeanne Botek. Treatment for diabetic foot ulcers. *The Lancet*, 366(9498):1725–1735, 2005.

- [75] Michael J Mueller, Jay E Diamond, David R Sinacore, Anthony Delitto, Vilray P Blair III, Dolores A Drury, and Steven J Rose. Total contact casting in treatment of diabetic plantar ulcers: controlled clinical trial. *Diabetes Care*, 12(6):384–388, 1989.
- [76] David G Armstrong, Lawrence A Lavery, Heather R Kimbriel, Brent P Nixon, and Andrew JM Boulton. Activity patterns of patients with diabetic foot ulceration: patients with active ulceration may not adhere to a standard pressure off-loading regimen. *Diabetes care*, 26(9):2595–2597, 2003.
- [77] Karen L Andrews, Matthew T Houdek, and Lester J Kiemele. Wound management of chronic diabetic foot ulcers: from the basics to regenerative medicine. *Prosthetics and orthotics international*, 39(1):29–39, 2015.
- [78] David J Margolis, Jayanta Gupta, Ole Hoffstad, Maryte Papdopoulos, Henry A Glick, Stephen R Thom, and Nandita Mitra. Lack of effectiveness of hyperbaric oxygen therapy for the treatment of diabetic foot ulcer and the prevention of amputation: a cohort study. *Diabetes care*, 36(7):1961–1966, 2013.
- [79] Peter Kranke, Michael H Bennett, Marrisona Martyn-St James, Alexander Schnabel, Sebastian E Debus, and Stephanie Weibel. Hyperbaric oxygen therapy for chronic wounds. *Cochrane Database of Systematic Reviews*, 32(6), 2015.
- [80] Lynda D Woodruff, Julie M Bounkeo, Windy M Brannon, Kenneth S Dawes, Cameron D Barham, Donna L Waddell, and Chukuka S Enwemeka. The efficacy of laser therapy in wound repair: a meta-analysis of the literature. *Photomedicine and laser surgery*, 22(3):241–247, 2004.
- [81] Alexandra J Bishop and Elizabeth Mudge. Diabetic foot ulcers treated with hyperbaric oxygen therapy: a review of the literature. *International wound journal*, 11(1):28–34, 2014.
- [82] Haris M Rathur and Andrew JM Boulton. The diabetic foot. *Clinics in dermatology*, 25(1):109–120, 2007.
- [83] Dean T Williams and Keith G Harding. New treatments for diabetic neuropathic foot ulceration: views from a wound healing unit. *Current Diabetes Reports*, 3(6):468–474, 2003.
- [84] JR Hilton, DT Williams, B Beuker, DR Miller, and KG Harding. Wound dressings in diabetic foot disease. *Clinical Infectious Diseases*, 39(Supplement\_2):S100–S103, 2004.
- [85] LL Lloyd, JF Kennedy, P Methacanon, M Paterson, and CJ Knill. Carbohydrate polymers as wound management aids. *Carbohydrate Polymers*, 37(3):315–322, 1998.
- [86] Selvaraj Dhivya, Viswanadha Vijaya Padma, and Elango Santhini. Wound dressings—a review. *BioMedicine*, 5(4):22, 2015.

- [87] Riley S Rees, Martin C Robson, Janice M Smiell, Barbara H Perry, and Pressure Ulcer Study Group. Becaplermin gel in the treatment of pressure ulcers: a phase ii randomized, double-blind, placebo-controlled study. *Wound repair and regeneration*, 7(3):141–147, 1999.
- [88] William J Jeffcoate, Loretta Vileikyte, Edward J Boyko, David G Armstrong, and Andrew JM Boulton. Current challenges and opportunities in the prevention and management of diabetic foot ulcers. *Diabetes care*, 41(4):645–652, 2018.
- [89] Simon Matoori, Aristidis Veves, and David J Mooney. Advanced bandages for diabetic wound healing. *Science translational medicine*, 13(585):eabe4839, 2021.
- [90] Charles E Hart, Andrea Loewen-Rodriguez, and Jan Lessem. Dermagraft: use in the treatment of chronic wounds. *Advances in wound care*, 1(3):138–141, 2012.
- [91] William H Eaglstein and Vincent Falanga. Tissue engineering and the development of apligraf®(R), a human skin equivalent. *Clinical therapeutics*, 19(5):894–905, 1997.
- [92] Jun Ishihara, Ako Ishihara, Kazuto Fukunaga, Koichi Sasaki, Michael JV White, Priscilla S Briquez, and Jeffrey A Hubbell. Laminin heparin-binding peptides bind to several growth factors and enhance diabetic wound healing. *Nature communications*, 9(1):1–14, 2018.
- [93] Priscilla S Briquez, Jeffrey A Hubbell, and Mikael M Martino. Extracellular matrix-inspired growth factor delivery systems for skin wound healing. *Advances in wound care*, 4(8):479–489, 2015.
- [94] Arsalan Latif, Leanne E Fisher, Adam A Dundas, Valentina Cuzzucoli Crucitti, Zeynep Imir, Karen Lawler, Francesco Pappalardo, Benjamin W Muir, Ricky Wildman, Derek J Irvine, et al. Microparticles decorated with cell-instructive surface chemistries actively promote wound healing. *Advanced Materials*, page 2208364, 2022.
- [95] Farida B Ahmad and Robert N Anderson. The leading causes of death in the us for 2020. *Jama*, 325(18):1829–1830, 2021.
- [96] Dídac Mauricio, Núria Alonso, and Mònica Gratacòs. Chronic diabetes complications: the need to move beyond classical concepts. *Trends in Endocrinology & Metabolism*, 31(4):287–295, 2020.
- [97] Andrew JM Boulton, Robert S Kirsner, and Loretta Vileikyte. Neuropathic diabetic foot ulcers. *New England Journal of Medicine*, 351(1):48–55, 2004.
- [98] Gayle E Reiber, LORETTA Vileikyte, EJ de Boyko, Michael Del Aguila, DOUGLAS G Smith, LAWRENCE A Lavery, and AJ Boulton. Causal pathways for incident lower-extremity ulcers in patients with diabetes from two settings. *Diabetes care*, 22(1):157–162, 1999.

- [99] Kate S Smigiel and William C Parks. Macrophages, wound healing, and fibrosis: recent insights. *Current rheumatology reports*, 20(4):1–8, 2018.
- [100] Johannes Westman, Sergio Grinstein, and Pedro Elias Marques. Phagocytosis of necrotic debris at sites of injury and inflammation. *Frontiers in immunology*, 10:3030, 2020.
- [101] Sofia De Oliveira, Emily E Rosowski, and Anna Huttenlocher. Neutrophil migration in infection and wound repair: going forward in reverse. *Nature Reviews Immunology*, 16(6):378–391, 2016.
- [102] João Moura, Elisabet Børsheim, and Eugenia Carvalho. The role of micrnas in diabetic complications—special emphasis on wound healing. *Genes*, 5(4):926–956, 2014.
- [103] João Moura, João Rodrigues, Marta Gonçalves, Cláudia Amaral, Margarida Lima, and Eugénia Carvalho. Impaired t-cell differentiation in diabetic foot ulceration. *Cellular & Molecular Immunology*, 14(9):758–769, 2017.
- [104] Ana Tellechea, Antonios Kafanas, Ermelindo C Leal, Francesco Tecilazich, Sarada Kuchibhotla, Michael E Auster, Iraklis Kontoes, Jacqueline Paolino, Eugenia Carvalho, Leena Pradhan Nabzdyk, et al. Increased skin inflammation and blood vessel density in human and experimental diabetes. *The international journal of lower extremity wounds*, 12(1):4–11, 2013.
- [105] Margaret A Fonder, Gerald S Lazarus, David A Cowan, Barbara Aronson-Cook, Angela R Kohli, and Adam J Mamelak. Treating the chronic wound: A practical approach to the care of nonhealing wounds and wound care dressings. *Journal of the American Academy of Dermatology*, 58(2):185–206, 2008.
- [106] Alexander J Whittam, Zeshaan N Maan, Dominik Duscher, Victor W Wong, Janos A Barrera, Michael Januszyk, and Geoffrey C Gurtner. Challenges and opportunities in drug delivery for wound healing. *Advances in wound care*, 5(2):79–88, 2016.
- [107] Mateusz S Wietecha and Luisa A DiPietro. Therapeutic approaches to the regulation of wound angiogenesis. *Advances in wound care*, 2(3):81–86, 2013.
- [108] Arturo J Martí-Carvajal, Christian Gluud, Susana Nicola, Daniel Simancas-Racines, Ludovic Reveiz, Patricio Oliva, and Jorge Cedeño-Taborda. Growth factors for treating diabetic foot ulcers. *Cochrane Database of Systematic Reviews*, 2(10), 2015.
- [109] Dr Nikolaos Papanas and Efstratios Maltezos. Benefit-risk assessment of becaplermin in the treatment of diabetic foot ulcers. *Drug safety*, 33(6):455–461, 2010.
- [110] Michael JV White, Priscilla S Briquez, David AV White, and Jeffrey A Hubbell. Vegf-a, pdgf-bb and hb-egf engineered for promiscuous super affinity to the extracellular matrix improve wound healing in a model of type 1 diabetes. *NPJ Regenerative Medicine*, 6(1):1–12, 2021.

- [111] YP Sharon Goh, Neil C Henderson, Jose E Heredia, Alex Red Eagle, Justin I Odegaard, Nadja Lehwald, Khoa D Nguyen, Dean Sheppard, Lata Mukundan, Richard M Locksley, et al. Eosinophils secrete il-4 to facilitate liver regeneration. *Proceedings of the National Academy of Sciences*, 110(24):9914–9919, 2013.
- [112] Deng Pan, Lauren Schellhardt, Jesús A Acevedo-Cintrón, Daniel Hunter, Alison K Snyder-Warwick, Susan E Mackinnon, and Matthew D Wood. Il-4 expressing cells are recruited to nerve after injury and promote regeneration. *Experimental Neurology*, 347:113909, 2022.
- [113] Syed Faaiz Enam, Sajidur Rahman Kader, Nicholas Bodkin, Johnathan G Lyon, Mark Calhoun, Cesar Azrak, Pooja Munnial Tiwari, Daryll Vanover, Haichen Wang, Philip J Santangelo, et al. Evaluation of m2-like macrophage enrichment after diffuse traumatic brain injury through transient interleukin-4 expression from engineered mesenchymal stromal cells. *Journal of Neuroinflammation*, 17(1):1–24, 2020.
- [114] Michael Stein, Satish Keshav, Neil Harris, and Siamon Gordon. Interleukin 4 potently enhances murine macrophage mannose receptor activity: a marker of alternative immunologic macrophage activation. *The Journal of experimental medicine*, 176(1):287–292, 1992.
- [115] Kyle A Jablonski, Stephanie A Amici, Lindsay M Webb, Juan de Dios Ruiz-Rosado, Phillip G Popovich, Santiago Partida-Sanchez, and Mireia Guerau-de Arellano. Novel markers to delineate murine m1 and m2 macrophages. *PloS one*, 10(12):e0145342, 2015.
- [116] Anna E Boniakowski, Andrew S Kimball, Benjamin N Jacobs, Steven L Kunkel, and Katherine A Gallagher. Macrophage-mediated inflammation in normal and diabetic wound healing. *The Journal of Immunology*, 199(1):17–24, 2017.
- [117] Robert D Stout, Chuancang Jiang, Bharati Matta, Illya Tietzel, Stephanie K Watkins, and Jill Suttles. Macrophages sequentially change their functional phenotype in response to changes in microenvironmental influences. *The Journal of Immunology*, 175(1):342–349, 2005.
- [118] FM Menzies, FL Henriquez, J Alexander, and CW Roberts. Sequential expression of macrophage anti-microbial/inflammatory and wound healing markers following innate, alternative and classical activation. *Clinical & Experimental Immunology*, 160(3):369–379, 2010.
- [119] Johanna A Knipper, Sebastian Willenborg, Jürgen Brinckmann, Wilhelm Bloch, Tobias Maaß, Raimund Wagener, Thomas Krieg, Tara Sutherland, Ariel Munitz, Marc E Rothenberg, et al. Interleukin-4 receptor  $\alpha$  signaling in myeloid cells controls collagen fibril assembly in skin repair. *Immunity*, 43(4):803–816, 2015.

- [120] Erwei Song, Nengtai Ouyang, Markus Hörbelt, Balazs Antus, Minghui Wang, and Michael S Exton. Influence of alternatively and classically activated macrophages on fibrogenic activities of human fibroblasts. *Cellular immunology*, 204(1):19–28, 2000.
- [121] Kara L Spiller, Rachel R Anfang, Krista J Spiller, Johnathan Ng, Kenneth R Nakazawa, Jeffrey W Daulton, and Gordana Vunjak-Novakovic. The role of macrophage phenotype in vascularization of tissue engineering scaffolds. *Biomaterials*, 35(15):4477–4488, 2014.
- [122] Rita E Mirza, Milie M Fang, William J Ennis, and Timothy J Koh. Blocking interleukin-1 $\beta$  induces a healing-associated wound macrophage phenotype and improves healing in type 2 diabetes. *Diabetes*, 62(7):2579–2587, 2013.
- [123] Rita E Mirza, Milie M Fang, Eileen M Weinheimer-Haus, William J Ennis, and Timothy J Koh. Sustained inflammasome activity in macrophages impairs wound healing in type 2 diabetic humans and mice. *Diabetes*, 63(3):1103–1114, 2014.
- [124] Rita Mirza and Timothy J Koh. Dysregulation of monocyte/macrophage phenotype in wounds of diabetic mice. *Cytokine*, 56(2):256–264, 2011.
- [125] Anca Sindrilaru, Peters Wieschalka, Corina Baican, and Adrian Baican. An unrestrained proinflammatory m1 macrophage population induced by iron impairs wound healing in humans and mice. *Journal of Clinical Investigation*, 121(3):985–997, 2011.
- [126] Ako Ishihara, Jun Ishihara, Elyse Watkins, Andrew Tremain, Mindy Nguyen, and Ani Solanki. Prolonged residence of an albumin-il-4 fusion protein in secondary lymphoid organs ameliorates experimental autoimmune encephalomyelitis. *Nature Biomedical Engineering*, 5(5):387–398, 2021.
- [127] Aslan Mansurov, Abigail Lauterbach, Erica Budina, Aaron T Alpar, Jeffrey A Hubbell, and Jun Ishihara. Immunoengineering approaches for cytokine therapy. *American Journal of Physiology-Cell Physiology*, 321(2):C369–C383, 2021.
- [128] Alessandro Ruggiero, Carlos H Villa, Evan Bander, Diego A Rey, Magnus Bergkvist, Carl A Batt, Katia Manova-Todorova, William M Deen, David A Scheinberg, and Michael R McDevitt. Paradoxical glomerular filtration of carbon nanotubes. *Proceedings of the National Academy of Sciences*, 107(27):12369–12374, 2010.
- [129] Zaverio M Ruggeri and G Loredana Mendolicchio. Adhesion mechanisms in platelet function. *Circulation research*, 100(12):1673–1685, 2007.
- [130] Jun Ishihara, Kazuto Fukunaga, Ako Ishihara, Hans M Larsson, Lambert Potin, Peyman Hosseinchi, Gabriele Galliverti, Melody A Swartz, and Jeffrey A Hubbell. Matrix-binding checkpoint immunotherapies enhance antitumor efficacy and reduce adverse events. *Science translational medicine*, 9(415):ean0401, 2017.

- [131] Aslan Mansurov, Jun Ishihara, Peyman Hosseinchi, Lambert Potin, Tiffany M Marchell, Ako Ishihara, John-Michael Williford, Aaron T Alpar, Michal M Raczy, Laura T Gray, et al. Collagen-binding il-12 enhances tumour inflammation and drives the complete remission of established immunologically cold mouse tumours. *Nature biomedical engineering*, 4(5):531–543, 2020.
- [132] Xiangrong Liu, Jia Liu, Shangfeng Zhao, Haiyue Zhang, Wei Cai, Mengfei Cai, Xunming Ji, Rehana K Leak, Yanqin Gao, Jun Chen, et al. Interleukin-4 is essential for microglia/macrophage m2 polarization and long-term recovery after cerebral ischemia. *Stroke*, 47(2):498–504, 2016.
- [133] Antonio Sica, Alberto Mantovani, et al. Macrophage plasticity and polarization: in vivo veritas. *The Journal of clinical investigation*, 122(3):787–795, 2012.
- [134] Alberto Mantovani, Silvano Sozzani, Massimo Locati, Paola Allavena, and Antonio Sica. Macrophage polarization: tumor-associated macrophages as a paradigm for polarized m2 mononuclear phagocytes. *Trends in immunology*, 23(11):549–555, 2002.
- [135] Amit K Mittal, Rohit Bhardwaj, Riya Arora, Aarti Singh, Monalisa Mukherjee, and Satyendra K Rajput. Acceleration of wound healing in diabetic rats through poly dimethylaminoethyl acrylate–hyaluronic acid polymeric hydrogel impregnated with a didymocarpus pedicellatus plant extract. *ACS omega*, 5(38):24239–24246, 2020.
- [136] Julia E Babensee. Interaction of dendritic cells with biomaterials. In *Seminars in immunology*, volume 20, pages 101–108. Elsevier, 2008.
- [137] Tatiana N Demidova-Rice, Michael R Hamblin, and Ira M Herman. Acute and impaired wound healing: pathophysiology and current methods for drug delivery, part 1: normal and chronic wounds: biology, causes, and approaches to care. *Advances in skin & wound care*, 25(7):304, 2012.
- [138] Moses Lee, Seung Hwan Han, Woo Jin Choi, Kwang Ho Chung, and Jin Woo Lee. Hyaluronic acid dressing (healoderm) in the treatment of diabetic foot ulcer: a prospective, randomized, placebo-controlled, single-center study. *Wound Repair and Regeneration*, 24(3):581–588, 2016.
- [139] HJ You, SK Han, and JW Rhie. Randomised controlled clinical trial for autologous fibroblast-hyaluronic acid complex in treating diabetic foot ulcers. *Journal of wound care*, 23(11):521–530, 2014.
- [140] Mikaël M Martino, Federico Tortelli, Mayumi Mochizuki, Stephanie Traub, Dror Ben-David, Gisela A Kuhn, Ralph Müller, Erella Livne, Sabine A Eming, and Jeffrey A Hubbell. Engineering the growth factor microenvironment with fibronectin domains to promote wound and bone tissue healing. *Science translational medicine*, 3(100):100ra89–100ra89, 2011.

- [141] Antony W Burgess and Donald Metcalf. The nature and action of granulocyte-macrophage colony stimulating factors. *Blood*, 56(6), 1980.
- [142] Christian Wetzler, Heiko Kämpfer, Birgit Stallmeyer, Josef Pfeilschifter, and Stefan Frank. Large and sustained induction of chemokines during impaired wound healing in the genetically diabetic mouse: prolonged persistence of neutrophils and macrophages during the late phase of repair. *Journal of Investigative Dermatology*, 115(2):245–253, 2000.
- [143] Hetvi Gandhi, Remigiusz Worch, Kristina Kurgonaite, Martin Hintersteiner, Petra Schwille, Christian Bökel, and Thomas Weidemann. Dynamics and interaction of interleukin-4 receptor subunits in living cells. *Biophysical journal*, 107(11):2515–2527, 2014.
- [144] Jaroslaw Cendrowski, Agnieszka Mamińska, and Marta Miaczynska. Endocytic regulation of cytokine receptor signaling. *Cytokine & growth factor reviews*, 32:63–73, 2016.
- [145] Masaaki Mori, Suzanne C Morris, Tatyana Orekhova, Mariarosaria Marinaro, Edward Giannini, and Fred D Finkelman. Il-4 promotes the migration of circulating b cells to the spleen and increases splenic b cell survival. *The Journal of Immunology*, 164(11):5704–5712, 2000.
- [146] Pauline Bannon, Sally Wood, Terry Restivo, Laura Campbell, Matthew J Hardman, and Kimberly A Mace. Diabetes induces stable intrinsic changes to myeloid cells that contribute to chronic inflammation during wound healing in mice. *Disease models & mechanisms*, 6(6):1434–1447, 2013.
- [147] Thanh Dinh, Francesco Tecilazich, Antonios Kafanas, John Doupis, Charalambos Gnardellis, Ermelindo Leal, Ana Tellechea, Leena Pradhan, Thomas E Lyons, John M Giurini, et al. Mechanisms involved in the development and healing of diabetic foot ulceration. *Diabetes*, 61(11):2937–2947, 2012.
- [148] Hao Lu, Xiaoyue Wu, Zejing Wang, Li Li, Wen Chen, Mingcan Yang, Da Huo, Wen Zeng, and Chuhong Zhu. Erythropoietin-activated mesenchymal stem cells promote healing ulcers by improving microenvironment. *journal of surgical research*, 205(2):464–473, 2016.
- [149] Dan Liu, Peilang Yang, Min Gao, Tianyi Yu, Yan Shi, Meng Zhang, Min Yao, Yan Liu, and Xiong Zhang. Nlrp3 activation induced by neutrophil extracellular traps sustains inflammatory response in the diabetic wound. *Clinical Science*, 133(4):565–582, 2019.
- [150] Tina Lucas, Ari Waisman, Rajeev Ranjan, Jürgen Roes, Thomas Krieg, Werner Müller, Axel Roers, and Sabine A Eming. Differential roles of macrophages in diverse phases of skin repair. *The Journal of Immunology*, 184(7):3964–3977, 2010.

- [151] Horacio A Ramirez, Irena Pastar, Ivan Jozic, Olivera Stojadinovic, Rivka C Stone, Nkemcho Ojeh, Joel Gil, Stephen C Davis, Robert S Kirsner, and Marjana Tomic-Canic. Staphylococcus aureus triggers induction of mir-15b-5p to diminish dna repair and deregulate inflammatory response in diabetic foot ulcers. *Journal of investigative dermatology*, 138(5):1187–1196, 2018.
- [152] Rivka C Stone, Olivera Stojadinovic, Ashley M Rosa, Horacio A Ramirez, Evangelos Badiavas, Miroslav Blumenberg, and Marjana Tomic-Canic. A bioengineered living cell construct activates an acute wound healing response in venous leg ulcers. *Science translational medicine*, 9(371):eaaf8611, 2017.
- [153] Laura Bonapace, Marie-May Coissieux, Jeffrey Wyckoff, Kirsten D Mertz, Zsuzsanna Varga, Tobias Junt, and Mohamed Bentires-Alj. Cessation of ccl2 inhibition accelerates breast cancer metastasis by promoting angiogenesis. *Nature*, 515(7525):130–133, 2014.
- [154] Chang Rae Rho, Mi-young Park, and Seungbum Kang. Effects of granulocyte-macrophage colony-stimulating (gm-csf) factor on corneal epithelial cells in corneal wound healing model. *PLoS One*, 10(9):e0138020, 2015.
- [155] Hyongbum Kim, Hyun-Jai Cho, Sung-Whan Kim, Bianling Liu, Yong Jin Choi, JiYoon Lee, Young-Doug Sohn, Min-Young Lee, Mackenzie A Houge, and Young-sup Yoon. Cd31+ cells represent highly angiogenic and vasculogenic cells in bone marrow: novel role of nonendothelial cd31+ cells in neovascularization and their therapeutic effects on ischemic vascular disease. *Circulation research*, 107(5):602–614, 2010.
- [156] Uzoagu A Okonkwo, Lin Chen, Da Ma, Veronica A Haywood, May Barakat, Norifumi Urao, and Luisa A DiPietro. Compromised angiogenesis and vascular integrity in impaired diabetic wound healing. *PloS one*, 15(4):e0231962, 2020.
- [157] Sabine Werner and Richard Grose. Regulation of wound healing by growth factors and cytokines. *Physiological reviews*, 83(3):835–870, 2003.
- [158] J Aaron Barnes, Mark A Eid, Mark A Creager, and Philip P Goodney. Epidemiology and risk of amputation in patients with diabetes mellitus and peripheral artery disease. *Arteriosclerosis, thrombosis, and vascular biology*, 40(8):1808–1817, 2020.
- [159] Misty D Humphries, Ann Brunson, Chin-Shang Li, Joy Melnikow, and Patrick S Romano. Amputation trends for patients with lower extremity ulcers due to diabetes and peripheral artery disease using statewide data. *Journal of vascular surgery*, 64(6):1747–1755, 2016.
- [160] David G Armstrong, Mark A Swerdlow, Alexandria A Armstrong, Michael S Conte, William V Padula, and Sicco A Bus. Five year mortality and direct costs of care for people with diabetic foot complications are comparable to cancer. *Journal of foot and ankle research*, 13(1):1–4, 2020.

- [161] Monika Vinish, Weihua Cui, Eboni Stafford, Leon Bae, Hal Hawkins, Robert Cox, and Tracy Toliver-Kinsky. Dendritic cells modulate burn wound healing by enhancing early proliferation. *Wound Repair and Regeneration*, 24(1):6–13, 2016.
- [162] Ariel Savina and Sebastian Amigorena. Phagocytosis and antigen presentation in dendritic cells. *Immunological reviews*, 219(1):143–156, 2007.
- [163] Andreas Patsalos, Laszlo Halasz, Miguel A Medina-Serpas, Wilhelm K Berger, Bence Daniel, Petros Tzerpos, Máté Kiss, Gergely Nagy, Cornelius Fischer, Zoltan Simandi, et al. A growth factor–expressing macrophage subpopulation orchestrates regenerative inflammation via gdf-15. *Journal of Experimental Medicine*, 219(1), 2022.
- [164] Holger Karsunky, Miriam Merad, Antonio Cozzio, Irving L Weissman, and Markus G Manz. Flt3 ligand regulates dendritic cell development from flt3+ lymphoid and myeloid-committed progenitors to flt3+ dendritic cells in vivo. *The Journal of experimental medicine*, 198(2):305–313, 2003.
- [165] Tomaz Velnar, Tracey Bailey, and Vladimir Smrkolj. The wound healing process: an overview of the cellular and molecular mechanisms. *Journal of international medical research*, 37(5):1528–1542, 2009.
- [166] Estelle Everett and Nestoras Mathioudakis. Update on management of diabetic foot ulcers. *Annals of the New York Academy of Sciences*, 1411(1):153–165, 2018.
- [167] Julien Bernatchez, Amanda Mayo, and Ahmed Kayssi. The epidemiology of lower extremity amputations, strategies for amputation prevention, and the importance of patient-centered care. In *Seminars in Vascular Surgery*, volume 34, pages 54–58. Elsevier, 2021.
- [168] David G. Armstrong and J. de Asla, Richard. *Management of Diabetic Foot Uclers*. UpToDate, 2022.
- [169] Henrike M Hamer, DMAE Jonkers, Koen Venema, SALW Vanhoutvin, FJ Troost, and R-J Brummer. The role of butyrate on colonic function. *Alimentary pharmacology & therapeutics*, 27(2):104–119, 2008.
- [170] JP Segain, D Raingeard De La Blétiere, A Bourreille, V Leray, N Gervois, C Rosales, L Ferrier, C Bonnet, HM Blottiere, and JP Galmiche. Butyrate inhibits inflammatory responses through  $\text{nf}\kappa\text{b}$  inhibition: implications for crohn’s disease. *Gut*, 47(3):397–403, 2000.
- [171] Hardi Lührs, T Gerke, JG Müller, R Melcher, J Schaubert, F Boxberger, W Scheppach, and T Menzel. Butyrate inhibits  $\text{nf}\kappa\text{b}$  activation in lamina propria macrophages of patients with ulcerative colitis. *Scandinavian journal of gastroenterology*, 37(4):458–466, 2002.
- [172] ANDREW J Wilson and PETER R Gibson. Short-chain fatty acids promote the migration of colonic epithelial cells in vitro. *Gastroenterology*, 113(2):487–496, 1997.

- [173] IA Finnie, AD Dwarakanath, BA Taylor, and JM Rhodes. Colonic mucin synthesis is increased by sodium butyrate. *Gut*, 36(1):93–99, 1995.
- [174] Laura Garcia-Bermejo, Nuria E Vilaboa, Concepcion Perez, Alba Galan, Elena De Blas, and Patricio Aller. Modulation of heat-shock protein 70 (hsp70) gene expression by sodium butyrate in u-937 promonocytic cells: relationships with differentiation and apoptosis. *Experimental cell research*, 236(1):268–274, 1997.
- [175] Mahmoud AO Dawood, Nabil M Eweedah, Zizy I Elbially, and Amr I Abdelhamid. Dietary sodium butyrate ameliorated the blood stress biomarkers, heat shock proteins, and immune response of Nile tilapia (*Oreochromis niloticus*) exposed to heat stress. *Journal of Thermal Biology*, 88:102500, 2020.
- [176] Rodrigo G Rosique, Marina J Rosique, and Jayme A Farina Junior. Curbing inflammation in skin wound healing: a review. *International journal of inflammation*, 2015, 2015.
- [177] Anna J Slezak, Aslan Mansurov, Michal M Raczky, Kevin Chang, Aaron T Alpar, Abigail L Lauterbach, Rachel P Wallace, Rachel K Weathered, Jorge EG Medellin, Claudia Battistella, et al. Tumor cell-surface binding of immune stimulating polymeric glyco-adjuvant via cysteine-reactive pyridyl disulfide promotes antitumor immunity. *ACS central science*, 2022.
- [178] D Scott Wilson, Sachiko Hirose, Michal M Raczky, Leonardo Bonilla-Ramirez, Laura Jeanbart, Ruyi Wang, Marcin Kwissa, Jean-Francois Franetich, Maria AS Broggi, Giacomo Diaceri, et al. Antigens reversibly conjugated to a polymeric glyco-adjuvant induce protective humoral and cellular immunity. *Nature materials*, 18(2):175–185, 2019.
- [179] Maiko Suzuki, Fumiaki Shinohara, K Sato, T Taniguchi, H Takada, and H Rikiishi. Interleukin-1 $\beta$  converting enzyme subfamily inhibitors prevent induction of cd86 molecules by butyrate through a creb-dependent mechanism in hl60 cells. *Immunology*, 108(3):375–383, 2003.
- [180] Richard P Phipps. Atherosclerosis: the emerging role of inflammation and the cd40–cd40 ligand system. *Proceedings of the National Academy of Sciences*, 97(13):6930–6932, 2000.
- [181] Gregory D Sempowski, Patricia R Chess, and Richard P Phipps. Cd40 is a functional activation antigen and b7-independent t cell costimulatory molecule on normal human lung fibroblasts. *The Journal of Immunology*, 158(10):4670–4677, 1997.
- [182] Linda Sealy and Roger Chalkley. The effect of sodium butyrate on histone modification. *Cell*, 14(1):115–121, 1978.
- [183] James R Davie. Inhibition of histone deacetylase activity by butyrate. *The Journal of nutrition*, 133(7):2485S–2493S, 2003.

- [184] Christopher J Lewis, Andrew Stevenson, Mark W Fear, and Fiona M Wood. A review of epigenetic regulation in wound healing: Implications for the future of wound care. *Wound Repair and Regeneration*, 28(6):710–718, 2020.
- [185] Muthusamy Thangaraju, Gail A Cresci, Kebin Liu, Sudha Ananth, Jaya P Gnanaprakasam, Darren D Browning, John D Mellinger, Sylvia B Smith, Gregory J Digby, Nevin A Lambert, et al. Gpr109a is a g-protein–coupled receptor for the bacterial fermentation product butyrate and functions as a tumor suppressor in colon. *Cancer research*, 69(7):2826–2832, 2009.
- [186] Ian B Robertson and Daniel B Rifkin. Regulation of the bioavailability of tgf- $\beta$  and tgf- $\beta$ -related proteins. *Cold Spring Harbor Perspectives in Biology*, 8(6):a021907, 2016.
- [187] Erich Bünemann, Norman-Philipp Hoff, Bettina Alexandra Buhren, Ulrike Wiesner, Stephan Meller, Edwin Bölke, Anja Müller-Homey, Robert Kubitzka, Thomas Ruzicka, Albert Zlotnik, et al. Chemokine ligand–receptor interactions critically regulate cutaneous wound healing. *European journal of medical research*, 23(1):1–17, 2018.
- [188] M Maurer and E Von Stebut. Macrophage inflammatory protein-1. *The international journal of biochemistry & cell biology*, 36(10):1882–1886, 2004.
- [189] Masae Ritsu, Kazuyoshi Kawakami, Emi Kanno, Hiromasa Tanno, Keiko Ishii, Yoshimichi Imai, Ryoko Maruyama, and Masahiro Tachi. Critical role of tumor necrosis factor- $\alpha$  in the early process of wound healing in skin. *Journal of Dermatology & Dermatologic Surgery*, 21(1):14–19, 2017.
- [190] Stefan Frank, Griseldis Hübner, Georg Breier, Michael T Longaker, David G Greenhalgh, and Sabine Werner. Regulation of vascular endothelial growth factor expression in cultured keratinocytes.: Implications for normal and impaired wound healing. *Journal of Biological Chemistry*, 270(21):12607–12613, 1995.
- [191] Philip Bao, Arber Kodra, Marjana Tomic-Canic, Michael S Golinko, H Paul Ehrlich, and Harold Brem. The role of vascular endothelial growth factor in wound healing. *Journal of Surgical Research*, 153(2):347–358, 2009.
- [192] Blair Z Johnson, Andrew W Stevenson, Cecilia M Prêle, Mark W Fear, and Fiona M Wood. The role of il-6 in skin fibrosis and cutaneous wound healing. *Biomedicines*, 8(5):101, 2020.
- [193] Guodong Li, Chung-Nga Ko, Dan Li, Chao Yang, Wanhe Wang, Guan-Jun Yang, Carmelo Di Primo, Vincent Kam Wai Wong, Yaozu Xiang, Ligen Lin, et al. A small molecule hif-1 $\alpha$  stabilizer that accelerates diabetic wound healing. *Nature communications*, 12(1):1–11, 2021.
- [194] Jesus Romo-Rico, Smriti Murali Krishna, Kateryna Bazaka, Jonathan Golledge, and Mohan V Jacob. Potential of plant secondary metabolite-based polymers to enhance wound healing. *Acta Biomaterialia*, 2022.

- [195] Jessica Hoff, Berit Karl, Jana Gerstmeier, Uwe Beekmann, Lisa Schmolz, Friedemann Borner, Dana Kralisch, Michael Bauer, Oliver Werz, Dagmar Fischer, et al. Controlled release of the  $\alpha$ -tocopherol-derived metabolite  $\alpha$ -13'-carboxychromanol from bacterial nanocellulose wound cover improves wound healing. *Nanomaterials*, 11(8):1939, 2021.
- [196] Maggie J Malone-Povolny, Sara E Maloney, and Mark H Schoenfisch. Nitric oxide therapy for diabetic wound healing. *Advanced healthcare materials*, 8(12):1801210, 2019.
- [197] Adrian Buganza Tepole and Ellen Kuhl. Systems-based approaches toward wound healing. *Pediatric research*, 73(2):553–563, 2013.
- [198] Marcello Chieppa, Giancarlo Bianchi, Andrea Doni, Annalisa Del Prete, Marina Sironi, Gordana Laskarin, Paolo Monti, Lorenzo Piemonti, Andrea Biondi, Alberto Mantovani, et al. Cross-linking of the mannose receptor on monocyte-derived dendritic cells activates an anti-inflammatory immunosuppressive program. *The Journal of Immunology*, 171(9):4552–4560, 2003.
- [199] Karen Ousey, KF Cutting, Alan A Rogers, and Mark G Rippon. The importance of hydration in wound healing: reinvigorating the clinical perspective. *Journal of wound care*, 25(3):122–130, 2016.
- [200] Roy Hajjar, Carole S Richard, and Manuela M Santos. The role of butyrate in surgical and oncological outcomes in colorectal cancer. *American Journal of Physiology-Gastrointestinal and Liver Physiology*, 320(4):G601–G608, 2021.
- [201] Hong-Bo Wang, Peng-Yuan Wang, Xin Wang, Yuan-Lian Wan, and Yu-Cun Liu. Butyrate enhances intestinal epithelial barrier function via up-regulation of tight junction protein claudin-1 transcription. *Digestive diseases and sciences*, 57(12):3126–3135, 2012.
- [202] Guangxin Chen, Xin Ran, Bai Li, Yuhang Li, Dewei He, Bingxu Huang, Shoupeng Fu, Juxiong Liu, and Wei Wang. Sodium butyrate inhibits inflammation and maintains epithelium barrier integrity in a tnbs-induced inflammatory bowel disease mice model. *EBioMedicine*, 30:317–325, 2018.
- [203] A Di Sabatino, R Morera, R Ciccocioppo, P Cazzola, S Gotti, FP Tinozzi, S Tinozzi, and GR Corazza. Oral butyrate for mildly to moderately active crohn's disease. *Alimentary pharmacology & therapeutics*, 22(9):789–794, 2005.
- [204] You-Hua Xu, Chen-Lin Gao, Heng-Li Guo, Wen-Qian Zhang, Wei Huang, Shan-Shan Tang, Wen-Jun Gan, Yong Xu, Hua Zhou, and Quan Zhu. Sodium butyrate supplementation ameliorates diabetic inflammation in db/db mice. *Journal of Endocrinology*, 238(3):231–244, 2018.
- [205] Marek Konop, Mateusz Rybka, Mateusz Szudzik, Łukasz Mazurek, Anna K Laskowska, Dorota Sulejczak, Zbigniew Ruszczak, Rafał Mazgaj, Bartłomiej Cieřlik, Robert A

- Schwartz, et al. Keratin-butyrate scaffolds promote skin wound healing in diabetic rats through down-regulation of il-1 $\beta$  and up-regulation of keratins 16 and 17. *Journal of Natural Fibers*, pages 1–16, 2022.
- [206] Fang Bian, Yangyan Xiao, Mahira Zaheer, Eugene A Volpe, Stephen C Pflugfelder, De-Quan Li, and Cintia S De Paiva. Inhibition of nlrp3 inflammasome pathway by butyrate improves corneal wound healing in corneal alkali burn. *International journal of molecular sciences*, 18(3):562, 2017.
- [207] Rohini Keshava and Rajalakshmi Gope. Sodium butyrate plus egf and pdgf-bb aids cutaneous wound healing in diabetic mice. *Advances in Biology*, 2015, 2015.
- [208] Agatha Schwarz, Anika Bruhs, and Thomas Schwarz. The short-chain fatty acid sodium butyrate functions as a regulator of the skin immune system. *Journal of Investigative Dermatology*, 137(4):855–864, 2017.
- [209] Jun Wang, Mei Yang, Shengyu Xu, Yan Lin, Lianqiang Che, Zhengfeng Fang, and De Wu. Comparative effects of sodium butyrate and flavors on feed intake of lactating sows and growth performance of piglets. *Animal Science Journal*, 85(6):683–689, 2014.
- [210] Kees Meijer, Paul de Vos, and Marion G Priebe. Butyrate and other short-chain fatty acids as modulators of immunity: what relevance for health? *Current Opinion in Clinical Nutrition & Metabolic Care*, 13(6):715–721, 2010.
- [211] Elizabeth Lebrun, Marjana Tomic-Canic, and Robert S Kirsner. The role of surgical debridement in healing of diabetic foot ulcers. *Wound repair and regeneration*, 18(5):433–438, 2010.
- [212] Tarig Elraiayah, Gabriela Prutsky, Juan Pablo Domecq, Apostolos Tsapas, Mohammed Nabhan, Robert G Frykberg, Belal Firwana, Rim Hasan, Larry J Prokop, and Mohammad Hassan Murad. A systematic review and meta-analysis of off-loading methods for diabetic foot ulcers. *Journal of vascular surgery*, 63(2):59S–68S, 2016.
- [213] Vanessa Jones, Joseph E Grey, and Keith G Harding. Wound dressings. *Bmj*, 332(7544):777–780, 2006.
- [214] Lihua Wu, Gill Norman, Jo C Dumville, Susan O’Meara, and Sally EM Bell-Syer. Dressings for treating foot ulcers in people with diabetes: an overview of systematic reviews. *Cochrane Database of Systematic Reviews*, 7, 2015.
- [215] Shan Bergin and Paul Wraight. Silver based wound dressings and topical agents for treating diabetic foot ulcers. *Cochrane Database of Systematic Reviews*, 1, 2006.
- [216] T Jeffery Wieman, Janice M Smiell, and Yachin Su. Efficacy and safety of a topical gel formulation of recombinant human platelet-derived growth factor-bb (becaplermin) in patients with chronic neuropathic diabetic ulcers: a phase iii randomized placebo-controlled double-blind study. *Diabetes care*, 21(5):822–827, 1998.

- [217] Julia E Babensee, Larry V McIntire, and Antonios G Mikos. Growth factor delivery for tissue engineering. *Pharmaceutical research*, 17(5):497–504, 2000.
- [218] Lara Lopes, Ocean Setia, Afsha Aurshina, Shirley Liu, Haidi Hu, Toshihiko Isaji, Haiyang Liu, Tun Wang, Shun Ono, Xiangjiang Guo, et al. Stem cell therapy for diabetic foot ulcers: a review of preclinical and clinical research. *Stem cell research & therapy*, 9(1):1–16, 2018.
- [219] Robert James Thomas, Paul C Hourd, and David J Williams. Application of process quality engineering techniques to improve the understanding of the in vitro processing of stem cells for therapeutic use. *Journal of biotechnology*, 136(3-4):148–155, 2008.
- [220] Thomas RJ Heathman, Alvin W Nienow, Mark J McCall, Karen Coopman, Bo Kara, and Christopher J Hewitt. The translation of cell-based therapies: clinical landscape and manufacturing challenges. *Regenerative medicine*, 10(1):49–64, 2015.
- [221] Ileana Ruxandra Botusan, Vivekananda Gupta Sunkari, Octavian Savu, Anca Irinel Catrina, Jacob Grünler, Stina Lindberg, Teresa Pereira, Seppo Ylä-Herttuala, Lorenz Poellinger, Kerstin Brismar, et al. Stabilization of hif-1 $\alpha$  is critical to improve wound healing in diabetic mice. *Proceedings of the National Academy of Sciences*, 105(49):19426–19431, 2008.
- [222] Laís P Pral, José L Fachi, Renan O Corrêa, Marco Colonna, and Marco AR Vinolo. Hypoxia and hif-1 as key regulators of gut microbiota and host interactions. *Trends in Immunology*, 42(7):604–621, 2021.
- [223] Wan Xing Hong, Michael S Hu, Mikaela Esquivel, Grace Y Liang, Robert C Rennert, Adrian McArdle, Kevin J Paik, Dominik Duscher, Geoffrey C Gurtner, H Peter Lorenz, et al. The role of hypoxia-inducible factor in wound healing. *Advances in wound care*, 3(5):390–399, 2014.
- [224] PH Maxwell, GU Dachs, JM Gleadle, LG Nicholls, AL Harris, IJ Stratford, O Hankinson, CW Pugh, and PJ Ratcliffe. Hypoxia-inducible factor-1 modulates gene expression in solid tumors and influences both angiogenesis and tumor growth. *Proceedings of the National Academy of Sciences*, 94(15):8104–8109, 1997.
- [225] Gregg L Semenza. Hydroxylation of hif-1: oxygen sensing at the molecular level. *Physiology*, 19(4):176–182, 2004.
- [226] Loredana Bergandi, Tania Flutto, Sabina Valentini, Laura Thedy, Rita Pramotton, Simona Zenato, and Francesca Silvagno. Whey derivatives and galactooligosaccharides stimulate the wound healing and the function of human keratinocytes through the nf-kb and foxo-1 signaling pathways. *Nutrients*, 14(14):2888, 2022.
- [227] Sandra Leon Carrion, Carrie Hayes Sutter, and Thomas R Sutter. Combined treatment with sodium butyrate and pd 153035 enhances keratinocyte differentiation. *Experimental dermatology*, 23(3):211–214, 2014.

- [228] Aurélien Trompette, Julie Pernot, Olaf Perdikj, Rayed Ali A Alqahtani, Jaime Santo Domingo, Dolores Camacho-Muñoz, Nicholas C Wong, Alexandra C Kendall, Andreas Wiederkehr, Laurent P Nicod, et al. Gut-derived short-chain fatty acids modulate skin barrier integrity by promoting keratinocyte metabolism and differentiation. *Mucosal Immunology*, pages 1–19, 2022.
- [229] Abdul Malik Tyagi, Mingcan Yu, Trevor M Darby, Chiara Vaccaro, Jau-Yi Li, Joshua A Owens, Emory Hsu, Jonathan Adams, M Neale Weitzmann, Rheinallt M Jones, et al. The microbial metabolite butyrate stimulates bone formation via t regulatory cell-mediated regulation of wnt10b expression. *Immunity*, 49(6):1116–1131, 2018.
- [230] Sachiko Hirosue, Iraklis C Kourtis, André J van der Vlies, Jeffrey A Hubbell, and Melody A Swartz. Antigen delivery to dendritic cells by poly (propylene sulfide) nanoparticles with disulfide conjugated peptides: Cross-presentation and t cell activation. *Vaccine*, 28(50):7897–7906, 2010.
- [231] Supriya Mallick, Rony Benson, and GK Rath. Radiation induced oral mucositis: a review of current literature on prevention and management. *European Archives of Oto-Rhino-Laryngology*, 273:2285–2293, 2016.
- [232] Osama Muhammad Maria, Nicoletta Eliopoulos, and Thierry Muanza. Radiation-induced oral mucositis. *Frontiers in oncology*, 7:89, 2017.
- [233] Aishan Shih, Christine Miaskowski, Marylin J Dodd, Nancy A Stotts, and Laurie MacPhail. Mechanisms for radiation-induced oral mucositis and the consequences. *Cancer nursing*, 26(3):222–229, 2003.
- [234] Serena Coppola, Carmen Avagliano, Antonia Sacchi, Sonia Laneri, Antonio Calignano, Luana Voto, Anna Luzzetti, and Roberto Berni Canani. Potential clinical applications of the postbiotic butyrate in human skin diseases. *Molecules*, 27(6):1849, 2022.
- [235] Maria MM Kaiser, Leonard R Pelgrom, Alwin J Van der Ham, Maria Yazdanbakhsh, and Bart Everts. Butyrate conditions human dendritic cells to prime type 1 regulatory t cells via both histone deacetylase inhibition and g protein-coupled receptor 109a signaling. *Frontiers in immunology*, 8:1429, 2017.
- [236] G Gabbiani, M Le Lous, AJ Bailey, S Bazin, and A Delaunay. Collagen and myofibroblasts of granulation tissue. *Virchows Archiv B*, 21(1):133–145, 1976.